Improving indoor localization accuracy through information fusion

Improving Indoor Localization Accuracy through Information Fusion

PROEFSCHRIFT

ter verkrijging van de graad van doctor aan de Technische Universiteit Eindhoven, op gezag van de rector magnificus prof.dr.ir. F. Baaijens voor een commissie aangewezen door het College voor Promoties, in het openbaar te verdedigen op dinsdag 10 december 2019 om 13:30 uur

door

Akis Kokkinis

geboren in Nicosia, Cyprus

Dit proefschrift is goedgekeurd door de promotoren en de samenstelling van de promotiecommissie is als volgt:

Voorzitter:	prof.dr.ir. M.J. Bentum
1e promotor:	prof.dr.ir A. Liotta
2e promotor:	prof.dr.ir S. Stavrou (Open University of Cyprus)
copromotor(en):	dr.ir. G. Exarchakos
leden:	dr. T. Dagiuklas (London South Bank University)
	prof.dr. A. Anjum (University of Derby)
	prof.dr.ir. I.G.M.M. Niemegeers
reserve	prof.ir. A.M.J. Koonen

Het onderzoek of ontwerp dat in dit proefschrift wordt beschreven is uitgevoerd in overeenstemming met de TU/e Gedragscode Wetenschapsbeoefening.

ISBN: 978-90-386-4925-2
NUR: 959

Acknowledgements

Special thanks to Sigint Solutions Ltd for sponsoring this PhD and also providing access to their laboratory equipment, test-beds and software tools. The opportunity that I was given to develop and test custom-made modules on **TruNET wireless** simulator, was undoubtedly a critical success factor.

I would also like to express my sincere gratitude to my wife, family, friends and to my supervisors for their support and guidance.

Akis Kokkinis
Eindhoven, The Netherlands, 2019

Summary

Improving Indoor Localization Accuracy through Information Fusion

Indoor user localization and tracking techniques and systems are instrumental to a broad range of services and applications that are supported by advanced wireless networks, sensors and Internet of Things (IoT). Applications utilizing localization information can assist people in shopping malls, through the provision of navigation services and geospatial marketing alerts; in hospitals, for monitoring the location of patients, doctors and critical equipment; in logistics, for tracking assets and optimizing empty spaces in ports or inland storage, even in homes or for providing relevant Ambient Assisted Living (AAL) services. Since Global Navigation Satellite System (GNSS) signals are not available in indoor environments, localization can be typically achieved by utilizing other off-the-shelf wireless communication technologies (Wi-Fi, Bluetooth, LTE, Zigbee, VLC etc.). Striving for accuracy, the research community investigates sophisticated solutions that are often sought through hybrid approaches. It is a fact that the accuracy achieved by any Real Time Localization System (RTLS) is affected by the volume and quality of information that is available during the position estimation procedure. The more useful information can be provided, the higher the probability of producing a more accurate estimate. Depending on the capabilities of the terminal or the overall RTLS, in retrieving, storing and processing location-specific information, advanced positioning algorithms can be developed in order to provide improved positioning services. The location-specific information may include radio parameters retrieved by one or more wireless technologies, such as Received Signal Strength (RSS), Angle of Arrival (AOA), Time of Arrival (TOA) and Impulse Responses (IR), or non-radio parameters, such as inertial measurements, prior map/layout knowledge etc. Among all, fingerprint-based positioning is one of the most popular indoor localization techniques implemented by RTLS due to its simplicity.

In this research work, we examine existing, and develop novel methodologies, for the purpose of improving indoor localization accuracy, through information fusion. In this context, by information fusion, we mean the usage of various available radio related parameters from heterogeneous wireless technologies, as well as nonradio parameters such as physical information retrieved from an environment map. More specifically, we have contributed in this research area by developing enhanced methodologies and algorithms in the following areas of Fingerprint-based Indoor Positioning:

(1) **Cross-Device Indoor Positioning**: We initially investigated the challenge of providing satisfactory positioning accuracy to users whose mobile device models vary significantly. Device diversity means in simple words different performance of characteristics like receiver sensitivity, antenna patterns, RSS and other radio parameter readings. In such environments indoor positioning platforms need to encapsulate such mechanisms that can handle the differences and still perform within the expected specifications. Our approach, was published in [**1**] and [**2**] and is described in Chapter 3 of this thesis.

(2) **Map-Aided Indoor Positioning**: The objective was to investigate potential accuracy improvements in the fingerprint-based indoor positioning processes, by imposing map-constraints into the positioning algorithms in the form of apriori knowledge. In our approach, we proposed the introduction of a Route Probability Factor (RPF), which reflects the probability of a user, to be located in one position instead of all others. Detailed analysis of the research work is provided in Chapter 4. The work is based on our scientific papers [**3**] and [**4**].

(3) **Combining Heterogeneous Technologies in Fingerprint-based Positioning**: In this research area, which is described in Chapter 5, we introduced two new algorithms that utilize information retrieved by IEEE 802.15.1 or IEEE 802.15.7 technologies in order to improve the accuracy and performance of conventional fingerprint-based localization platforms which use IEEE 802.11 wireless networks. Both algorithms (i-KNN for IEEE 802.15.1 and vlp-KNN for IEEE 802.15.7) are filtering the initial RSS fingerprint dataset in order to narrow it down to a subset of the data that is used by the conventional positioning algorithm KNN. In this way, mean error is reduced significantly and positioning speed is improved. Further analysis is presented Chapter 5 as per the published work in [**5**] and [**6**].

(4) **Utilizing Polarization for Improved Single Access Point Indoor Localization**: In this work, which has been submitted to *Sensors Journal, MDPI*, we investigated a Multiple Input, Multiple Output (MIMO) 802.11 system, and its polarization effects on RSS, in order to achieve single access point localization in indoor environments. Extended experimental testing indicated that the presence of differently polarized antennas and signals can be utilized to provide unique fingerprints in a multi-layered radiomap approach and improve accuracy through an RSS-based localization method. The details are presented in Chapter 6.

During the thesis, further contributions were made, relevant to the topic of the thesis. Contributions include:

(1) Quality evaluation of Real Time Localization Systems (RTLS) as per the work published in [**7**], [**8**], [**9**] and [**10**] and
(2) Supportive work in optimizing Wireless Sensor Networks (WSN) deployment for providing better coverage in RTLS as per [**11**].

Contents

List of Figures

List of Tables

Abbreviations

Abbreviation	Description
AAL	Ambient Assisted Living
AR-WFL	Aging-Resistant Wi-Fi Fingerprinting Localization
AOA	Angle of Arrival
AP	Access Point
BDS	BeiDou Navigation Satellite System
BLE	Bluetooth Low Energy
BSN	Body Sensor Networks
CEP	Circular Error Probability
CDF	Cumulative Distribution Function
DAS	Delay and Sum
DCM	Database Correlation Method
DOA	Direction of Arrival
DOAJ	Directory of open access journals
ESPRIT	Estimation of Signal Parameters via Rotational Invariance Technique
FOV	Field Of View
FSL	Free Space Loss
GFSK	Gaussian Frequency Shift Key
GLONASS	Global Navigation Satellite System
GNSS	Global Navigation Satellite System
GPS	Global Positioning System
GPU	Graphics Processing Unit
GO	Geometrical Optics
GTD	Geometrical Theory of Diffraction
HLF	Hyperbolic Location Fingerprinting
i-KNN	Intelligent KNN
IMU	Inertial Measurement Unit
IoT	Internet of Things
IW-KNN	Iterative Weighted KNN
KNN	K Nearest Neighbour
LBS	Location Based Services
LED	Light-Emitting Diode
LOS	Line of Sight
LT	Linear Transformation
LTE	Long Term Evolution
MAP	Maximum A Posteriori

MDPI	Multidisciplinary Digital Publishing Institute
MIMO	Multiple Input, Multiple Output
MMSE	Minimum Mean Square Error
MS	Mobile Station
MU	Mobile User
MUSIC	Multiple Signal Classification
NLOS	Non-Line of Sight
NMF	Neighbour Mean Filter
NN	Nearest Neighbour
OWC	Optical Wireless Communication
RFID	Radio Frequency Identification
RSS	Received Signal Strength
RSSD	RSS Difference
RT	Ray Tracing
RTLS	Real Time Localization System
SDR	Software Defined Radio
SON	Self-Organizing Networks
SSDA	Sample Size Determination Algorithm
TDOA	Time Difference of Arrival
TOA	Time of Arrival
TOF	Time of Flight
UE	User Equipment
UI	User Interface
UTD	Uniform Theory of Diffraction
UWB	Ultra Wide Band
VLC	Visible Light Communication
VLP	Visible Light Positioning
WKNN	Weighted K Nearest Neighbour
WSN	Wireless Sensor Networks

CHAPTER 1

Introduction

Localization is the process of using wireless technologies in order to locate and track users or assets in outdoor or indoor environments. As a term, in the concept of this thesis, *localization* is interchangeable with the term *positioning*. As a service, it became of extreme importance in both military and civilian applications. Such applications include the tracking of military forces in fast changing battle environments, personal navigation and tracking of emergency calls. It is also implemented in the logistics industry for managing the flow of assets and goods, the medical sector for monitoring patients, as well as in the marketing domain for advertising products to specific geographically located target groups [**13**]. Due to the more recent technological advances and the trend towards the utilization of internet cloud applications, localization service has been further expanded to support location-sensitive billing and cellular phone fraud detection. The related more advanced localization methodologies involve the utilization of heterogeneous wireless technologies as well as the fusion of sensor and Internet of Things (IoT) data ([**14**], [**15**], [**16**], [**17**]). Currently, the most active research topics concern the provision of affordable localization solutions with improved accuracy through the combination of technologies and fusion of information of radio and non-radio parameters.

There are four fundamental localization techniques, for both indoor and outdoor localization, and these are (i) **Range-based (lateration)**, (ii) **Direction-based (angulation)**, (iii) **Dead reckoning** and (iv) **Fingerprinting**. Details on Wireless Indoor Positioning Techniques and Systems can be found in [**18**], [**19**] and [**20**]. The theoretical background is explained in Chapter 2. An analysis and comparison of outdoor positioning methodologies is provided in [**21**], [**22**], [**23**] and [**24**]. A brief overview on outdoor and indoor localization systems will follow in Sections 1.1 and 1.2. The research scope is defined in Section 1.3 and the thesis structure is explained in Section 1.4.

1.1. Outdoor Localization

The dominant wireless communication systems used for outdoor localization, are the Global Navigation Satellite Systems (GNSS) and cellular networks. GNSS implement purely TOA and TDOA-based localization techniques, while in cellular networks the techniques are much more broad with some of them being more attractive than others, as will be presented in the coming subsections.

1.1.1. Global Navigation Satellite Systems

GNSS systems are positioning and navigation systems that utilize the information provided by a constellation of satellites in orbits around the earth. They implement the TOA-based estimation and consequently they require a LOS condition to perform satisfactory. They are the dominant outdoor positioning system. There are currently four well known GNSS systems: The US *Global Positioning System (GPS)*, the Russian *Global Navigation Satellite System (GLONASS)*, the European *GALILEO* and the Chinese *BeiDou Navigation Satellite System (BDS)* [**25**].

For the implementation of GNSS concept, three segments are required: i. The satellite constellation, ii. the ground control stations, and iii. the user equipment. Satellites and ground control stations are synchronized with accurate clocks, which is a prerequisite for the accomplishment of localization accuracy with the Time-based technique. Conceptually, there are four steps during the localization procedure in GNSS, as shown in figure 1.1 and summarized below:

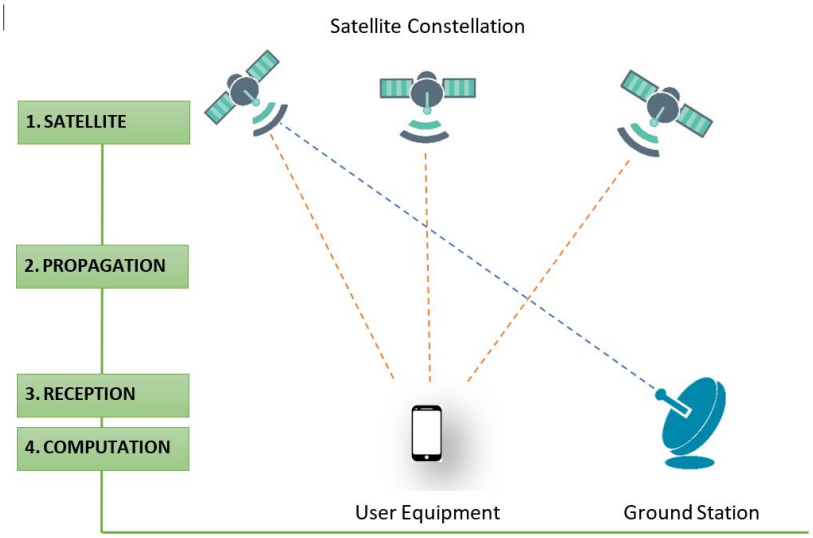

Figure 1.1 – GNSS Schematic

(1) **Satellite:** A constellation of satellites is required to be in orbit in such a way so that 4 satellites are always visible from a user device in order to accomplish 3D localization. Their orbit ephemerides (the parameters that define their orbit) are known with a high degree of precision at any given time. Ground-based control stations adjust the satellites' ephemerides and clocks, when necessary.

(2) **Propagation:** Every satellite broadcasts periodically its ephemerides and its internal time. Radio signals follow the basic rules of propagation

as they pass through the different layers of the atmosphere until they are eventually received by the user equipment.

(3) **Reception:** Signals from at least 4 satellites are required to be received by the user's equipment or device. These radio signals contain the data required for the calculation of the propagation time.

(4) **Computation:** Upon receiving the radio signals, the user equipment computes the propagation time and consequently calculates the relative position.

(5) **Application:** At an application level, the relative position is utilized for navigation, mapping, or any other service.

GNSS applications can be found on every level of our lives and in every industry sector. Typical examples include personal and commercial navigation and LBS services, emergency location, security and humanitarian services, science, environment, weather and agriculture [**26**].

The technical characteristics of the typical GNSS systems [**27**], are shown in table 1.1.

Table 1.1 – GNSS Positioning System Characteristics

Parameter	**GPS**	**GLONASS**	**GALILEO**	**Beidou**
Satellites in orbit	31	26	28	23
Max Satellites	33	24	30	35
Orbital Planes	6	3	3	3
Orbit Altitude	$20.183km$	$19.100km$	$23.222km$	$21.500km$
Inclination	55°	64.8°	56°	55°
Orbital Period	$11h55m$	$11h15m$	$14h05m$	$12h50m$
Frequencies	L1, L2, L5	G1, G2, G3	E1, E5a, E5b, E6	B1-2, B1, B2, B3
Coding	CDMA	FDMA	CDMA	CDMA
Accuracy [m]	5	2.8-7.38	1	10

1.1.2. Cellular Networks for Localization Services

Since their introduction to the market, cellular networks have being evolving and incorporating new technologies, offering their users a broad number of services in addition to mobile telephony. They have transformed from the 1^{st} generation to the 5^{th} generation which offers transfer of information at extremely high data rates. This capability has provided the opportunity for developing mobile applications, cloud based or not, which are nowadays accessible from almost everywhere. A wide range of such applications require user localization information. The opportunity was triggered after the decision of Federal Communications Commission of the United States which defined enhanced 911 (E911) location requirements in the mid 1990s. A similar decision was taken in the European Commission (EC) within the framework of harmonizing emergency services. For this task, a coordination group was formulated, to coordinate the access to location information by

emergency services (CGALIES). Having the mandate of user localization in emergency scenarios, the cellular service providers gradually included such Location Based Services (LBS) in all cellular technologies.

The most widely utilized localization technique in cellular networks, is time-based estimation. They implement methods such as Uplink TOA (UToA), Uplink Time Difference of Arrival (UTDoA), Observed Time Difference of Arrival (OTDoA), Enhanced Cell ID (E-CID) -TA/CID and Enhanced Observed Time Difference (E-OTD) [**21**]. Some solutions also use outdoor fingerprinting, also known as scene analysis [**23**].

A brief comparison of localization accuracy per method and technology is summarized in Table 1.2 based on [**21**], [**22**], [**23**] and [**24**].

Table 1.2 – Cellular Networks Localization methods

Method	**Technology**	**Type**	**67%-Accuracy[m]**
CID+TA/CID+RTT	2G, 3G, 4G	Proximity	$\geqslant 100$
E-CID	3G, 4G	Proximity	~ 50
RFPM	2G, 3G, 4G	Fingerprinting	$\geqslant 50$
U-ToA	2G	Trilateration	$\geqslant 100$
UTDoA	3G, 4G	Trilateration	$\geqslant 50$
E-OTD	2G	Trilateration	$\geqslant 100$
OTDoA	3G, 4G	Trilateration	≤ 50
TBS	4G	Trilateration	≤ 50

Location Based Services (LBS) provided by cellular networks is currently a very active topic in the research community, which investigates ways to improve the communication capacity, by supporting decisions for better network management and for radio re-configurable spectrum. A typical example of LSB utilization for optimizing the network and improving quality of service, is the self-organizing networks (SON) technology. SON is a mechanism to ease and improve the operation of the network exploited commercially by the network operator or the application developer, with an aim to obtain a revenue [**28**].

1.2. Indoor Localization

During the last decade, several indoor localization methods have been proposed, a number of which is summarized in [**29**], [**30**] and [**31**]. In all cases, and depending on the technology and equipment available, the localization methodology utilizes parameters, such as Received Signal Strength (RSS), Time of Flight (TOF) and Angle of Arrival (AOA). Methods based on TOF and AOA require usage of specialized equipment in order to measure time or ray angles with high accuracy, synchronization of transceivers and calibration of antennas [**32**].

With the advancement of computational power and the introduction of new technologies, more sophisticated solutions have emerged. They typically include hybrid approaches where information from different sources is fused in order to

achieve improved localization accuracy. In this scope, two new novel approaches are proposed in this thesis, which refer to the combination of Wi-Fi and Bluetooth Low Energy (BLE) beacons [**5**], and Wi-Fi with Visual Light Positioning (VLP) [**6**]. Other related work includes also the combination of VLP with ultra sound [**33**].

With regard to fusion of information of non-radio parameters with radio parameters, details can be found in [**34**], [**35**], [**36**] where researchers utilize input from inertial, magnetic or other sensors. In this area, information fusion retrieved from maps is presented , as per work in [**37**] and [**4**].

A summary of the most common technologies utilized in indoor positioning, with a brief analysis of their cons and pros is presented in table 1.3.

Table 1.3 – Indoor Positioning:Technologies comparison

Technology	**Advantages**	**Disadvantages**
RFID [**38**]	Non-line of sight (NLOS)	Short range, limited coverage
UWB [**39**]	High accuracy even in multipath, limited interference with other RF systems	High cost, increased errors if metallic materials exist
VLP [**6**]	High accuracy	Infrastructure required, Line of sight (LOS), UE constraints
ZigBee [**40**]	Low energy, low cost	Vulnerable to interference (IS band)
Infrared [**41**]	LOS (helps with security aspects)	LOS, short range, vulnerable to lighting conditions
Ultrasonic [**41**]	Does not interfere with RF	Loss of signal due to obstructions
Wi-Fi [**9**]	Widely used, adequate range and coverage	Fingerprinting technique is labour-intensive and not resilient to dynamic changes
Bluetooth [**42**]	Widely used	Low range, low accuracy
BLE [**5**]	Low energy, upcoming trend, range information provided	Low range, low coverage, easily interfered
IoT [**11**]	Widely spread	Low range, sensitive to interference

The most popular localization technique that is widely used, is based on RSS fingerprinting. The popularity of this method, lies on the utilization of existing wireless communication infrastructures, the simplicity of the localization algorithms, and the achieved levels of accuracy. In RSS fingerprint-based localization, the procedure involves an offline and an online phase. During the offline phase, a data–set of RSS fingerprints, named *a radiomap*, is generated by recording the RSS

value of each Access Point (AP), for each location in the area of interest. The RSS values are then calibrated in order to improve the quality of the *radiomap* [**8**]. Such datasets can be generated rapidly and at a relatively low cost, through the use of a deterministic radio propagation simulator. The conventional approach involves performing a time consuming and expensive measurement campaign in the actual environment [**1**]. The *radiomap* of such a campaign represents a *static snapshot* of the APs' RSS values at each measured location, requiring the repetition of measurements every time that the environment or the wireless network is modified. During the online phase, the Mobile Station (MS) performs network discovery as well as real time RSS measurements. Different positioning algorithms are then applied in order to identify the best match between the observed RSS fingerprint and the respective mean value of the fingerprints recorded in the *radiomap* during the offline phase. An overview of typical fingerprint-based methods is provided in [**43**].

A significant drawback of these systems, is that they require the deployment of several APs in order to generate unique fingerprints at each location and achieve a satisfactory positioning accuracy [**9**]. Due to this characteristic, fingerprint-based localization applications and platforms cannot be easily utilized in small indoor environments (i.e., residential places or open-plan business spaces), where only a single AP is typically being deployed.

1.3. Research Scope

In this research work, existing methodologies have been examined, and new novel methodologies have been developed, for the purpose of improving indoor localization accuracy, through information fusion. In this context, information fusion means the usage of various available radio related parameters from heterogeneous wireless technologies, as well as non-radio parameters, such as physical information retrieved from the environment map. More specifically, contribution to this research area has been the development of the following enhanced methodologies/algorithms:

(1) **Cross-Device Indoor Positioning**: The proposed work was directed towards facing the device diversity issue in indoor localization. The wide variety of mobile devices which provide different signal measurement values, is an error generating factor during user location estimation. In this approach, which was published in [**1**] and [**2**] a linear transformation method between different devices, was implemented and tested, in order to calibrate the *radiomap* used in fingerprinting positioning.

(2) **Map-Aided Fingerprint-based Indoor Positioning:** The objective was to investigate potential accuracy improvements in the fingerprint-based indoor positioning processes, by imposing map-constraints into the positioning algorithms in the form of apriori knowledge. In this approach in [**3**] and [**4**], the introduction of a Route Probability Factor (RPF), was proposed, which reflects the probability of a user, to be located at one position instead of all others. The RPF does not only affect the probabilities of the points along the pre-defined frequent routes, but also influences

all the neighbouring points that lie in proximity to each frequent route. The outcome of the evaluation process indicates the validity of the RPF approach, demonstrated by the significant reduction of the positioning error. It was finally further investigated how positioning accuracy is affected in map-aided positioning systems, when a user's typical route is described by different probability distribution types. Probability distributions are introduced in an effort to better explain any reasonable route deviations from the user's centre line of movement.

(3) **Fusing Bluetooth Beacon Data with Wi-Fi Radiomaps:** Due to the widespread availability of IEEE 802.11, many localization platforms are based on Wi-Fi RSS, using algorithms such as KNN, MAP and MMSE. Yet, accuracy achieved can greatly vary and can be considered insufficient depending on the application. In [**5**], a hybrid method was introduced, which combines the information retrieved from low cost Bluetooth Low Energy (BLE) beacons and other existing Wi-Fi infrastructure. Building on KNN, a new positioning algorithm (dubbed i-KNN) was proposed, which is able to filter the initial fingerprint dataset (i.e., the *radiomap*), by taking into consideration the proximity of RSS fingerprints with respect to the BLE devices. In this way, i-KNN provides an optimized small subset of possible user locations, based on which it finally estimates the user position. The proposed methodology achieves fast positioning estimation due to the utilization of a fragment of the initial fingerprint dataset and, at the same time, improves positioning accuracy by minimizing estimation errors.

(4) **Combining Smart Lighting and Radio Fingerprinting for Improved Indoor Localization:** Following a similar methodology as described above, in [**6**] and further expansion of research, a hybrid indoor positioning system was proposed, which combines a minimal smart lighting deployment, for Visible Light Positioning (VPL) purposes, with an IEEE 802.11 RSS Fingerprint-based Indoor Positioning System. Such a hybrid deployment improves the localization performance by utilizing the benefits of both the visible light and radio technologies. Improvement is demonstrated in terms of accuracy, coverage and processing requirements. At the same time, the deployment cost and complexity remain in affordable levels, due to the minimal deployment of the smart lighting system and the utilization of an existing IEEE 802.11 wireless network.

(5) **Utilizing Polarization for Improved Single Access Point Indoor Localization:** Finally, a MIMO 802.11 system was investigated, as well as its polarization effects on RSS, in order to achieve improved single access point indoor localization. Extended experimental testing indicated that the presence of differently polarized antennas and signals can be utilized to provide unique fingerprints in a *multi-layered radiomap* approach and improve accuracy through an RSS-based localization method.

1.4. Structure of Thesis

After the general introduction of outdoor and indoor localization concepts presented in Chapter 1, the rest of the thesis is organized as follows: In Chapter 2 the fundamental localization techniques are analyzed and the respective mathematical models are explained as per Section 2.2. In the same chapter, under Section 2.3, the research work performed in information fusion and combination of wireless technologies was further investigated, with an aim to provide more reliable and accurate indoor localization. Chapter 2 ends with Section 2.4, where the most common RTLS performance evaluation methodologies are presented. Chapters 3, 4, 5 and 6 include an analysis of the most important research contribution of this thesis. More specifically, in Chapter 3 the challenge of cross device positioning is explained and a linear transformation methodology is proposed to overcome such issues. In Chapter 4, an advanced localization methodology is introduced, which imposes map constraints and improves accuracy provided by fingerprint-based platforms. In Chapter 5, an enhanced KNN algorithm is proposed. The aforementioned algorithm combines information from two different technologies (either Wi-Fi and BLE or Wi-Fi and VLP) and improves the performance in terms of computational speed and location prediction accuracy. The research contribution ends with Chapter 6, where a novel methodology for single MIMO-type access point indoor localization is presented. The method is based on utilization of polarization effects as they occur in complex environments. The thesis ends with conclusions and suggestions for future work, as per Chapter 7.

CHAPTER 2

Related Work

2.1. Introduction

In this Chapter the fundamentals on localization techniques are presented, while giving emphasis on fingerprint-based methodologies and core positioning algorithms as per Section 2.2. A review of the research work performed in information fusion for the purposes of improving indoor localization accuracy (Section 2.3) is also presented, focusing in three areas: the introduction of map-constraint parameters, the combination of IEEE 802.15.1 and IEEE 802.15.7 wireless technologies and the utilization of polarization mechanisms for positioning purposes. Finally, in Section 2.4 the evaluation methodologies widely used in testing the performance of localization platforms is briefly explored.

2.2. Localization Techniques

The core localization techniques widely used for both indoor and outdoor localization are the following:

(1) **Range-based lateration**, which estimates the location by measuring the distance between the Mobile Station (MS) and a number of Base Stations (BS). In 2D space, this technique requires at least three measurements, while in 3D space four measurements are required. Distance measurements are typically performed by calculating the Time of Flight (TOF) or Time of Arrival (TOA). A more advanced methodology incorporates Time Difference of Arrival (TDOA) between each pair of BS. Received Signal Strength (RSS) attenuation can be also utilized in order to estimate the aforementioned distance.

(2) **Direction-based angulation**, that involves the calculation of the Direction of Arrival (DOA) - or the Angle of Arrival (AOA) - of at least two signals from known locations in a 2D-space scenario.

(3) **Dead reckoning** which estimates the position of a mobile station by using an anchor point or a previously determined position. In this case, the technique uses sensors to calculate distance, speed and/or drift angle data from the known fixed positions.

(4) **Fingerprinting**, which is the most popular technique in indoor positioning. With this technique, location is identified by comparing and matching the signal characteristics of pre-collected data named **fingerprints** with the characteristics of the user real time signals in a specific environment.

All the above techniques can be also combined with, or supported by, information retrieved by heterogeneous technologies. Details on Wireless Indoor Positioning Techniques and Systems can be found in [**18**], [**19**] and [**20**]. A comprehensive analysis in outdoor positioning is provided in [**21**] and [**23**].

2.2.1. Range-based lateration

2.2.1.1. ***RSS Estimation***. It is assumed that the Received Signal Strength typically follows an exponential decay model, which is a function of the transmitted power, the path loss constant and the distance between the source and the receiver. RSS estimation, is based on the calculation of the aforementioned **Path Loss**. Mathematically, path loss is defined as the ratio of the received power P_r to the transmitted power P_t, expressed in dB [**44**] as shown in equation 2.1.

$$PL(dB) = 10\log(\frac{P_r}{P_t}) \tag{2.1}$$

The free space path loss (FSPL) model is derived from the Friis Transmission Formula, according to which, the path loss follows an inverse square law with respect to the distance R between the transmitter and the receiver. The radio propagation loss refers to an obstacle free environment (i.e., Line of Sight (LOS) between the transmitter and the receiver). It also depends on the frequency - or the wavelength λ - and the antenna patterns of both the transmitter and the receiver, which specify the gains G_t and G_r respectively, as per equation 2.2.

$$PL(dB) = 10\log\left(\frac{G_t G_r \lambda^2}{(4\pi)^2 R^2}\right) \tag{2.2}$$

In the case of Free Space Loss (FSL), the model assumes isotropic antennas for both the transmitting and receiving antennas, and therefore the equation is simplified to:

$$FSL(dB) = 10\log\left(\frac{\lambda^2}{(4\pi)^2 R^2}\right) \tag{2.3}$$

or

$$FSL(dB) = 20\log(d) + 20\log(f) - 147.55 \tag{2.4}$$

The FSL model is useful for simple LOS scenarios and for rough preliminary estimations, but is an oversimplified model that fails to provide accurate results in most real life cases. For this reason, other models were developed. Empirical models are based on extensive outdoor measurement campaigns that took place under specific conditions, representing categories of environments that follow similar characteristics [**45**]. Some examples of empirical models are the **Okumura-Hata Model**, working in the frequency range $150MHz - 1.5GHz$ for Tokyo-like cities [**46**], [**47**], the **Cost-231-Hata model**, that is an extension of the Okumura-Hata and covers the frequencies $1500MHz - 2000MHz$ [**48**], and the **Ibrahim and Parsons Model**, which is based on a measurement campaign executed around London [**49**]. Typical semi-empirical models are the **Allsebrook and Parsons**

Model, for suburban predictions and in the frequencies $86MHz$, $167MHz$ and $441MHZ$ [**50**] and **Walfish-Bertoni Model**, that predicts multiple diffraction over building rooftops [**51**].

The aforementioned indicative models, gather a large number of measurements and perform mathematical methods like least squares to extract conversion graphs. As it can be understood, such methods can provide only indications and rough estimations of the RSS values in the outdoor study areas. They usually fail to perform reliably and accurately in complex outdoor environments, in the presence of fast fading and multipath effects.

Extensive research work has been done towards the direction of developing indoor attenuation models that could more accurately calculate the RSS in such complex environments [**52**], [**53**], [**54**]. The *large-scale attenuation model*, was the basis for many proposed models. This model calculates the radio propagation path loss as a function of an *attenuation exponent* α as indicated in equation 2.5. P_d is the power at distance d from the transmitter and P_{d_0} is the power at a reference distance of $1m$. α typically receives a value of 2 for free space scenarios and may increase up to 5 in an indoor environment. An implementation example can be found in [**55**], where by setting $n = 2.6$, researchers managed to achieve an average difference of $3.0dB$ between measurements and estimates, in their specific study area.

$$P_d[dB] = P_{d_0}[dB] - 10\alpha \log\left(\frac{d}{d_0}\right) \tag{2.5}$$

Hence, in lognormal form, the average power received by the lth sensor, denoted as $P_{r,l}$ is expressed as:

$$\ln(P_{r,l}) = \ln(K_l) + \ln(P_t) - \alpha \ln(d_l) + n_{RSS,l} \tag{2.6}$$

where $l = 1, 2, \ldots, L$, with $L \geq 3$ and α are known a priori. K_l accounts for all factors that affect the received power, including antenna gain and height. $n_{RSS,l}$ is the disturbance, which for simplicity is assumed to be zero-mean uncorrelated Gaussian process with variance $\sigma^2_{RSS,l}$.

If the range measurement $r_{RSS,l}$ is set as:

$$r_{RSS,l} = \ln(P_{r,j}) - \ln(K_l) - \ln(P_t) \tag{2.7}$$

then the RSS signal model can be expressed as:

$$r_{RSS,l} = -\alpha \ln(d_l) + n_{RSS,l} \tag{2.8}$$

And can be converted in a vector form:

$$\vec{r_{RSS}} = \vec{f_{RSS}}(\vec{x}) + \vec{n_{RSS}} \tag{2.9}$$

where

$$\vec{r_{RSS}} = [\vec{r_{RSS,1}}, \vec{r_{RSS,2}}, \ldots \vec{r_{RSS,L}}]^T \tag{2.10}$$

$$n_{\vec{RSS}} = [n_{\vec{RSS},1}, n_{\vec{RSS},2}, \dots n_{\vec{RSS},L}] \tag{2.11}$$

and

$$f_{\vec{RSS}}(\vec{x}) = \vec{p} = -\alpha \begin{bmatrix} \sqrt{(x-x_1)^2 + (y-y_1)^2} \\ \sqrt{(x-x_2)^2 + (y-y_2)^2} \\ \vdots \\ \sqrt{(x-x_L)^2 + (y-y_L)^2} \end{bmatrix} \tag{2.12}$$

The calculation of the Probability Density Function (PDF) for $r_{\vec{RSS}}$, denoted as $p(r_{\vec{RSS}})$, is then performed by the following formula:

$$p(r_{\vec{RSS}}) = \frac{1}{(2\pi)^{L/2}|C_{\vec{RSS}}|^{1/2}} \exp\left(-\frac{1}{2}(r_{\vec{RSS}} - \vec{p})^T C_{\vec{RSS}}^{-1}(r_{\vec{RSS}} - \vec{p})\right) = \tag{2.13}$$

$$= \frac{1}{(2\pi)^{L/2}\prod_{l=1}^{L}\sigma_{RSS,l}} \exp\left(-\frac{1}{2}\sum_{l=1}^{L}\frac{(r_{\vec{RSS},l} + \alpha\ln(d_l))^2}{\sigma_{RSS,l}^2}\right) \tag{2.14}$$

where $C_{\vec{RSS}} = diag\left(\sigma_{RSS,1}^2, \sigma_{RSS,2}^2, \dots, \sigma_{RSS,L}^2\right)$

All the above RSS measurement models are based on a number of assumptions and include several parameters. In scenarios where accuracy is critical, the researchers should use *radio deterministic models*. Deterministic models implement electromagnetic formulas and numerical methods (such as Ray Tracing) to a site-specific environmental description [**56**].

Ray Tracing is the dominant deterministic technique used to predict propagation effects in wireless communication environments. It is based on Geometrical Optics (GO) and its extension, Uniform Theory of Diffraction (UTD). Ray tracing can be easily applied for approximately predicting a high-frequency electromagnetic field. It is used to identify all the possible ray paths between the transmitter and possible receiver locations and uses high-frequency electromagnetic theory to calculate the amplitude, phase, delay and polarization of each ray.

As mentioned earlier, GO is the basis of RT. It assumes an infinite frequency for the propagating signal in such a way so as to consider all the propagating energy to be contained inside very thin tubes, called rays [**57**]. Using this theory the reflected and transmitted fields can be determined. However, this theory is subject to assumptions [**58**]:

(1) Waves are locally plane to the points of interaction.
(2) Wavelength is small compared to the distance between the source and the first interactions along each ray path and the distance between individual interactions.
(3) Surfaces are large compared to the wavelength of transmission.
(4) Curvature of surfaces is small compared to the wavelength.

However, by utilizing the Geometric Optics theory it is not possible to predict diffraction over obstructions because it fails to account for the energy that propagates into the shadowing regions For this reason, the RT method has included the UTD. Based on these techniques, a ray obliquely incident upon the edge of an obstruction at an angle β to the edge, produces a cone (Keller cone) of diffracted rays having a semi-angle β. Ray Tracing is a method implemented in *TruNET wireless* 3D polarimetric deterministic simulator [**12**], which is heavily utilized in generating all the study area *radiomaps* for evaluating all the positioning methodologies proposed in this thesis.

2.2.1.2. *TOA and TDOA Estimation.* TOA is the propagation time that a signal requires to travel from a transmitter to a receiver [**20**]. By accurately measuring TOA and multiplying with the speed of light, we can calculate the distance between the transmitter and the receiver. However, the practical implementation of Time-based localization technique, requires accurate estimation of the signal propagation delay, hence high resolution clock synchronization between all nodes and mobile user equipment [**59**]. Additionally, multipath effects can generate large localization errors, restricting the reliable implementation of such a technique to only Line of Sight (LOS) scenarios.

For a 2D TOA positioning three transmitters are required, as shown in the simplified TOA positioning concept of figure 2.1. The position of the user, lies within the area where all circles overlap.

The localization problem, as analyzed in [**20**], is solved as follows: It is assumed that $\vec{X} = [x, y]^T$ is the unknown user position, while $\vec{X_l} = [x_l, y_l]^T$ are the known coordinates of the l^{th} receiver, where $l = 1, 2, \ldots, L$ and $L \geqslant 3$. The distance between the user and the l^{th} sensor, denoted by d_l, is given by:

$$d_l = \|\vec{X} - \vec{X_l}\|_2 = \sqrt{(x - x_l)^2 + (y - y_l)^2} \tag{2.15}$$

With no loss of generality, it is assumed that the source emits a signal at time 0 and the l^{th} receiver receives it at time t_l; which means that t_l are the measured times which have the following relationship with the d_l:

$$t_l = \frac{d_l}{c}, l = 1, 2, \ldots, L. \tag{2.16}$$

In practice, range measurements $r_{\vec{TOA}}$ include the inherent errors of the technique as explained earlier and are denoted as $n_{\vec{TOA}}$. Hence, the range measurement is the sum of the actual distance d_l as given by equation 2.15, but in a vector form, plus the error $n_{\vec{TOA}}$. In a vector form the above concept is expressed as follows:

$$r_{\vec{TOA}} = f_{\vec{TOA}}(\vec{X}) + n_{\vec{TOA}} \tag{2.17}$$

where

$$n_{\vec{TOA}} = [n_{\vec{TOA},1}, n_{\vec{TOA},2}, \ldots, n_{\vec{TOA},L}]^T \tag{2.18}$$

$$r_{\vec{TOA}} = [r_{\vec{TOA},1}, r_{\vec{TOA},2}, \ldots, r_{\vec{TOA},L}]^T \tag{2.19}$$

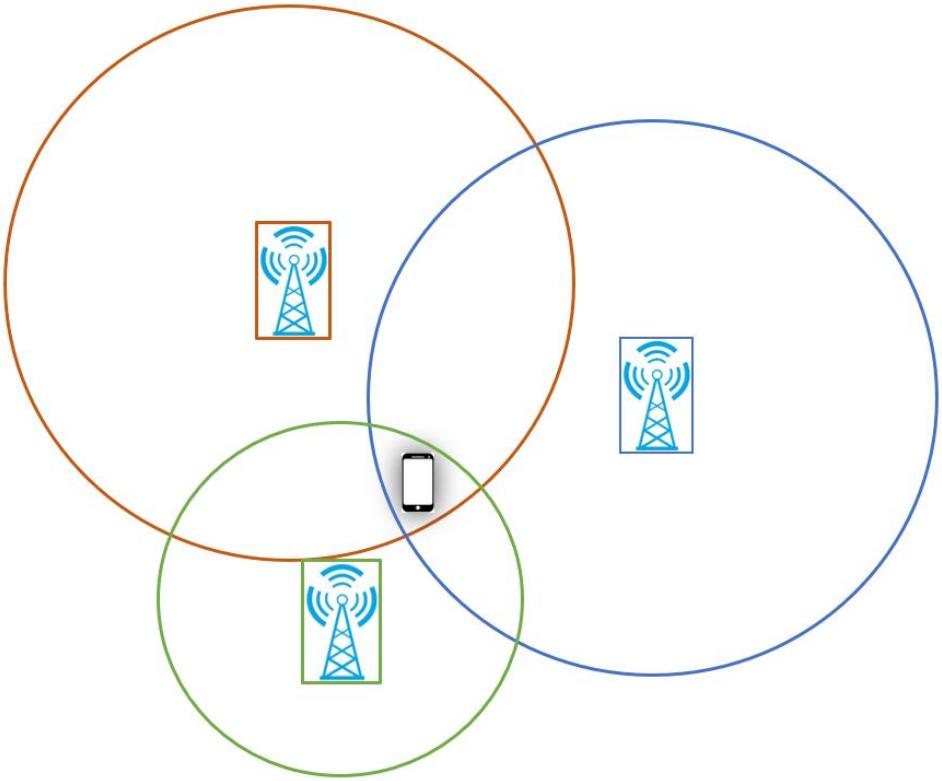

Figure 2.1 – TOA Localization Technique

and

$$f_{TOA}(\vec{x}) = \begin{bmatrix} \sqrt{(x-x_1)^2 + (y-y_1)^2} \\ \sqrt{(x-x_2)^2 + (y-y_2)^2} \\ \vdots \\ \sqrt{(x-x_L)^2 + (y-y_L)^2} \end{bmatrix} \tag{2.20}$$

The calculation of the Probability Density Function (PDF) for each $R_{TOA,i}$ is calculated by formula 2.21:

$$p(r_{TOA,i}) = \frac{1}{\sqrt{2\pi\sigma^2_{TOA,i}}} \exp\left[-\frac{1}{2\sigma^2_{TOA,i}}\left(r_{TOA,i} - d_i\right)^2\right] \tag{2.21}$$

Node and user device synchronization issues can be overcome if time difference of arrival (TDOA) between all pairs of nodes is implemented. However, the synchronization between the nodes themselves is still required. Each calculated TDOA forms a hyperbola in the localization space and the intersection of all hyperbolas represents the possible location of the mobile terminal. The TDOA measurement method can be formulated [**20**] in the following way. Assuming that the

source emits a signal at an unknown time t_0 and the l^{th} receiver receives it at time $t_l, l = 1, 2, \ldots, L$ with $L \geqslant 3$, there are $\frac{L(L-1)}{2}$ distinct TDOAs from all possible receiver pairs, denoted by $t_{k,l} = (t_k - t_0) - (t_l - t_0) = t_k - t_l$, where $l = 1, 2, \ldots, L$ with $k > l$. The solution of TDOA is similar to the TOA as described previously.

Summing up, TOA and TDOA localization is a popular technique for outdoor scenarios where a LOS condition can be ensured. The most known and popular implementation is a GNSS systems, which utilize a number of satellites and embed a high accuracy clock.

2.2.2. DOA Estimation

DOA localization technique is based on the measurement of the arrival angles of the transmitted signal from the source, as this is observed at the receiver [**20**]. Hence, by determining the direction of propagation of a signal and its angle of arrival at a minimum of two nodes, the location of the user can be estimated, as illustrated in figure 2.2.

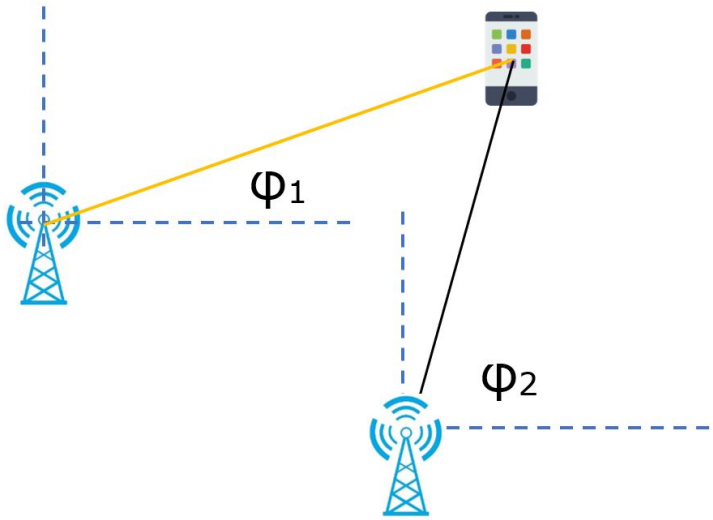

Figure 2.2 – DOA Localization Technique

The mathematical model of DOA method is based on the geometrical formula of angle ϕ_l, which represents the DOA between the source and the l^{th} receiver [**20**]:

$$\tan(\phi_l) = \frac{y - y_l}{x - x_l}, l = 1, 2, \ldots, L \tag{2.22}$$

with $L \geqslant 2$.

As in the case of TOA, during DOA measurements denoted as $r_{DOA,l}$, an error $n_{DOA,l}$ is included, which occurs from noises (assumed to be zero) mean

uncorrelated Gaussian processes with variances $\sigma^2_{DOA,l}$. In this case $r_{DOA,l}$ can be expressed by equation 2.23:

$$r_{DOA,l} = \phi_l + n_{DOA,l} = \tan^{-1}\left[\frac{y - y_l}{x - x_l}\right] + n_{DOA,l}, l = 1, 2, \ldots, L \tag{2.23}$$

Vector wise, 2.23 can be re-written as:

$$r_{\vec{DOA}} = f_{\vec{DOA}}(\vec{x}) + n_{\vec{DOA}} \tag{2.24}$$

where

$$n_{\vec{DOA}} = [n_{\vec{DOA},1}, n_{\vec{DOA},2}, \ldots, n_{\vec{DOA},L}]^T \tag{2.25}$$

$$r_{\vec{DOA}} = [r_{\vec{DOA},1}, r_{\vec{DOA},2}, \ldots, r_{\vec{DOA},L}]^T \tag{2.26}$$

and

$$f_{\vec{DOA}}(\vec{x}) = \vec{\phi} = \begin{bmatrix} \tan^{-1}\left(\frac{y-y_1}{x-x_1}\right) \\ \tan^{-1}\left(\frac{y-y_2}{x-x_2}\right) \\ \vdots \\ \tan^{-1}\left(\frac{y-y_L}{x-x_L}\right) \end{bmatrix} \tag{2.27}$$

Typical examples of methods that are based on DOA are: (i) Delay and Sum (DAS) [**60**] which is a spatial spectral estimation method and (ii) Multiple Signal Classification (MUSIC) [**61**] which is an eigenstructure method. A more recent work where DOA technique was utilized ispresented in [**62**]. In this approach, authors proposed the utilization of sectorized antennas instead of antenna arrays. They introduced a DOA estimator that is broadly applicable with different sectorized antenna types and signal wave-forms, and has low computational complexity. Finally, taking advantage of the technological evolution, researchers in [**60**] introduced hardware novelties, such as Software Defined Radios (SDRs) and/or propose the fusion of multiple DOA techniques in order to combine the benefits of each category.

Summing up, although the DOA-based localization technique does not require clock synchronization, has several challenges to overcome, such as the requirement for sophisticated antenna arrays and NLOS conditions, especially in indoor environments.

2.2.3. Dead Reckoning

Dead reckoning is the technique of estimating the position of a mobile station by using an anchor point or a previously determined position. The estimation is performed considering a number of parameters, such as the speed and direction of movement of the user, etc.

Systems implementing dead reckoning typically use sensors on the user's device to estimate relative, rather than absolute location (i.e., the change in position since the last update), by knowing angle $\theta_i[^\circ]$ and distance $r_i[m]$, as shown in Figure 2.3. The infrastructure requirements are nil or minimal, but the localization

error accumulates with time. For this reason they are usually combined with other localization techniques and work supportively, exchanging and retrieving information for correcting the relative location [**63**].

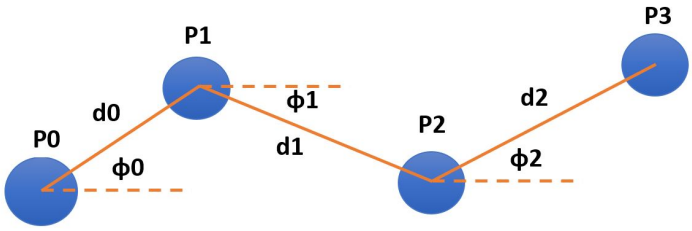

Figure 2.3 – Dead Reckoning Technique

With the sensors and processing nodes getting smaller and more affordable, several solutions have been proposed for Pedestrian Dead Reckoning (PDR) systems, especially for indoor tracking. These use inertial and other sensors, often combined with domain-specific knowledge about walking, to track user movements. There is currently rich research and relevant literature, which is summarized in [**63**]. From the aforementioned survey, the work done in [**64**] is highlighted, where researchers fused data retrieved from dead reckoning sensors using the extended Kalman filter (EKF) algorithm, in a *multi-robot distributed cooperative localization method*. In this way, the authors aim to correct the accumulative error of the dead reckoning. In another approach, authors of [**65**] propose an effective indoor localization method for automated guided vehicles (AGVs), utilizing dead reckoning while eliminating its inherent drawbacks, based on an encoder, and particle filters, based on a 2D laser range finder. The proposed method involves an asynchronous localization algorithm. Finally, in [**66**], authors presented a smartphone-based pedestrian dead reckoning system, which uses data from inertial sensors embedded in off-the-shelf smart-phones, without the support from any other infrastructure or system.

2.2.4. Fingerprinting

As briefly explained in Chapter 1, Section 1.2, fingerprinting is a localization technique, where the Mobile User (MU) device, through a dedicated positioning application, retrieves the RSS values from all surrounding nodes, and "attempts" to find the best match from a number of pre-existing RSS values - called *fingerprints*. *Fingerprints* are recorded beforehand and stored in a database. For the prediction of the best match and consequently the real time location estimation of the user, the application utilizes numerous mathematical algorithms.

It can be easily understood that, for the aforementioned procedure to be executed, two phases are required: (i) the offline phase, and (ii) the online phase, as indicated in Figure 2.4. During the offline phase, a set of fingerprints is collected from predetermined locations and recorded in a database, together with the information of the transmitting nodes (usually the MAC addresses), their location

coordinates and any other supportive information. Such databases are named ***radiomaps***. During the second online phase, initially the MU scans the area and identifies all the existing transmitters within range. It then collects the real time RSS values and implements the positioning algorithm, which is either deterministic or statistical. The task of such an algorithm is to find the best match of the current online RSS value set, retrieved from all nodes, with the fingerprint sets that exist in the *radiomap*. In this way location estimation is performed.

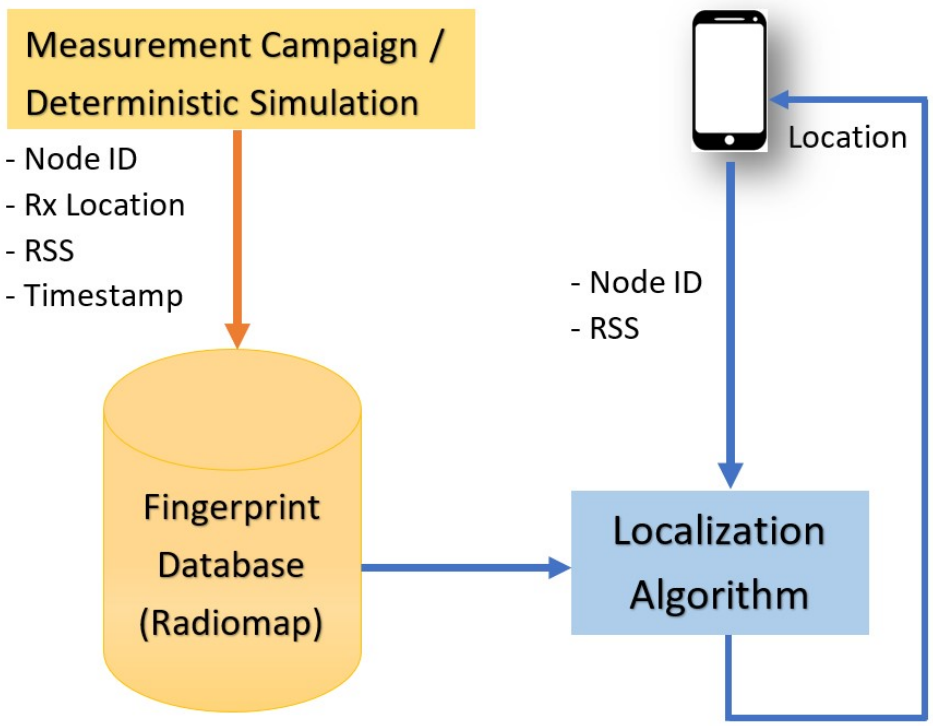

Figure 2.4 – Fingerprinting Concept

2.2.4.1. ***Radiomap Generation.*** In the literature, two map generation methods are used during the offline phase; actual measurements and utilization of simulation tools. The actual measurements method is extremely time consuming, costly and more difficult to maintain, since the radiomaps produced are static. In other words, in case of changes in the environment setup, new measurements must be taken. For the execution of a measurement campaign, special equipment can be used, such as spectrum analyzers, or typical smart devices which have the necessary data collection application installed. Examples of this method can be found in [**67**] and [**68**]. The simulated map generation method is faster and much easier to maintain. During this procedure, the indoor environment is created in a simulator and different radio propagation models are used to generate the RSS fingerprints. Examples include the adoption of *2D Ray Tracing (RT)* models in [**69**] and [**70**], and full *3D Ray Tracing Models* in [**71**], [**1**] and [**2**]. The

3D RT algorithm typically utilizes the 3D electromagnetic formulation of reflection, refraction and diffraction based on the Uniform Theory of Diffraction (UTD).

In both cases, a reliable calibration procedure is required in order to achieve device diversity matching. The calibration challenge is investigated in more detail in Chapter 3.

2.2.4.2. ***Fingerprint–based Positioning Algorithms***. Fingerprint–based positioning using RSS can be classified into two main categories (1) Deterministic and (2) Probabilistic approaches. The *deterministic* positioning methods estimate location as a convex combination of the reference locations [**72**]. Usually, the K reference locations with the shortest distance between $\overline{r}_i$ and s in the n-dimensional RSS space are used and the estimated location $\widehat{\ell}$ is given by

$$\widehat{\ell} = \sum_{i=1}^{K} \left(\frac{w_i}{\sum_{j=1}^{K} w_j} \ell'_i \right). \tag{2.28}$$

The set $\{\ell'_1, \ldots, \ell'_l\}$ denotes the ordering of reference locations with respect to increasing distance between the respective fingerprint $\overline{r}_i$ and the observed measurement during positioning s, i.e., $\|\overline{r}_i - s\|$. The distance can be calculated using standard norms, such as the Manhattan (1-norm) [**73**], the Euclidean (2-norm) [**67**], the general p-norm with modifications [**74**] or the Mahalanobis norm that employs the sample means and variances of the reference fingerprint [**75**].

One possible option for the non–negative weights w_i in Eq. (2.28) is the inverse of $\|\overline{r}_i - s\|$ and in this case the positioning method is known as Weighted K-Nearest Neighbour (WKNN) [**73**]. The K-Nearest Neighbour (KNN) method assumes equal weights for the candidate reference locations, while setting $K = 1$ leads to the simple Nearest Neighbour (NN) method [**67, 76, 77**]. In general, the KNN and the WKNN methods have been reported to provide higher level of accuracy compared to the NN method, particularly with parameter values $K = 3$ and $K = 4$ [**67, 73**]. However, if the density of the RSS radio map is high, NN method performs equally well compared to more complicated methods [**72**]. Several variants of the KNN method have been discussed in the literature, including the Database Correlation Method (DCM) which introduces an additional term in the error function to penalize missing RSS values in the fingerprints [**78, 79**].

In probabilistic methods, location ℓ can be estimated by calculating and maximizing the conditional posterior probabilities $p(\ell_i|s),\ i = 1, \ldots, l$ given an observed fingerprint s and a fingerprint database (l is the number of fingerprints in the database). These methods have been extensively used in the Maximum A Posteriori (MAP) approach [**80, 81, 82**] and the Minimum Mean Square Error (MMSE) approach [**68**] to estimate the expected value of ℓ.

The posterior probability $p(\ell_i|s)$ is obtained by applying Bayes' rule:

$$p(\ell_i|s) = \frac{p(s|\ell_i)p(\ell_i)}{\sum_{i=1}^{l} p(s|\ell_i)p(\ell_i)} \tag{2.29}$$

where $p(s|\ell_i)$ is a conditional probability calculated through statistics at the survey stage and $p(\ell_i)$ is the a–priori probability, a weighting factor based on the probability distribution of the target over the reference position candidates (database fingerprints). If we assume that we do not have any prior knowledge then this *prior* can be assumed to be unity providing equal a-priori probability to all the fingerprint candidates in the database.

2.3. Information Fusion in Indoor Positioning

2.3.1. Map Information Extraction

Most of the work carried out in the direction of utilizing map information for indoor positioning purposes, is related to the robotics area and the enhancement of the respective mobility models. In this scope, Liao et al. in [**83**] and Evennou et al. in [**84**] proposed the use of particle filters to make use of the inherent structure of indoor environments. In order to simplify the calculation complexity of the unconstrained particle filters, they suggested the estimation of the locations of people based on the Voronoi graph of the environment. By restricting particles to a graph, they achieved a more efficient algorithm and at the same time simulated a basic human motion in the indoor environment.

In the work presented in Chapter 4, instead of adopting the Voronoi graphs and particle filters, the frequent –or most probable– routes are defined, based on observations. The recording of the *frequent routes* based on simple observations, can be replaced by the adoption of supervised or unsupervised learning techniques. As the names suggest, in the case of supervised learning, the researcher must involve some supervision by an external source in order to improve the algorithm, while in the case of unsupervised learning, the algorithm will self-evolve, and gradually achieve a very representative snapshot of the most frequently used routes.

2.3.2. Retrieving Information from IEEE 802.15.1 Technology

Bluetooth Low Energy was introduced as part of Bluetooth 4.0 specifications, allowing devices to support both BLE and classic Bluetooth protocols simultaneously [**85**]. The power efficiency of Bluetooth was especially created for IoT applications. It allows devices to run for long periods of time on extremely low power sources, such as coin-cell batteries or energy-harvesting devices.

BLE operates at $2.4\,GHz$ and uses Gaussian Frequency Shift Key (GFSK) modulation in 40 channels of $2\,MHz$ each. Three of the channels, called "advertising channels", are used to ensure connectivity with other nodes, while the remaining 37, are the "data channels". BLE has a range of around $100m$ in an outdoor environment, a maximum data rate of $1\,Mbps$ and an application throughput of up to $305\,kbps$ [**85**]. Lastly, it supports point-to-point and mesh networks.

iBeacon was developed by Apple in order to provide a higher level of location awareness, by utilizing BLE technology. iBeacon is a cross platform technology for both Android and iOS devices which are able to support the BLE standard [**86**]. Devices, acting as beacons, generate iBeacon advertisements through which

they establish a region around them. Android and iOS mobile devices receiving the advertisements can determine the entrance and exit border from each beacon's region, estimate the nearest beacon and approximate the distance between the two devices. The aforementioned advertisements contain three identifying fields, as described in [**87**]:

- **UUID:** Universally Unique Identifier, is a 128-bit integer used as an ID for all beacons in an application
- **Major:** is a 16-bit integer, used to differentiate Beacons with the same UUID.
- **Minor:** is a 16-bit integer, used to further differentiate Beacons that have the same UUID and Major values.

Due to their design philosophy, iBeacons are flexible in deployment and can be used in mobile objects or to temporarily define a region and sub-regions.

The possibilities introduced by BLE and iBeacon technologies in indoor positioning, are currently a topic of investigation from the research community. The authors of [**88**] proposed a software framework which can be used to automate IoT applications based on the proximity, which is triggered by AltBeacon devices. AltBeacon is an open and interoperable specification that defines the format of the advertisement message that BLE proximity beacons broadcast. In [**89**], InLoc is introduced, which is a positioning and tracking system using commercial mobile devices, with navigation (routing) capability. With InLoc, authors propose, among others, a method for independent fusion of location information from a smart phone's Inertial Measurement Unit (IMU) sensors and BLE beacons.

In [**90**], the authors propose a solution for the creation of study groups in future smart libraries, featuring a smart phone application to create study groups and a hybrid BLE and Wi-Fi indoor positioning system. Their hybrid indoor positioning system calculates two probable user locations every time, utilizing each technology separately, compares the estimated conditional probabilities and selects the most reliable. Following a different approach, researchers in [**91**] assume a very dense IoT environment with BLE compatible devices and propose an Iterative Weighted KNN (IW-KNN) indoor localization method based on the RSS of the BLE, which has a low power consumption and hence long life expectancy. Finally, a combination of Wi-Fi and BLE fingerprints was implemented in [**92**], utilizing the conventional WKNN algorithm. The test case included the deployment of 17 Estimote BLEs on top of the existing Wi-Fi network, in a study area of $52m$ x $43m$. Positioning was performed by utilizing both BLE and Wi-Fi RSS fingerprints, resulting in a 23% accuracy improvement of the RTLS system.

A different and novel approach is proposed in Chapter 5, Section 5.4.3, where IEEE 802.15.1 technology is utilized in a filtering algorithm that creates a subset of fingerprints from the initial IEEE 802.11 *radiomap*. In this way errors are minimized and computational speed is improved.

2.3.3. Retrieving Information from IEEE 802.15.7 Technology

A Visible Light Positioning (VLP) system is graphically illustrated in Figure 2.5. It consists of a transmitter (Tx_{SL}) which is the Smart Light, the receiver (Rx) which is the mobile station (user smart phone, wearable device with a light sensor etc.) and the environment [**93**]. The transmitter emits at a power P_{SL} which follows a certain radiation pattern ($R_E(\phi_i)$). The encoded light follows the well known optical geometry, i.e travels in a direct path (LOS), reflects, diffracts or scatters on different obstacles and falls onto the receiver (NLOS). In the case of indoor positioning, the channel can be considered flat, since no high data rates are expected in the case of VLP, making the channel response more simple and taking into consideration only the LOS paths [**31**], [**94**]. The mobile station is equipped with either a photodiode or an image sensor that converts the optical signal back to an electrical signal. The received power P_R depends on the transmitted power PTx and radiation pattern $R_E(\phi_i)$, the AOA (θ_i), the Active Area (A_R) related to the FOV and clear ceiling-user height hcl and the spectral response. If an optical concentrator ($G(\theta_i)$, or optical filter ($T(\theta_i)$) exists in the receiver, it is taken into consideration. The aforementioned relations are expressed with the following formulas:

$$P_R = \frac{P_{Tx}}{d^2} R_E(\phi_i) T(\theta_i) G(\theta_i) A_R \cos(\theta_i) \tag{2.30}$$

and

$$d = \sqrt[4]{\frac{P_{Tx}}{P_R} \frac{h^2}{\pi} A_R} \tag{2.31}$$

In order to achieve accurate localization in VLP systems, the mobile station must be able to receive and process signals from multiple smart lighting sources. This fundamental requirement is the origin of most of the challenges in this specific research area. Several methods have been investigated depending on whether the mobile station uses an image sensor or a single photodiode. In the case of image sensor, each smart light can be processed by a different part of the sensor, without any synchronization requirements. Hence, Spatial Division Multiple Access (SDMA) can be used [**95**], [**96**]. On the other hand, in the case of a single photodiode, either the Time Division Multiple Access (TDMA) is implemented [**97**] or the Frequency Division Multiple Access (FDMA) [**93**]. TDMA requires synchronization in order to manage the time slots of every smart light communication channel and both RSS and TOF parameters can be utilized for positioning. FDMA does not require any backbone since each smart light is allocated a specific carrier frequency, but only the RSS can be used. Code Division Multiple Access (CDMA) is another option, where every smart light is assigned a unique sequence to encode its information. However, several interference issues occur due to the fact that none of the used codes are fully orthogonal [**98**].

The aforementioned methods, although they benefit from the inherent properties of the Visible Light Communication (VLC), at the same time they suffer from the physical propagation constraints of light and from technological limitations. Technological challenges faced, are related to low sample rate processing capabilities

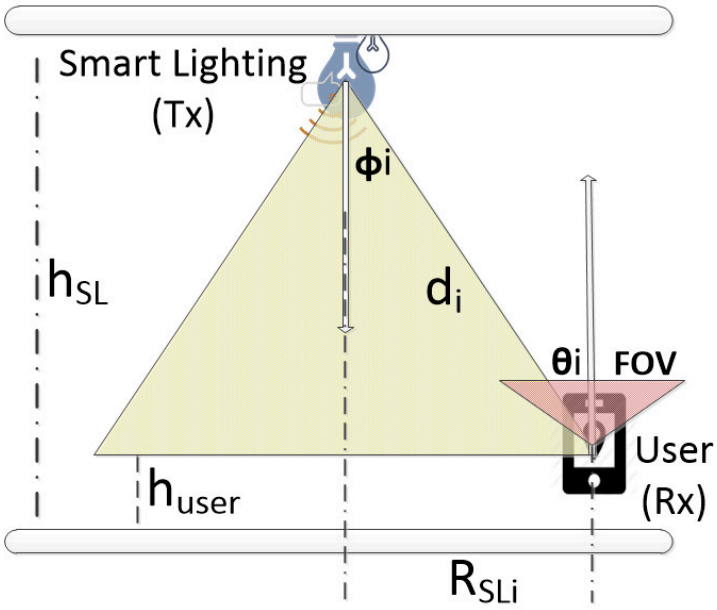

Figure 2.5 – Angles ϕ and θ to compute channel impulse response and SL Radius

of the commercial image sensors, high processing power requirements, increased power consumption, necessity for dense smart light grids and/or expensive dedicated infrastructure for synchronization purposes [**31**].

2.3.4. Utilizing Polarization Effects

2.3.4.1. ***Polarization Mechanisms.*** Before investigating the related research work performed in the area of utilizing polarization for localization purposes, a brief explanation on how the polarization mechanism works and how it may affect the indoor positioning accuracy, is first given.

Polarization is the alignment of the axis of the electric field $\overrightarrow{E}$ oscillation, relative to the direction of propagation. Such an alignment, can sometimes be parallel to one of the two planes of a typical orthogonal system, providing a vertically or a horizontally polarized wave. In these two cases the electric field has a single direction of oscillation along the direction of propagation and the waves are described as linearly polarized. If two plane waves of the same frequency, unequal magnitude and a phase difference of 90° are combined, the result is a wave of elliptical polarization; if the magnitude of these waves is equal, then the combined wave becomes circularly polarized. Electric field and magnetic field $\overrightarrow{H}$ are transverse waves, meaning that their plane waves are perpendicular to the direction of wave propagation. They are also perpendicular to each other.

Focusing on the electric field, it can be expressed using a complex expression as a function of time t and spatial position z, as per equation 2.32:

$$\overrightarrow{E}(z,t) = \begin{bmatrix} e_x \\ e_y \\ 0 \end{bmatrix} e^{i2\pi(\frac{z}{(\lambda\backslash n)} - (t\backslash T))} = \begin{bmatrix} e_x \\ e_y \\ 0 \end{bmatrix} e^{(kz-\omega t)} \tag{2.32}$$

where $\lambda\backslash n$ is the wavelength in a medium whose refractive index is $n = \sqrt{\epsilon\mu}$, $T = 1\backslash f$ is the period of the wave and e_x, and e_y, are complex numbers. In the second part of the equation, the electric field is described using the wavenumber $k = 2\pi n/\lambda$ and angular frequency $\omega = 2\pi f$.

All the different polarization states of the electric field can be represented by a compound electric field composed of x- and y-linearly polarized plane waves as in equation 2.33:

$$\overrightarrow{E} = \overrightarrow{E_x}\hat{\chi} + \overrightarrow{E_y}\hat{\psi} \tag{2.33}$$

In order to understand the importance of polarization effects in indoor environments, we recall the basic principles of radio propagation that whenever a propagating wave impinges on an obstruction, its amplitude, phase, direction and polarization will change. For the calculation of the kinematic properties of the wave, *Snell's Law of reflection and refraction* is applied. The dynamic properties, such as amplitude, phase, polarization and the *Fresnel Reflection (R) and Transmission (T) Coefficients* need to be considered as per the following formulas:

$$E_r = RE_i \tag{2.34}$$

and

$$E_t = TE_i \tag{2.35}$$

where E_i is the incident electric field, E_r is the reflected electric field and E_t is the transmitted electric field. The calculation of the reflection and transmission coefficients can be performed by utilizing the Boundary Model, the Single Slab Model or the Multi-layer Model.

The Boundary Model [**58**] assumes that the two media are semi-infinite as shown in figure 2.6. It can be observed that, although the angle of incidence of the rays is kept the same in both sub-figures, the direction of the electric field vector is different, depending solely on the polarization. Such a mechanism influences the RSS value calculation in all possible mobile user locations that fall within the path of the wave. The Fresnel Coefficients of reflection and refraction which need to be calculated, depend on the constitutive parameters of the materials, the wave angle of incidence and its polarization. At this point, it is critical to highlight that each of the two polarization cases should be considered separately, since the Fresnel Coefficients vary significantly with respect to polarization. The two cases are the horizontal or transverse electric (TE) polarization, where the electric field vector is perpendicular to the plane of incidence, and the vertical or transverse magnetic (TM) polarization where the electric field vector is parallel to the plane of incidence. The Fresnel Coefficients for dielectric materials are given by the following formulas:

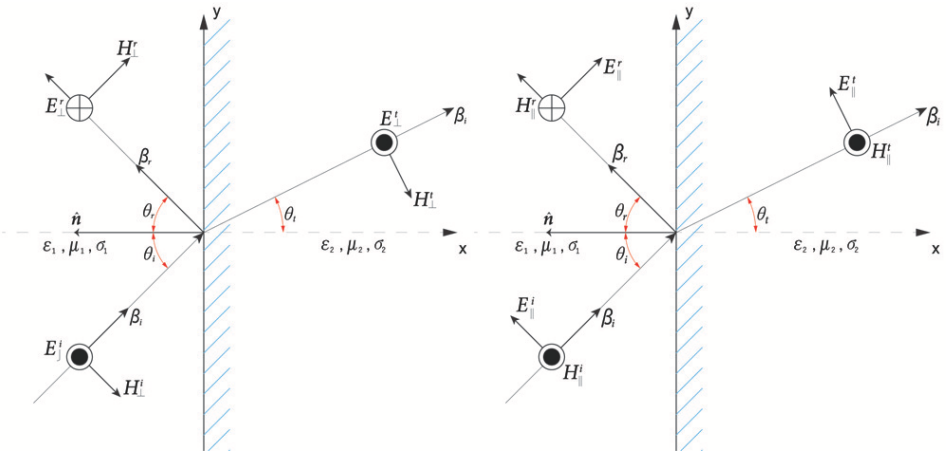

(a) Horizontal **(b)** Vertical

Figure 2.6 – Boundary Layer Model - Horizontal and Vertical polarization

$$R_\perp = \frac{\cos(\theta_i) - \sqrt{\frac{\epsilon_2}{\epsilon_1}}\sqrt{1 - \frac{\epsilon_1}{\epsilon_2}\sin^2(\theta_i)}}{\cos(\theta_i) + \sqrt{\frac{\epsilon_2}{\epsilon_1}}\sqrt{1 - \frac{\epsilon_1}{\epsilon_2}\sin^2(\theta_i)}} \tag{2.36}$$

$$T_\perp = \frac{2\cos(\theta_i)}{\cos(\theta_i) + \sqrt{\frac{\epsilon_2}{\epsilon_1}}\sqrt{1 - \frac{\epsilon_1}{\epsilon_2}\sin^2(\theta_i)}} \tag{2.37}$$

$$R_\parallel = \frac{-\cos(\theta_i) - \sqrt{\frac{\epsilon_1}{\epsilon_2}}\sqrt{1 - \frac{\epsilon_1}{\epsilon_2}\sin^2(\theta_i)}}{\cos(\theta_i) + \sqrt{\frac{\epsilon_1}{\epsilon_2}}\sqrt{1 - \frac{\epsilon_1}{\epsilon_2}\sin^2(\theta_i)}} \tag{2.38}$$

$$R_\parallel = \frac{2\sqrt{\frac{\epsilon_1}{\epsilon_2}}\cos(\theta_i)}{\cos(\theta_i) + \sqrt{\frac{\epsilon_2}{\epsilon_1}}\sqrt{1 - \frac{\epsilon_1}{\epsilon_2}\sin^2(\theta_i)}} \tag{2.39}$$

The aforementioned formulas can be used for lossy media ($(\sigma/2\pi f\epsilon)^2 >> 1$), if ϵ is replaced by its complex value $\epsilon_{complex}$:

$$\epsilon_{complex} = \epsilon_r(1 - j\tan\delta) \tag{2.40}$$

where $\tan\delta$ is the loss tangent:

$$\tan\delta = \frac{\sigma}{2\pi f\epsilon_r\epsilon_0} \tag{2.41}$$

Moving a step further, it is understood that the obstructions are not semi-infinite in a real environment. For this reason, the Single Slab Model [**99**] is utilized for providing more realistic results, by taking into consideration the thickness of the media. This mechanism is preferable for fully deterministic radio propagation modelling, and this is one of the models implemented in *TruNET wireless* simulator

[**12**], which is chosen for the experiments. This model assumes that multiple interactions exist between the incident ray and the two facets of the obstruction, as shown in Figure 2.7.

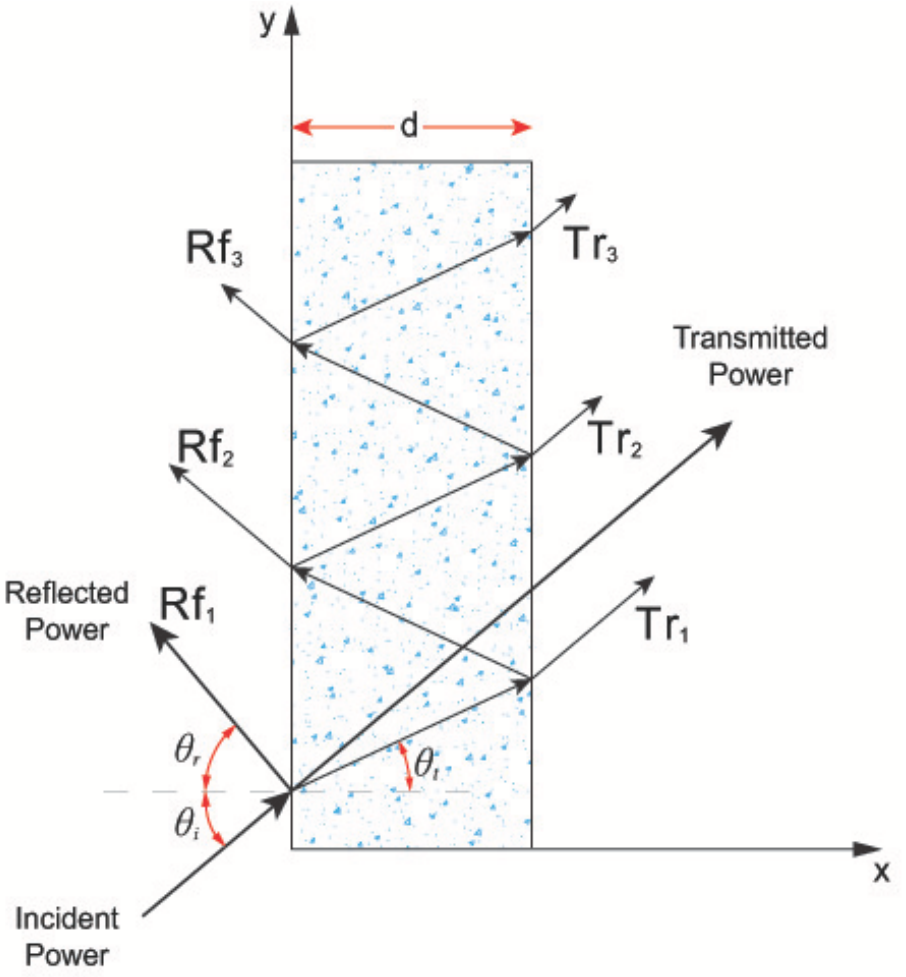

Figure 2.7 – Single Slab Model

Taking into consideration the multiple interactions, the total transmission and total reflection coefficients, are finally influenced by the phase delay of the field in a single crossing of the layer ϕ_d and the phase difference between adjacent rays leaving the layer ϕ_α, as per Formula 2.42:

$$T = \frac{(T_1 T_2 \sum_{i=1}^{n} (\phi_\alpha^{2i} \phi_d^{i-1} R_2^{2i})}{\phi_\alpha R_2^2} \tag{2.42}$$

Expanding 2.42, authors in [**100**] proved that:

$$T = \frac{(1 - \acute{R}^2)e^{-j(\delta - k_0 d)}}{1 - \acute{R}^2 e^{-j2\delta}} \tag{2.43}$$

and

$$R = \frac{1 - e^{-j2\delta}}{1 - \acute{R}^2 e^{-j2\delta}} \acute{R} \tag{2.44}$$

where

$$\delta = \frac{2\pi d}{\lambda} \sqrt{\epsilon_{complex} - \sin^2(\theta_i)} \tag{2.45}$$

and $k_0 = 2\pi/\lambda$, λ is the free space wavelength and $\epsilon_{complex}$ is the complex relative permittivity and d is the thickness of the material. $\acute{R}$ is then replaced by the respective Fresnel equations, depending on the polarization (vertical or horizontal).

Summarizing the theoretical background of this subsection, it was shown that for each wave interaction with an obstruction, the rays are reflected, refracted or diffracted in different directions, causing the polarization to change, and the power to be attenuated differently based on the equations described above. Additionally, due to the multipath effects in an indoor environment, time of flight for each ray is affected, resulting in ray phase difference, finally causing an impact on the total 3D vectorially summed RSS at the receiver locations.

The previously described mechanism dominates in indoor environments, where multiple obstacles exist, forcing the waves to interact multiple times within the area of interest. Based on the above, it can be safely concluded that any modification on the antenna polarization axis, either at the transmitter or at the receiver level, will finally influence the Power Delay Profile (PDP), and the generated *radiomap*. The aforementioned modifications will finally affect the localization estimation and the achieved accuracy of any method.

2.3.4.2. ***Related work with Polarization in Localization***. Research work performed in the area of indoor localization referencing polarization, or multipath, tends to focus on the minimization of their influence on the received signal, instead on how to use polarization to improve the localization process. In this scope, authors of [**101**] presented a method for decreasing errors of TOA-based indoor positioning systems, based on directional antennas with small side lobes. They additionally utilized circular polarization antennas for attenuating multipath components arriving from the Line of Sight (LOS) direction.

Authors of [**102**] investigated the effects of polarization on the accuracy of an indoor location tracking system and established an experimental model that includes parameters which take into account the environmental effects. Based on their observations, they concluded that the accuracy of the location calculation is mainly dependent on the accuracy of the range measurements and that antenna polarization angle will affect RSSI and thus range accuracy.

In another approach, in [**10**], researchers investigated potential accuracy improvements in the RSS indoor localization process, through the introduction of

directional antennas in the radio network infrastructure. The positions and orientations of the directional antennas was carefully selected in order to decrease the correlation levels of the Received Signal Strength fingerprints which form the *radiomap*.

Research community also proposed sophisticated and specialized RF designs for enabling spatial re-usability, and polarization diversity in order to mitigate multipath propagation. Authors of [**103**] and [**104**] designed a switched beam array optimized for 2.45 GHz wireless indoor applications. The proposed antenna also supports absolute 2D target localization using measurements from a single anchor node, achieving an average localization error of 1.7 m.

Polarization scenarios were also investigated in Ultra wide-band (UWB) fingerprinting [**105**]. Comparisons between vertical and horizontal polarization cases at a frequency range from 3 GHz to 11 GHz, suggested that horizontal polarization provides greater accuracy than vertical polarization.

The combination of linear and circular polarized antennas for RSS-based indoor positioning techniques was proposed in [**106**]. In this work, it was shown that the utilization of linear and circular polarized antennas, instead of only linear polarized antennas, decreases the standard deviation of the received power and enhances the effective range.

All the aforementioned work, focuses in mitigating multipath and polarization effects, rather than utilizing their inherent properties for the benefit of improving localization accuracy in RSS fingerprint–based indoor localization. In the author's best knowledge, no previous work has been performed in developing a methodology where the impact of polarization is utilized to provide unique fingerprints, as this is presented in Chapter 6, and has been submitted to *EURASIP Journal on Wireless Communications and Networking, Special issue on Smart Cyber-Physical Systems* for publishing.

2.4. RTLS Performance Evaluation Techniques

A typical RTLS evaluation method refers to the development of benchmark standards for the comparison of the performance of different localization schemes [**107**]. Such schemes usually include environment type categorization, and their dynamic behaviour. The main disadvantages of benchmarks are the complexity and the abstract procedures that need to be implemented.

More precise methods were presented by researchers in [**108**] and [**109**], who suggested the enumeration of a number of critical factors that influence the performance of localization platforms. These factors included the number of transmitters, the number of reference measurements and the signal measurement dynamics. They examined a set of localization mechanisms and evaluated their performance robustness under various configuration settings using two typical types of building environments: an office building and an underground floor-plan. Although they enumerated several critical factors, they have not provided a direct relation between each factor. The difficulty of assessing the performance of different localization systems due to different testing conditions, was also reported in [**110**].

The performance of *radiomaps*, using dynamically collected measurements was later exploited in [**111**]. In this research work, *radiomaps* were generated from

dynamically collected measurements during the offline phase, and the KNN algorithm was employed for positioning during the online phase. The positioning performance was then compared with different grid spacing and with various K numbers for a KNN algorithm. However, the proposed methodology is algorithm specific, and the general outcome was that the positioning performance is affected by various parameters, which should be thoroughly decided. Authors do not define such critical factors and they do not propose a holistic evaluation methodology.

In order to assess already deployed positioning platforms, in a previous contribution, the utilization of binomial distribution was proposed[**7**]. Especially for the evaluation of the quality of RSS fingerprint databases, a contribution to the development of a dedicated correlation algorithm named Tolerance Based - Normal Probability Distribution (TBNPD) [**9**] has also been made. This algorithm calculates the correlation level for every pair of fingerprint entries forming the *radiomap*, taking into consideration the possible RSS fluctuations (RSS_{tol}), occurring due to the dynamic nature of the environment. TBNPD algorithm offers the possibility to assess the uniqueness of each fingerprint entry in a *radiomap*, prior to its utilization in a Real-Time Locating System (RTLS). For this reason, the TBNPD algorithm is considered suitable and convenient to be used for the assessment of the candidate *radiomaps* and will be used especially in Chapter 6 where a large number of *radiomaps* are generated and need to be assessed.

Based on the analysis of this algorithm, the Correlation Score (CS_{pairAB}) of any pair of random fingerprint entries, A (x_A, y_A) and B (x_B, y_B), for any active AP (AP_i), without introducing the RSS_{tol} parameter, is given by the formula:

$$CS_{pairAB} = \frac{1}{\sigma_{\overline{RSS}_{AP_i}}\sqrt{2\pi}} e^{-\frac{1}{2}\left(\frac{\overline{RSS}_B - \overline{RSS}_A}{\sigma_{\overline{RSS}_{AP_i}}}\right)^2} \tag{2.46}$$

where random fingerprint entries $A, B \in Area_{radiomap}$, and $\sigma_{\overline{RSS}_{AP_i}}$ is the standard deviation of the $\overline{RSS}$ values observed from each AP_i as follows:

$$\sigma_{\overline{RSS}_{AP_i}} = \sqrt{\frac{\sum_{i=1}^{n} \overline{RSS}_i^2 - \left(\frac{\sum_{i=1}^{n} \overline{RSS}_i}{n}\right)^2}{n-1}} \tag{2.47}$$

where n is the number of fingerprint entries in the radio map and $\overline{RSS}_i \geq MS_{Sensitivity}$.

By introducing the RSS_{tol} parameter in formula 2.46, the correlation score CS_{TBNPD}, is formulated. The CS_{TBNPD} for a pair of random points $A, B \in Area_{radiomap}$ and for any AP_i is calculated by 2.48 below:

$$CS_{TBNPD_{pairAB}} = \frac{1}{\sigma_{\overline{RSS}_{AP_i}}\sqrt{2\pi}} e^{-\frac{1}{2}\left(\frac{\overline{RSS}_{diff}}{\sigma_{\overline{RSS}_{AP_i}}}\right)^2} \tag{2.48}$$

where

$$\overline{RSS}_{diff} = \left| \left(\overline{RSS}_A\right)_{AP_i} - \left(\overline{RSS}_B\right)_{AP_i} \right| - 2RSS_{tol} \tag{2.49}$$

In formula 2.49, $RSS_{diff} \geq 0$. For $RSS_{diff} < 0$ the value is explicitly set to 0, since the range of the RSS values of the two fingerprint entries overlap indicating a high level of correlation.

The total correlation score ($CS_{TBNPD_{total}}$), to be utilized for candidate *radiomap* assessment during the implementation of the proposed approach, is the product of the correlation scores of all active APs:

$$CS_{TBNPD_{total}} = \prod_{AP=1}^{m} \left(CS_{TBNPD_{pairAB}}\right) \tag{2.50}$$

The latter algorithm is extensively utilized in Chapter 6 during the performance and quality evaluation of a single access point localization methodology.

CHAPTER 3

Cross-Device Fingerprint-based Positioning

3.1. Introduction

As discussed in Chapter 2, the most important part of fingerprint-based methods is the construction and maintenance of the *radiomap*. It can either be created through an extensive measurement campaign or through radio propagation modeling techniques. Despite the fact that experimental measurements might lead to more accurate fingerprints, collecting them might be very laborious and also their applicability is reduced if the geometry or morphology of the wireless environment is changed. The availability of accurate Radio Propagation modeling techniques, such as Ray Tracing (RT), and the growth of computational systems, makes this solution more attractive for the creation and maintenance of the *radiomap*. Still, RT accuracy is subject to the precise definition of the geometry and morphology (e.g., wall electrical parameters) of the environment and also the accurate definition of the transmitter and receiver antennas. Precise information of these RT input parameters is usually hard to obtain, therefore in order to achieve higher accuracy, crude calibration of the RT tool might be required [**112**].

A second significant limitation of fingerprint-based techniques is that the device heterogeneity may degrade the positioning performance when the device to be positioned is different from the device that was used to train (create) the *radiomap*. Differences may arise due to the different antenna characteristics of the mobile terminals, which are usually difficult to know or predict, or due to RF receiver chain differences. There is work reported in literature that tries to address the issue of device diversity; mainly by calibrating the RSS measurements collected from a mobile device to be positioned, to match the fingerprints contained in the *radiomap*, which has been created using a different device.

In this Chapter the work published in [**1**] and [**2**] is presented, where both challenges are addressed by using artificial *radiomaps* generated through 3D RT Simulations and then through the use linear transformation with an aim to correlate the *radiomaps* to a set of fingerprints collected using four different WLAN-enabled devices. Specifically, focus is on the on the amount of fingerprints that need to be collected to obtain appropriate linear transformation parameters that guarantee low positioning error for each device.

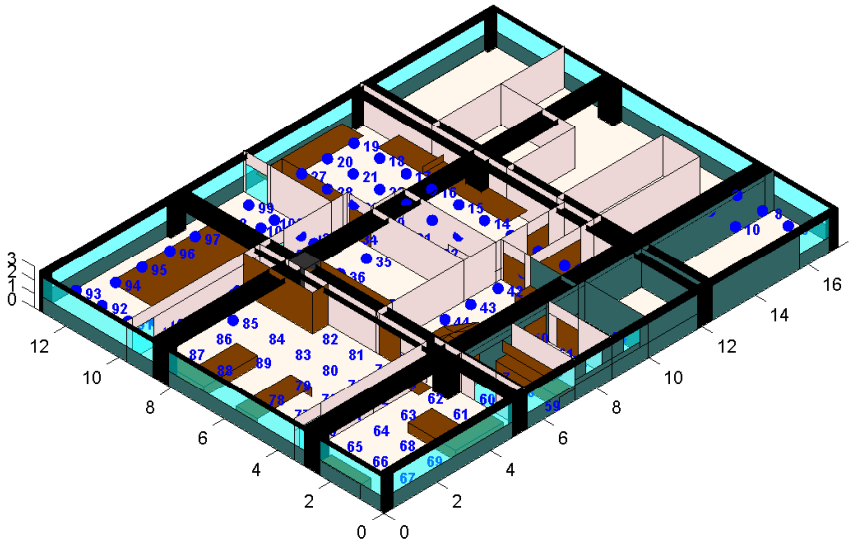

Figure 3.1 – 3D Model of the Indoor Environment for Ray Tracing Simulations

3.2. Proposed Approach

3.2.1. Ray Tracing Radiomap

For the creation of the fingerprinting *radiomap*, *TruNET wireless* has been used, which is a powerful 3D Ray Tracing polarimetric Simulator developed by Sigint Solutions Ltd. Its calculation engine uses a RT algorithm which utilizes the 3D EM formulation of reflection, refraction and diffraction based on the UTD. The 3D environment description can be defined by means of a built-in 3D-CAD application or by importing standard CAD files. It offers the ability to define the receiver and transmitter antenna characteristics from a wide range of antennas, as well as the flexibility to import a custom-made antenna by defining its radiation pattern. A snapshot is shown in Figure 3.2.

The indoor environment shown in Figure 3.4 has been modeled into the RT Simulator by importing the CAD file into its CAD designer including features of the environment such as desks, tables etc. Figure 3.1 shows the 3D model of the indoor environment. In this case 110 receiving locations have been defined at the same positions where the measurements have been carried out. In every receiving location a rectangular grid of 36 equally-spaced ($10cm$) isotropic receivers (at $90cm$ height) have been defined in order to remove potential fast fading behaviour by obtaining their local average. The 6 access points were equipped with an omni-directional antenna and placed at a height of $2.3m$. Typical values of the electrical parameters obtained from literature [**113**] have been used in order to characterize the building walls and geometric features. These parameters have been further tuned in order to better match the measurements collected with the Nexus S mobile device; see Table 3.1. This latter process is known as Ray Tracing calibration [**112**]. The Ray

Table 3.1 – Electrical Parameters used to characterize the morphology of the indoor environment

Material	Electrical Permittivity (F/m)	Loss Tangent
Concrete	3.9	0.23
Wood	2	0.025
Brick	5.5	0.03
Metal	1	1000000
Plasterboard	3	0.067
Glass	4.5	0.007

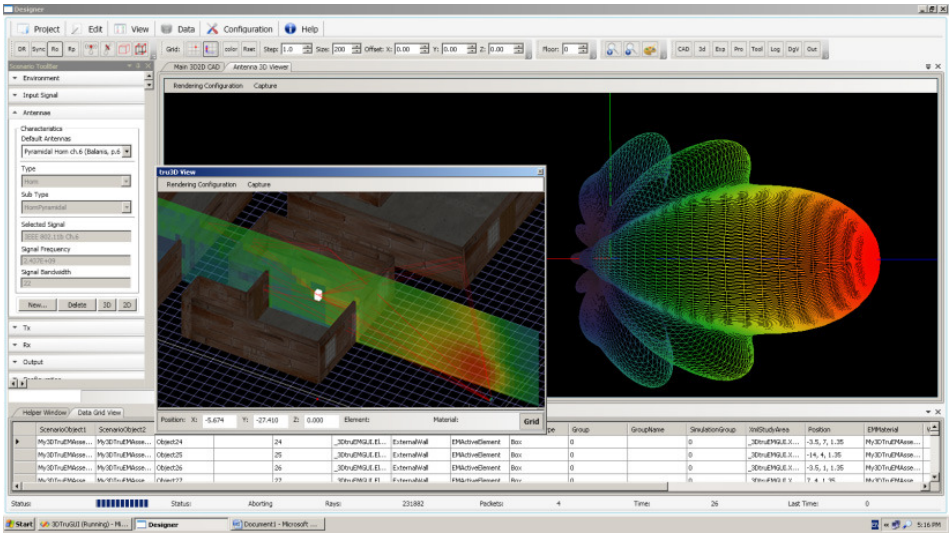

Figure 3.2 – *TruNET wireless* Ray Tracing Simulator [**12**]

Tracing simulations (compared to the measurements) have achieved a mean error of $5.62dB$ with a standard deviation of $4.23dB$ using all the measured locations. This error is assumed to be mainly due to the uncertainties of the exact values of the electrical parameters, the exact radiation pattern of the transmitting antennas, the environment clutter (chairs, computers etc.) but more importantly due to the fact that the receiver antenna pattern is unknown and it has been assumed as isotropic. However, since the objective is to devise a methodology where we have to collect as few measurements as possible, the RT accuracy using part of the measured data has been evaluated. Specifically, 1000 combinations of 4 training locations per region weew randomly selected, as described in Section 3.3, leading to the observation that similar behaviour is achieved (mean error is $5.6 \pm 0.3dB$ and the standard deviation is $4.3 \pm 0.2dB$). This effectively means that with very few measurements we can achieve reasonably good fine-tuning of the RT Simulator.

3.2.2. Device Calibration

The RT *radiomap* can be used as a reference *radiomap* for cross device positioning. However, the mobile devices report different RSS values depending on the hardware vendor of the WLAN adapter, the antenna sensitivity and its pattern. Therefore, the range of RSS values can greatly vary among devices, thus rendering the direct use of a single reference *radiomap* questionable. Consequently, device calibration is necessary to deliver a consistent level of performance, regardless of the device used during positioning. In order to increase the applicability of the mentioned approach, only a small amount of training data is used for the device calibration; otherwise, if a lot of training data is required to achieve adequate performance for a particular device, then such training data might as well be used to build a device-specific *radiomap* that ensures optimum performance.

In this approach linear transformation was investigated by using the training data for mapping the RSS values recorded with each target device to the RT *radiomap*. The RT *radiomap* contains the expected (mean) RSS value of each AP at every training location inside the area of interest. For this reason, the linear data fitting is performed in a least-squares sense using the mean RSS values of each device averaged over multiple fingerprints, collected at each training location. In this fashion, the two linear coefficients are estimated and can be used in a pre-processing step during positioning in order to scale the observed RSS values accordingly.

The data fitting is plotted for all four devices in Figure 3.3 indicating a strong linear correlation between the mean RSS values of each device and the RT *radiomap*. The linear fitting parameters are also indicated in the figures. The Lenovo X100e (laptop) behaves differently compared to the three Android devices and exhibits a large number of values ranging from -50dBm to -45dBm that correspond to values between -65dBm and -35dBm with respect to the RT data; see Figure 3.3a. This is also the reason for the hard limit appearing in Figure 3.3a. For this specific range of RSS values a higher order fitting could be applied to address this non-linearity. As it will be shown later in the performance evaluation (Section 3.4), this behaviour leads to a large positioning error if the RT *radiomap* is used to localize the X100e device without any calibration. Interestingly, the linear fitting obtained by using only 10% of the training data (dashed line), i.e., the mean RSS values in the fingerprints from 11 randomly selected locations, is very close to the respective fitting when all available training data are considered (solid line). This implies that we may use only few of the data for the device calibration and considerably reduce the data collection time for all target devices.

3.3. Test Environment

In order to assess the use of RT-generated *radiomaps* for enabling fingerprint-based positioning with diverse devices, WLAN RSS measurements have been collected in an indoor environment using four different devices. Three Android-based handsets (HTC Desire HD, Samsung Nexus S and Samsung Galaxy Tab) and one laptop (Lenovo X100e) have been used. Measurements have been performed at the same time with all four devices logging data from up to 6 D-Link 802.11b APs

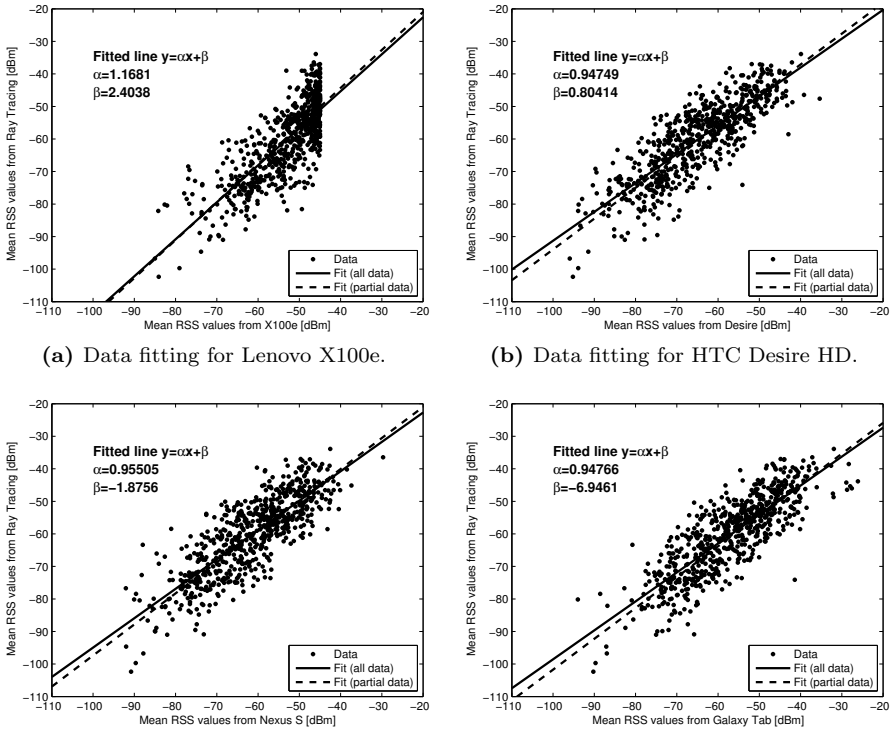

(a) Data fitting for Lenovo X100e.

(b) Data fitting for HTC Desire HD.

(c) Data fitting for Samsung Nexus S.

(d) Data fitting for Samsung Galaxy Tab.

Figure 3.3 – Device calibration using the Ray Tracing radiomap.

installed inside the building, and the RSS values range from -98dBm to -15dBm. Data was measured at 110 equally-spaced ($1m$ spacing) training locations. At every training location 30 fingerprints have been recorded (1 sample/sec) and the mean value fingerprint, averaged for each AP, has been computed in every location to build each device-specific *radiomap*. The whole data collection process took 2 hours to complete. For testing purposes additional RSS fingerprints have been collected with all devices along a route that comprises 40 distinct locations, while 10 fingerprints were measured at every test location with no averaging. The floorplan of the experimentation area, the installed APs, the training locations and test route are depicted in Figure 3.4. To enable random selection of data which are distributed uniformly in the environment, the whole area was divided into seven non-overlapping regions $A_i, i = 1, \ldots, 7$ representing rooms and large open spaces (see Figure 3.4), i.e., $\{A_1 : \ell_j, j = 1, \ldots, 11\}$, $\{A_2 : \ell_j, j = 12, \ldots, 30\}$, $\{A_3 : \ell_j, j = 31, \ldots, 40\}$, $\{A_4 : \ell_j, j = 41, \ldots, 59\}$, $\{A_5 : \ell_j = 60, \ldots, 69\}$, $\{A_6 : \ell_j, j = 70, \ldots, 89\}$, $\{A_7 : \ell_j, j = 90, \ldots, 110\}$ where j is the training location index.

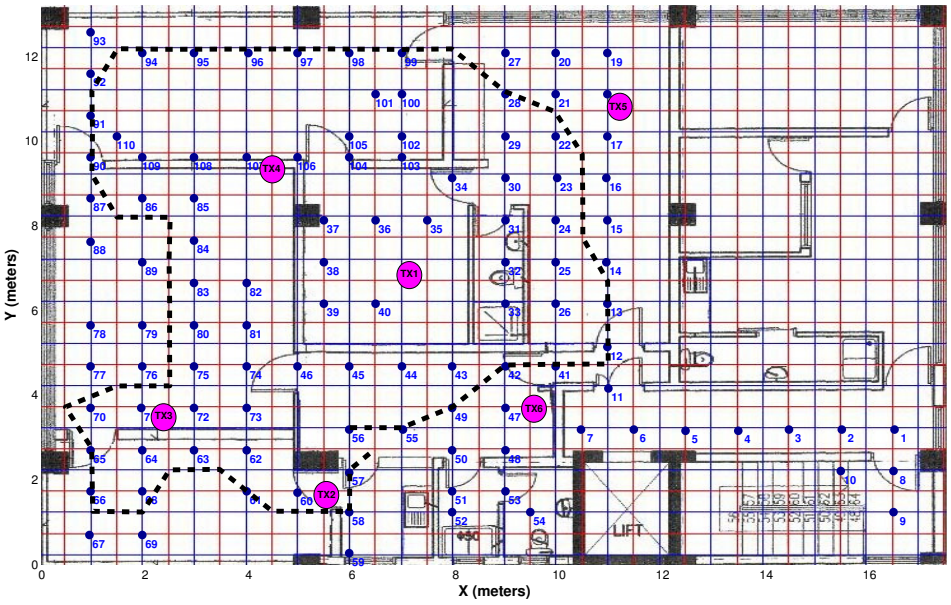

Figure 3.4 – Experimentation Area Floor Plan (Reference Locations and APs).

3.4. Performance Evaluation

The effectiveness of the proposed approach is assessed with respect to the positioning accuracy in an indoor environment and compare it with the case of using device-specific *radiomaps* collected with each device. Specifically, the experimental data collected with all four commercial devices, as detailed in Section 3.3, was employed to investigate the positioning error pertaining to the testing dataset. The focus was on the improvement achieved solely by combining the RT *radiomap* with the device calibration, rather than the fingerprint-based positioning method itself. Thus, the results are obtained using the well known closest Nearest Neighbour (NN) method [**67**]. Note that the proposed approach is independent of the underlying fingerprint-based method and using a more sophisticated approach, such as the probabilistic method described in [**114**], would incur additional accuracy improvement in the overall positioning system. Positioning accuracy results by such approaches are reported in [**1**].

The NN method estimates location by minimizing the Euclidean distance D_i, between the observed fingerprint during positioning $s = [s_1, \ldots, s_6]^T$ and the fingerprints $r_i = [r_{i1}, \ldots, r_{i6}]^T$ in the *radiomap*

$$\widehat{\ell}(s) = \arg\min_{\ell_i} D_i, \;\; D_i = \sqrt{\sum_{j=1}^{6} \left(r_{ij} - s_j\right)^2} \tag{3.1}$$

where r_{ij} and s_j denote the RSS value related to the j-th AP ($j = 1, \ldots, 6$). Essentially, all training locations $\ell_i, i = 1, \ldots, 110$ are ordered according to D_i and the location with the shortest distance between r_i and s in the RSS space is returned as the location estimate.

3.4.1. No Device Calibration

First, the performance in the case where the Ray Tracing *radiomap* is utilized without any device calibration is examined and the findings are summarized in Table 3.2. The accuracy results in the case where manually collected, device-specific *radiomaps* are used, are shown in parentheses for comparison. Apart from the mean, median and maximum positioning error pertaining to the dataset the 67^{th} and 95^{th} percentiles of the cumulative distribution function (CDF) are also reported, which represent the accuracy achieved for 67% and 95% of the time, respectively.

The first observation is that for the Nexus S the performance is marginally worse when the Ray Tracing *radiomap* is employed for positioning. This is justified by the fact that part of the training data from this device was used to fine-tune the Ray Tracing Simulator during the construction of the artificial *radiomap* as discussed in Section 3.2.1. For the Galaxy Tab device, this *radiomap* delivers similar accuracy with the device-specific *radiomap* (mean error $2.2m$ compared to $1.9m$), however it fails to provide adequate performance for the Desire and X100e devices. For these two devices the mean error is increased by 0.9m and 1.3m, respectively and this suggests that there is room for improving accuracy by means of device calibration.

Table 3.2 – Positioning error [m] using an uncalibrated RT *radiomap* compared to device-specific radiomaps.

	X100e	**Desire**	**Nexus S**	**Galaxy Tab**
Mean	4.4 (3.1)	3.0 (2.1)	2.2 (2.2)	2.2 (1.9)
Median	4.4 (2.6)	2.5 (1.6)	2.1 (2.0)	2.1 (1.5)
67% cdf	5.1 (3.5)	3.3 (2.2)	2.8 (2.5)	2.7 (2.5)
95% cdf	7.6 (7.1)	6.7 (4.4)	4.9 (4.7)	4.7 (4.6)
Max	11.3 (11.1)	8.4 (10.2)	7.5 (8.5)	8.6 (9.4)

3.4.2. Device Calibration with Partial Data

The question is how much training data is required to calibrate each device and ensure a good mapping between the RSS values observed during positioning and the RT *radiomap*. In this experimental analysis device-specific training data is employed and the effect of using part of the data for calibrating the devices is studied, as detailed in Section 3.2.2. Partial data is selected by varying the number of training locations in the setup that contribute their mean value fingerprints in the calibration process. In order to achieve a uniform distribution of the training data utilized for calibration, a specific number of locations from each region that is described in Section 3.3 is randomly selected. The average and standard deviation of the mean and 95% CDF positioning error, obtained over 100 runs using a variable number of randomly selected locations per region in each run, are tabulated in Table 3.3. In this case, all 30 fingerprints available for each location are used to calculate the mean RSS fingerprints for the device calibration.

Regarding the mean positioning error, shown in rows 1-3, it seems that using the data from only one location per region, provides the same performance with the case when using the data from all 110 training locations. The standard deviation is also very low, indicating that the mean error is not affected by the selection of specific locations in each region. On the other hand, data from more locations per region should be used to narrow the confidence interval for the 95% CDF positioning error (rows 4-6). The 95% CDF error provides an insight of the high errors anticipated during positioning and it is preferable to keep it as low as possible. Using data from 4 locations per region decreases further the uncertainty around the expected value of the 95% CDF error. These results indicate that by using training data from only a few locations for the device calibration suffices to reach the same level of accuracy as with the case of using all available data. This is justified because this subset of the data actually contains several RSS values from all APs, which cover a wide range of values, thus the data fitting during the device calibration is very effective.

However, another important issue is the number of fingerprints, containing raw RSS values, that need to be collected at each location in order to calculate the mean RSS fingerprints. This is directly related to the time spent at a particular location for recording a sequence of samples. Thus, the number of fingerprints that contribute to the mean RSS fingerprint at each location was additionally varied. Findings suggest that by using only 5 fingerprints per location does not affect the performance of the proposed approach and provides the same positioning accuracy, as with the case of using all 30 fingerprints per location; see Table 3.3. Essentially, this means that only a small fraction of time needs to be spent for collecting data and the device calibration overhead can be significantly reduced.

Table 3.3 – Positioning error [m] using a variable number of training locations per region.

	X100e	**Desire**	**Nexus S**	**Galaxy Tab**
			Mean error	
1 location	3.3±0.1	2.4±0.1	2.3±0.1	2.5±0.2
4 locations	3.3±0.0	2.4±0.0	2.3±0.0	2.5±0.1
All locations	3.3	2.4	2.3	2.4
			95% CDF error	
1 location	7.9±0.4	5.6±0.7	4.9±0.3	5.9±0.8
4 locations	8.0±0.1	5.8±0.3	5.0±0.1	5.9±0.3
All locations	8.0	5.9	4.9	5.8

3.4.3. Discussion

The statistics of the positioning error, assuming data from only four locations per region and five fingerprints per location are used in the device calibration, are

Table 3.4 – Performance of the proposed approach using 4 locations per region and 5 fingerprints per location for device calibration.

	X100e	**Desire**	**Nexus S**	**Galaxy Tab**
Mean	3.4±0.0 (3.1)	2.4±0.0 (2.1)	2.3±0.0 (2.2)	2.5±0.1 (1.9)
Median	2.7±0.1 (2.6)	2.1±0.0 (1.6)	2.1±0.0 (2.0)	2.1±0.1 (1.5)
67% CDF	3.6±0.1 (3.5)	2.5±0.0 (2.2)	2.8±0.0 (2.5)	2.8±0.1 (2.5)
95% CDF	8.0±0.0 (7.1)	5.8±0.3 (4.4)	5.0±0.1 (4.7)	5.9±0.2 (4.6)
Max	10.4±0.4 (11.1)	9.0±0.3 (10.2)	7.5±0.1 (8.5)	8.5±0.2 (9.4)

reported in Table 3.4. For the X100e and Desire devices the proposed approach improves considerably the performance compared to using the RT *radiomap* without any calibration, while the positioning error is close to the error achieved when device-specific *radiomaps* are employed; the positioning accuracy obtained using device specific measurements is shown in parentheses for comparison. For the Nexus S device similar behaviour was observed, while in the case of Galaxy Tab the device calibration leads to some higher errors during positioning that slightly increase the mean error. In any case, the traditional fingerprint-based approach can be replaced by the proposed approach. Here only five fingerprints at four random locations in each of the seven regions inside the experimentation area for device calibration need to be collected.

This translates into less than five minutes of data collection for each device to be positioned, compared to around two hours of RSS data logging for building each device-specific *radiomap*. If we also consider that RT simulations for this wireless environment took about 40 minutes to generate the *radiomap* the total time saving is around 60%. Larger scale setups would lead to greater savings in time and labour.

3.5. Conclusion

Fingerprint-based positioning with respect to device diversity is an active research field because the time consuming data collection process, using several target devices, is involved in the construction of the necessary *radiomap*. This work focuses on the use of a 3D Ray Tracing polarimetric simulator to automatically obtain a reference *radiomap* with much less effort. Subsequently, that is combined with a device calibration phase, which is based on linear fitting, to effectively map the RSS values observed during positioning to the reference RT *radiomap*, irrespectively of the user device. The proposed approach mitigates the cumbersome task of recording large datasets of RSS values throughout the area of interest with multiple devices. The performance evaluation indicates that only a small amount of device-specific data is required to reach the same level of positioning accuracy attained with a manually collected *radiomap*. Thus, the mentioned approach is

far less laborious compared to traditional *radiomap* construction. Moreover, the *radiomap* can be easily updated if the propagation environment changes in the future (e.g., APs are added or removed, or furniture is relocated, etc.) by running the RT simulator, instead of collecting the *radiomap* data from scratch.

CHAPTER 4

Map-Aided Fingerprint-based Indoor Positioning

4.1. Introduction

The accuracy achieved by any Real Time Localization System (RTLS) is affected by the volume and quality of information that is available during the position estimation procedure. The more useful information can be provided, the higher the probability for producing a more accurate estimate.

Depending on the capabilities of the terminal or the overall RTLS, in retrieving, storing and processing location-specific information, advanced positioning algorithms can be developed in order to provide improved positioning services.

The location-specific information may include radio parameters, such as Received Signal Strength (RSS), Angle of Arrival (AOA), Time of Arrival (TOA) and Impulse Responses (IR) or non-radio parameters, such as inertial measurements, prior map/layout knowledge etc.

In many cases, the sole utilization of the radio parameters, during the position estimation, imposes limits that are hard to overcome. By introducing and fusing additional non-radio parameters to the localization process, it is expected that one could potentially improve the positioning accuracy.

In this direction, the information retrieved from the inertial sensors can be used in conjunction with environment maps. The idea presented in this Chapter, which is based on the work in [**3**], is to utilize the available environment description of building databases and blueprints/architectural drawings of indoor areas, for the purpose of aiding the localization process. By using map–related information, the possible movement and location of the user is expected to be constrained and different probabilities can be assigned to different areas of the environment where the User/Mobile Station (MS) might reside. As a result, long–term error stability can be achieved when the map is sufficiently accurate and effectively constrains the motion.

Proper use of any available information into the positioning process, is definitely a challenge and can contribute noticeably to the minimization of the positioning error. In fact, the information retrieved from environment maps, can offer this extra knowledge. This paper describes how such environment knowledge can be extracted and exploited into a fingerprint-based positioning process. The proposed approach utilizes a-priori knowledge of the likelihood of a user being at a specific location. This a-priori knowledge can be made available as a means of probabilistic map constraints.

4.2. Methodology and Test Environment

4.2.1. Route Probability Factor

This Section introduces a new map–aided method, using what was named as Route Probability Factor (RPF). The RPF reflects the likelihood of a user to be located at a specific position instead of all other positions. This means that along a frequent route, the RPF will be increased, while in unlikely areas it will be decreased. The RPF does not only affect the probabilities along the specified route, but also the positions at its proximity. For this purpose, a normally distributed approach was implemented, at a radius ρ across the route, creating *route tubes*. For every location on each frequent route, the algorithm assigns a decaying probability to all those fingerprints in the fingerprint database, which reside within a circle with radius ρ around this location. This decaying probability is given by the following formula:

$$RPF_{\ell_i} = RPF_{\ell} \left(\frac{1}{\sigma_{route}\sqrt{2\pi}} \right) e^{-\frac{1}{2}\left(\frac{\|\overline{\ell}-\overline{\ell_i}\|}{\sigma_{route}}\right)^2} \tag{4.1}$$

where RPF_{ℓ} is the route probability factor at the location ℓ which lies exactly on the route and $\|\overline{\ell}-\overline{\ell_i}\|$ is the distance between location ℓ and any other location ℓ_i within the range of ρ. Finally, σ_{route} is given with respect to the selected ρ for a 99% confidence level $\sigma_{route} = \rho/3$, since statistically 3σ provides this confidence level.

This iterative process results in a normalized probability matrix for every location along each frequent route tube. All these matrices are then summed up to result into an accumulated probability matrix which describes the likelihood of a user being in any location in the environment. This matrix has a one to one relation to the fingerprints database and is then used in conjunction with the positioning algorithm to improve the localization accuracy.

In this research work, the WKNN deterministic algorithm was employed to perform fingerprint–based positioning, extended with the probabilistic part of the RPF. This approach takes into consideration a-priori knowledge of the frequent user routes, as well as the weighted Euclidean distance of the observed location. The former allows to incorporate map constraints into the position estimation, by assigning the different probabilities of likelihood of each location in the environment, in the form of a matrix as described above. In this context each fingerprint in the database is given a prior probability $P_i = RPF_i$, which multiplies the Euclidean Distance as $P_i\|\overline{r}_i - s\|$. This gives less likelihood to fingerprints in constrained areas to appear higher in the ordered vector $\{\ell'_1, \ldots, \ell'_l\}$ which is then used in Eq. (2.28). These prior probabilities can also be combined with the probabilities explicitly set to a minimum, in areas that are not accessible by the user (e.g., locked rooms, dangerous and forbidden areas etc.).

The normalized distribution of RPF in the test environment is visually presented in Figure 4.1.

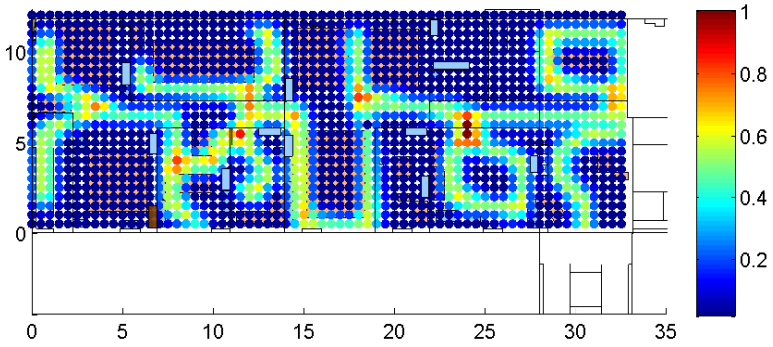

Figure 4.1 – Prior Probabilities

4.2.2. Generation of Fingerprint Database and Test Results

In this work, the generation of the fingerprint database of the testing environment was carried out in *TruNET wireless* simulator [**12**]. The 3D model of the building shown in Figure 4.2, including the furniture set up, was imported in the simulator in a digital form (.OBJ). The calculation algorithm of the Route Probability Factor, which was utilized in this research work, was developed and added into the source code of *TruNET wireless*.

For the creation of the fingerprint database, 1584 isotropic receivers (Rx) were defined in the floor plan. They were equally-spaced with a step of 0.5m, at a height of 1.5m. The underlying wireless network included 8 Wi-Fi (2.4GHz) Access Points (APs) with omni-directional antennas, installed at a height of 2.2m. The locations of the APs are depicted in Figure 4.2. Typical values of the electrical parameters obtained from literature [**113**], were used to characterize the morphology of the walls and other geometric features of the building.

4.3. Performance Evaluation

In order to assess the performance of the proposed approach, two separate simulations have been carried out for estimating the position of a user moving along the test route shown in Figure 4.3. The purpose of the test route is to evaluate the positioning accuracy before and after imposing the map constrains. It consists of 520 equally spaced (0.25m) locations at a height of 1.5m. When a positioning platform is deployed under real operating conditions, several factors

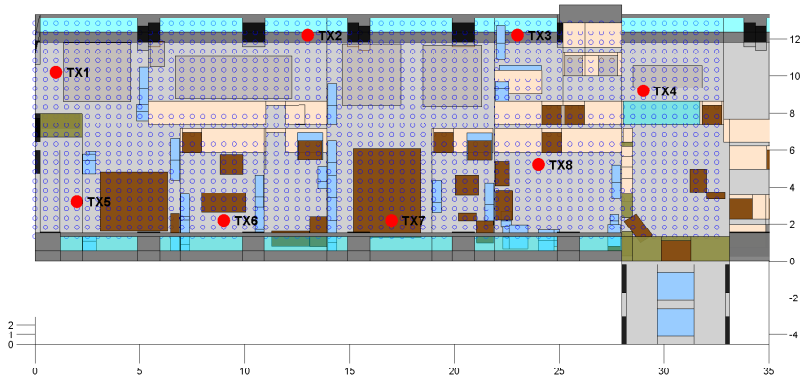

Figure 4.2 – 3D Model of the Indoor Environment with Fingerprint Locations

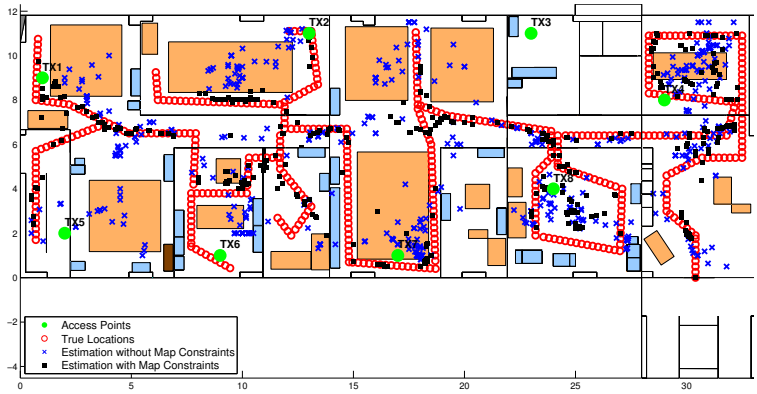

Figure 4.3 – Estimates along the Test Route

affect the positioning accuracy. The user might not be using the same device as the one used to collect the database fingerprints (device diversity issue), or even the geometric environment might have changed (displacement of furniture, new partitions etc.). Moreover, the movement of people create a more dynamic environment. To incorporate this profile variability onto the RSS values estimated along the test route, an uncertainty factor (normally distributed with standard deviation $\sigma = \pm 3dB$) has been introduced on the RSS values of the Mobile Station (MS) [**114**],[**1**]. The WKNN positioning method was tested iteratively for various values of K in the case where no map constraints are used and it was found that the optimum one that minimizes the mean error was $K = 5$. This value was then also used for the case where map constrains are incorporated into the positioning process.

The results from the two aforementioned positioning estimations (with and without map constraints) are summarized in Table 4.1, while the respective graphs showing the CDF of the obtained localization accuracy are depicted in Figure 4.4.

Table 4.1 – Positioning Accuracy with and without map Constraints

Positioning Estimation	**Parameter**	**Error** m
Without Map Constraints	Mean	2.03
	CEP 50%	1.79
	CEP 67%	2.35
	CEP 95%	4.53
	Max	17.09
With Map Constraints	Mean	1.46
	CEP 50%	1.09
	CEP 67%	1.62
	CEP 95%	3.77
	Max	5.95

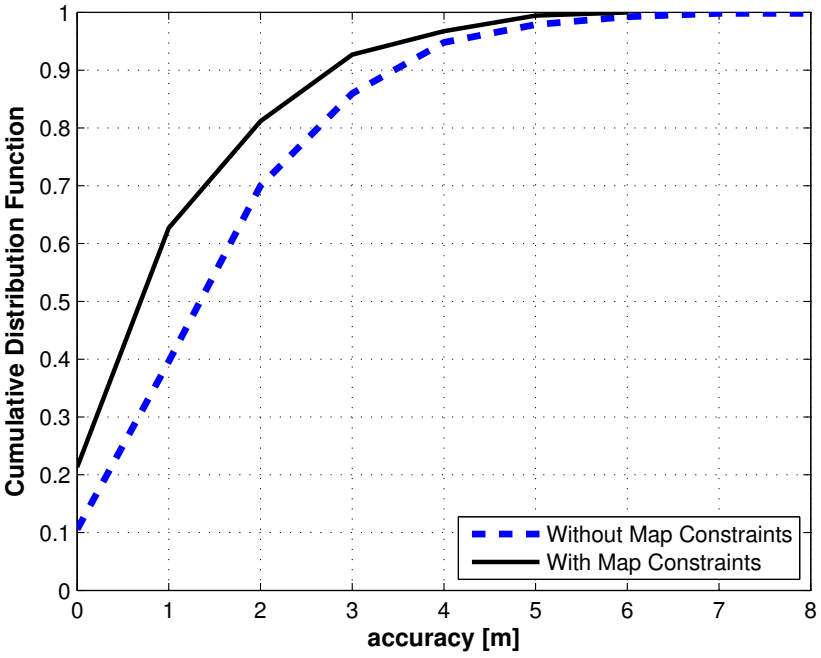

Figure 4.4 – CDF of Localization Accuracy

From the above findings it is noted that, when the map constraints are used, a significant improvement of 28% occurs on the mean positioning accuracy (from $2.03m$ to $1.46m$). A radical reduction of 65% on the maximum error ($5.95m$

instead of $17.09m$) is also be observed. The improvement is sustained in the whole range of Circular Error Probable (CEP), as it can be seen in Figure 4.4. The position estimation for all points along the test route in the map-aided scenario, is presented in Figure 4.3 with square symbols. It can be observed that, as a result of the implementation of the RPF in the positioning procedure, the estimated locations were shifted from the areas captured by furniture (asterisk symbols) towards more reasonable positions, near the test route.

Given the above improvements in the positioning accuracy, it is interesting to investigate what would be the effect of the radius ρ around each of the locations of the frequent route used for the generation of the a-priori probabilistic knowledge by the RPF method. In this context, for the optimization of the RPF, different values of route radius ρ were investigated. As it is illustrated in Figure 4.5, the value of ρ affects the localization accuracy and should be $\rho \geq d_{Rx}$, where d_{Rx} is the fingerprint radiomap resolution (step between the receivers).

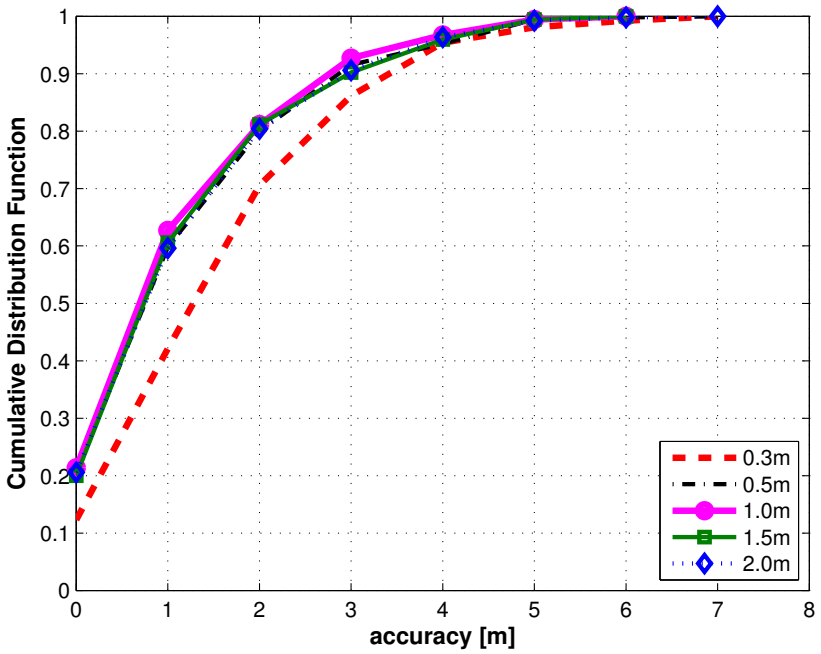

Figure 4.5 – Effect of RPF radius ρ on accuracy

4.4. Route Prior Knowledge for Map-Aided Fingerprint-based Positioning

In this Section the concept of Map-aided positioning was further extended. Within the work performed in [**4**], the positioning accuracy behaviour in map-aided positioning systems is investigated, when different probability distribution types are employed along typical predefined user routes. The aforesaid routes refer

to the most frequent user paths. These are given higher probability scores in an a–priori knowledge probability matrix, which includes all fingerprint locations. Such a–priori knowledge is usually retrieved from environment maps and the user mobility behaviour. It is assumed that the user's behaviour can be recorded through observations, or can be predicted through learning techniques. The effect of the probability distribution width, radius ρ, on positioning accuracy is also examined, by varying the value of ρ for both sides of the route. In this way, the allocated weight probability for locations near the user center line route, can be controlled.

4.4.1. Methodology and Test Environment for Route Prior Knowledge Concept

As discussed in previous Sections, map information utilization is also investigated in [**3**], where the implementation of a Route Probability Factor (RPF) is proposed. RPF reflects the probability of a user to be located at a position along the typical route, instead of all other positions. This is calculated by Equation 4.1 and is implemented in the form of a matrix that includes a probability factor for all fingerprint locations. In the aforementioned research work, the probability distribution width of the typical user route, called radius ρ, is used to calculate the standard deviation σ_{route}. Hence, varying the value of ρ, affects the probability factor value for locations near the user's route. In this way, *route tubes* are formed instead of one-dimensional line paths. The value of ρ depends on the fingerprint radio–map resolution, and can be optimized accordingly, to minimize positioning error [**3**].

In the following subsections, the effect of different probability distribution types on positioning accuracy, when employed to describe a user's movement along typical predefined routes is investigated.

4.4.1.1. ***Route Probability Distribution Types***. The a–priori knowledge of typical user routes, defines probable paths (routes) within the indoor environment. Probability distributions are introduced in an effort to better explain any reasonable route deviations from the user's center line of movement. Introduction of probability distributions on each fingerprint location of these paths, influences the weight factor of a number of neighbouring points that fall within the width of the applied distribution (radius ρ). In this respect, uniform, linear, distance ratio and exponential distribution types were applied and tested. The respective RPFs, are extracted by modification of formula 4.1, and are given in the following Equations 4.2, 4.3, 4.4 and 4.5:

Uniform distribution:

$$RPF_{\ell_i} = RPF_{\ell} \tag{4.2}$$

Linear distribution:

$$RPF_{\ell_i} = RPF_{\ell} \left(\rho - \|\overline{\ell} - \overline{\ell_i}\|\right) \tag{4.3}$$

Exponential distribution:

$$RPF_{\ell_i} = RPF_{\ell}\left(\frac{\rho}{e^{\|\overline{\ell}-\overline{\ell_i}\|}}\right) \tag{4.4}$$

Distance Ratio distribution:

$$RPF_{\ell_i} = RPF_{\ell}\left(\frac{\rho}{\|\overline{\ell}-\overline{\ell_i}\|}\right) \tag{4.5}$$

where RPF_{ℓ} is the route probability factor at location ℓ, which is positioned exactly on the center line of the route and $\|\overline{\ell}-\overline{\ell_i}\|$ is the distance between locations ℓ and ℓ_i within the range of ρ.

The aforesaid probability distributions within the route tube, are illustrated in Figure 4.6. The value of the tube radius ρ, is directly related to the fingerprint radiomap resolution [**3**]. In order to test the stability of each distribution with different values of ρ, ρ was varied from $1.0m$ to $2.0m$, with a step of $0.5m$. Tube radius however, being scenario specific, should be optimized based on the layout of the indoor environment (e.g., width of corridors, furniture setup, radiomap resolution etc.).

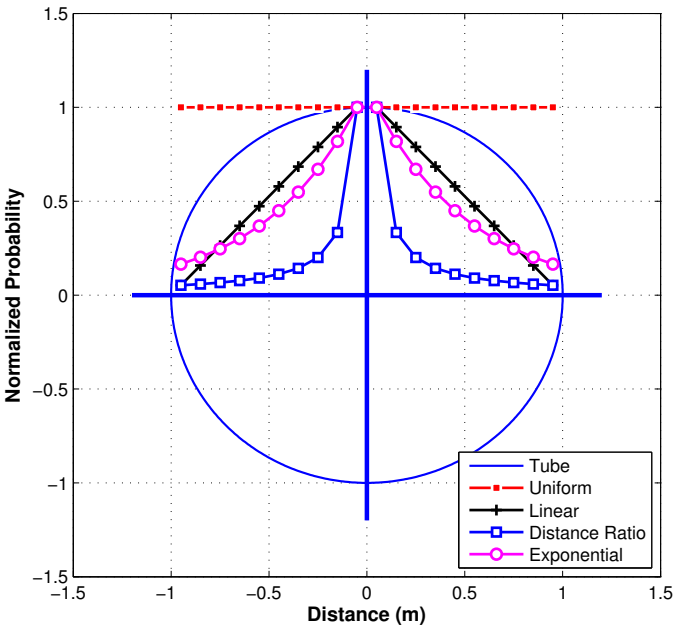

Figure 4.6 – Probability Distribution Types in Route Tube

For each distribution type, an iterative process along all points that fall within the route tube, was performed. This process results in a normalized probability matrix for all fingerprint locations in the environment. Each fingerprint in the radiomap is directly related to a probability value in the normalized matrix, hence it can be injected in the positioning algorithm in the form of a weight factor.

In all experiments, the WKNN deterministic algorithm is employed, extended with the probabilistic part of the RPF for each distribution type. The test environment and typical routes are shown if Figure 4.7. Along the typical routes, the weight probability is higher than other fingerprint locations in the environment, since users tend to move more frequently on this specific path, than on any other.

Figure 4.7 – Test Environment and Test Route

4.4.1.2. ***Radiomap Generation.*** A 3D Ray Tracing simulator (*TruNET wireless* [**12**]), was used to generate the radiomap of the test environment The simulator implements and applies the 3D electromagnetic formulation of reflection, refraction, and diffraction based on the Uniform Theory of Diffraction (UTD).

The area of interest was equally split every 0.5m in order to form a uniform grid area. In this way, 1584 isotropic receivers (Rx) were defined in the floor plan, at a height of $1.5m$. An 802.11 wireless network with 8 Access Points (APs) was placed at a height of $2.2m$, as shown in Figure 4.8. The constitutive parameters of the building and furniture materials were obtained from literature [**113**], and an initial simulation was performed to populate the RSS values of each fingerprint entry in the database.

4.4.2. Performance Evaluation of Route Prior Knowledge Concept

In order to assess the performance of each probability distribution type, separate simulations have been carried out, for the purpose of estimating the position of a user moving along the test route as shown in Figure 4.7. The test route consisted of 520 locations at the height of $(1.5m)$. To realistically simulate dynamic effects of a real case study, a normally distributed RSS fluctuation with a $\sigma = \pm 3dB$ was injected in the estimated RSS values. The aforesaid RSS fluctuations can be typically observed in real operating conditions due to the distortions caused by human/machine movement, device diversity etc. [**1**]. The positioning

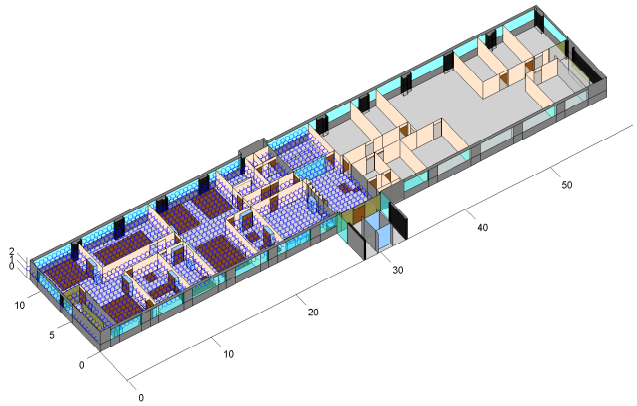

Figure 4.8 – 3D Model of the Indoor Environment with Fingerprint Locations

estimation was performed by implementing the WKNN algorithm with a $K = 5$, which minimizes the positioning error in the case where no map constraints are imposed.

Results of the aforementioned positioning estimations, including the case of "no map constraints", are summarized in Table 4.2. The respective graphs presenting the Cumulative Distribution Functions (CDF) of the obtained localization accuracy are depicted in Figure 4.9.

The results of the experiments indicate that all map-aided methods outperform the conventional positioning estimation where no map constraints are imposed, as depicted in Figure 4.10. Even the implementation of a *simple uniform* probability distribution within the route tube, results in an improvement of 23% of the mean positioning accuracy (from $2.03m$ to $1.57m$). The best performance was observed when the *distance ratio* probability distribution is used, with an accuracy improvement of 28% of the mean (from $2.03m$ to $1.46m$) and 65% of the maximum error. It can be also observed that, as the tube width increases from $1m$ to $2m$, the positioning accuracy of all probability distribution types under investigation, slightly degrades. This is noted along the whole range of Circular Error Probable (CEP).

4.5. Conclusion

The introduction of weight coefficients in the form of a–priori knowledge, that reflect the map constraints, can result in significant improvements of position estimation in indoor environments. In this direction the implementation of RPF as a matrix was proposed, which can be either populated manually, by observing the human movement behaviour, or through the implementation of supervised or unsupervised learning methods. The value of the radius ρ which defines the range of effect of the frequent routes, depends on the fingerprint radiomap resolution and should be optimized accordingly to minimize positioning error.

Table 4.2 – Positioning Error (m) for Different Distribution Types

Method	**Parameter**	**1m Tube**	**1.5m Tube**	**2m Tube**
No map	Mean	2.03	2.03	2.03
	CEP 50%	1.79	1.79	1.79
	CEP 67%	2.35	2.35	2.35
	CEP 95%	4.53	4.53	4.53
	Max	17.09	17.09	17.09
Uniform	Mean	1.57	1.72	1.77
	CEP 50%	1.07	1.25	1.40
	CEP 67%	1.83	1.86	1.91
	CEP 95%	4.16	4.60	4.76
	Max	6.83	6.15	6.46
Linear	Mean	1.48	1.55	1.65
	CEP 50%	1.10	1.11	1.20
	CEP 67%	1.62	1.82	1.87
	CEP 95%	4.19	4.20	4.55
	Max	5.77	5.97	6.10
Exponential	Mean	1.49	1.62	1.67
	CEP 50%	1.06	1.12	1.28
	CEP 67%	1.77	1.85	1.90
	CEP 95%	3.94	4.54	4.52
	Max	5.78	6.01	6.78
Distance Ratio	Mean	1.46	1.54	1.57
	CEP 50%	1.09	1.17	1.24
	CEP 67%	1.62	1.79	1.80
	CEP 95%	3.77	4.18	4.22
	Max	5.95	6.13	6.84

Additionally, different probability distributions were applied and tested on predefined, typical user routes, which are utilized as a–priori knowledge in map-aided positioning. Results indicate a significant improvement on positioning accuracy, when distribution types are applied to describe a user's probable deviation from the center line of a predefined route. The type of the probability distribution to be used, has small influence to the overall localization error. However, optimum results have been observed when the *distance ratio* distribution was used.

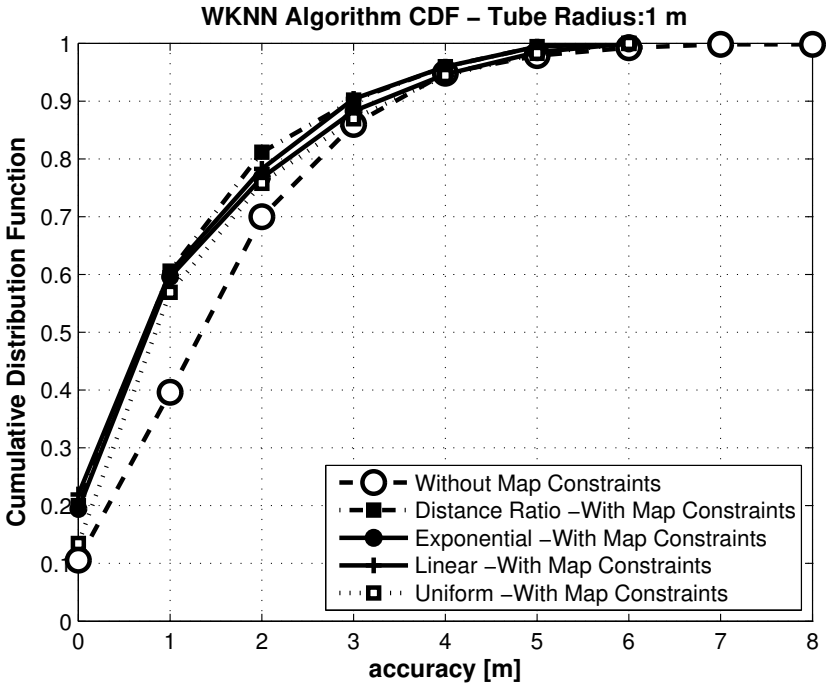

Figure 4.9 – CDF of Localization Accuracy - Tube Radius $1m$

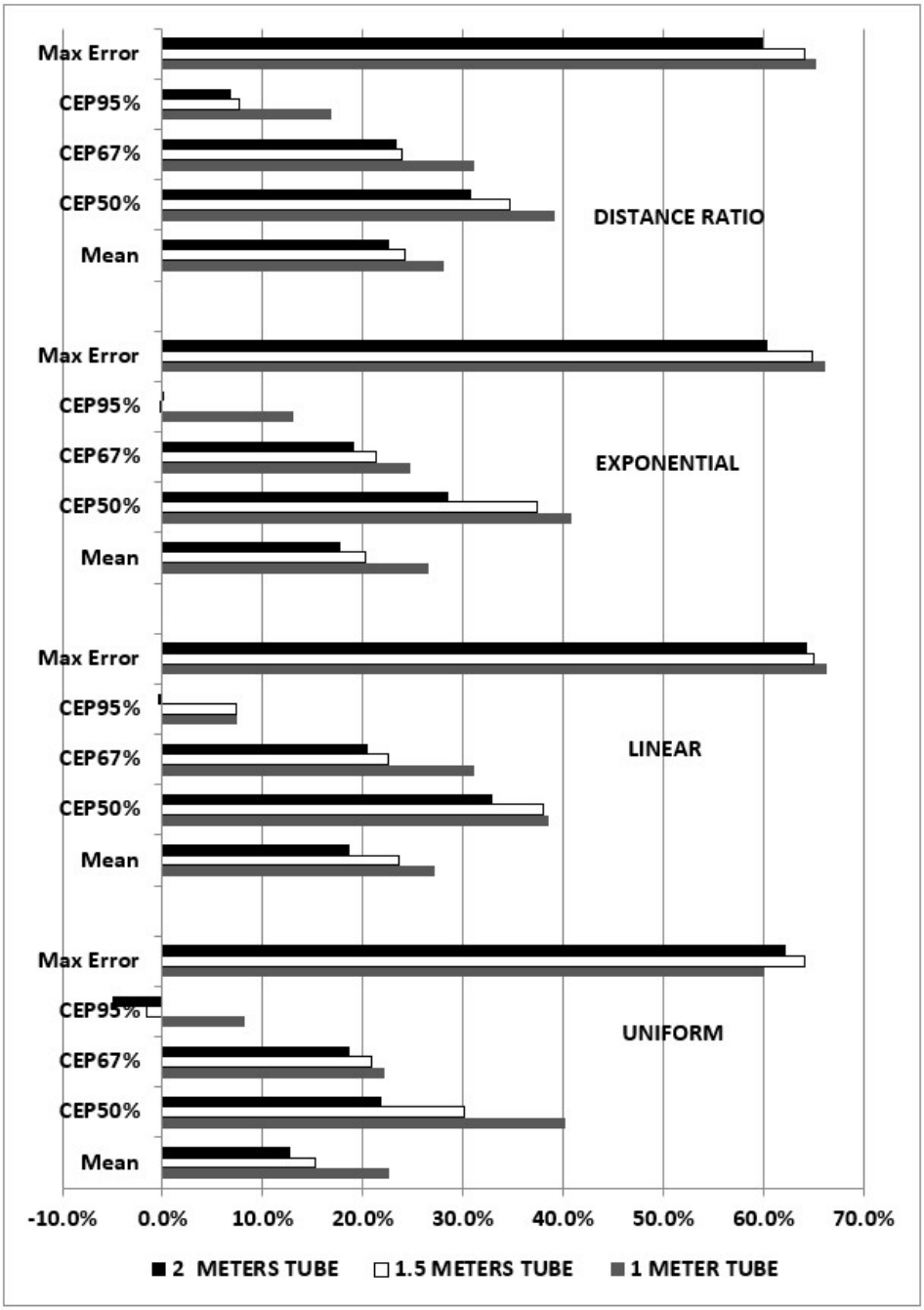

Figure 4.10 – Positioning Accuracy Improvement

CHAPTER 5

Combination of Heterogeneous Technologies in Fingerprint-based Positioning

5.1. Introduction

In this Chapter two new algorithms are introduced, which utilize information retrieved by IEEE 802.15.1 or IEEE 802.15.7 technologies in order to improve the accuracy and performance of conventional fingerprint-based localization platforms, which use IEEE 802.11 wireless networks. Both algorithms (*i-KNN* for IEEE 802.15.1 and *vlp-KNN* for IEEE 802.15.7), filter the initial RSS fingerprint dataset, in order to narrow it down to a subset of the data that is used by the conventional positioning algorithm KNN. The filtering procedure takes advantage of the low energy and hence low range characteristics of BLE in the first case, and of the LOS property of VLP. By taking advantage of these properties, an initial rough estimation of a much smaller area is performed, where the MS is assumed to lie within. In this way, mean error is reduced significantly by excluding other areas (where fingerprint characteristics might be similar) from the matching procedure during positioning. Having a much smaller subset of fingerprints to perform positioning, the calculation time decreases and consequently the energy consumption is minimized.

Detailed analysis of the proposed approach is presented in Section 5.2. For testing the aforementioned positioning algorithms an experimental positioning platform dubbed ϕ**-map** has been developed, which is described in Section 5.3. Finally, both algorithms were tested and evaluated with the procedure and results being presented in Sections 5.4 and 5.5. The work is based on scientific publications [**5**] and [**6**].

5.2. Proposed Approach

The proposed approach aims to gather general localization data from either BLE devices deployed in an IoT environment, or from a VLP system deployed in a smart lighting environment. The scope is to use this data to optimize the data retrieved from existing popular and low cost IEEE 802.11 RSS fingerprint-based indoor positioning systems in order to improve the provided positioning accuracy. By implementing this concept, two new enhanced KNN positioning algorithms were developed: *i-KNN* for BLE combination and *vlp-KNN* for smart lighting scenario.

Algorithms implement the same novel concept, i.e., to filter the initial Wi-Fi fingerprint dataset (*radiomap*), taking into consideration the proximity of the RSS fingerprints to the devices of the supporting technology (IEEE 802.15.1 or IEEE 802.15.7). By choosing to filter the initial dataset, instead of simply combining the fingerprints of all technologies together, the proposed algorithms utilize an optimized small size subset of possible user locations for the final position estimation.

5.2.1. Combining IEEE 802.15.1 with 802.11

In the case of *i-KNN*, the algorithm uses the range estimation data transmitted from the iBeacons. The range refers to the distance between a BLE device and the mobile user (mobile device or body sensor). The data package also includes information referring to the nearest iBeacon and the ranges from all visible BLE devices in the network. This data is used as an input to the filtering processes of the *i-KNN* in order to roughly estimate a probable area A, which encloses the user's position. The aforementioned donut-shape area A, is formulated between a minimum and a maximum radius ($R_{BLE_{min}}$ and $R_{BLE_{max}}$) measured from a center point, where the BLE device is located. The $R_{BLE_{min}}$ and $R_{BLE_{max}}$ values are calculated, taking into consideration a predefined tolerance (Tol) parameter, which accommodates any positioning error factors.

As illustrated in Figure 5.1, area A is then used to screen the number of candidate fingerprints, down to a subset ($S : \{\ell_1, \ldots, \ell_k\}$) extracted from the initial IEEE 802.11 fingerprint dataset ($D : \{\ell_1, \ldots, \ell_j\}_{Wi-Fi}$). The filtered fingerprint data subset S is finally used as the optimized input, to typical indoor positioning algorithms (in this case the KNN). The proposed methodology serves two purposes: Firstly, achieving fast positioning estimation due to the utilization of a fragment of the initial fingerprint dataset, and secondly achieving improved positioning accuracy by constraining any possible calculation errors within a very specific area A, where the user is actually located. The latter is achieved due to the inherited short range of IEEE 802.15.1 and its capability to identify the nearest iBeacon device to each mobile user. For clarity, a self-explanatory pseudocode of the *i-KNN* filtering algorithm used to calculate the subset $S : \{\ell_1, \ldots, \ell_k\}$, is presented in algorithm 5.2.1, and explained in subsection 5.2.1.1.

5.2.1.1. ***i-KNN Algorithm Explanation.*** *i-KNN* receives as input the Wi-Fi *radiomap* $D : \{\ell_1, \ldots, \ell_j\}_{Wi-Fi}$ and the BLE locations $B : \{BLE_1 \ldots, BLE_i\}$. A procedure named FINGERPRINTS TO BLE DISTANCE pre-calculates the distances between BLE devices and all fingerprint locations for easier estimation of the final output, which is subset S. Calculated distances are given in the form of a matrix $L : \{r_{\ell_1,BLE_1} \ldots, r_{\ell_j,BLE_i}\}$.

During the real-time positioning estimation, the algorithm initially scans for traceable BLEs by running BLE DISCOVERY procedure, retrieves their parameters and

sorts them based on their Received Signal Strength. Upon retrieval of BLE information, *i-KNN* selects the nearest BLE device and utilizes the distance information broadcasted by the beacon ($Range_{BLE_i}$) in order to additionally calculate the Tolerance (Tol) level and define the donut-shape area A, shown in Figure 5.1.

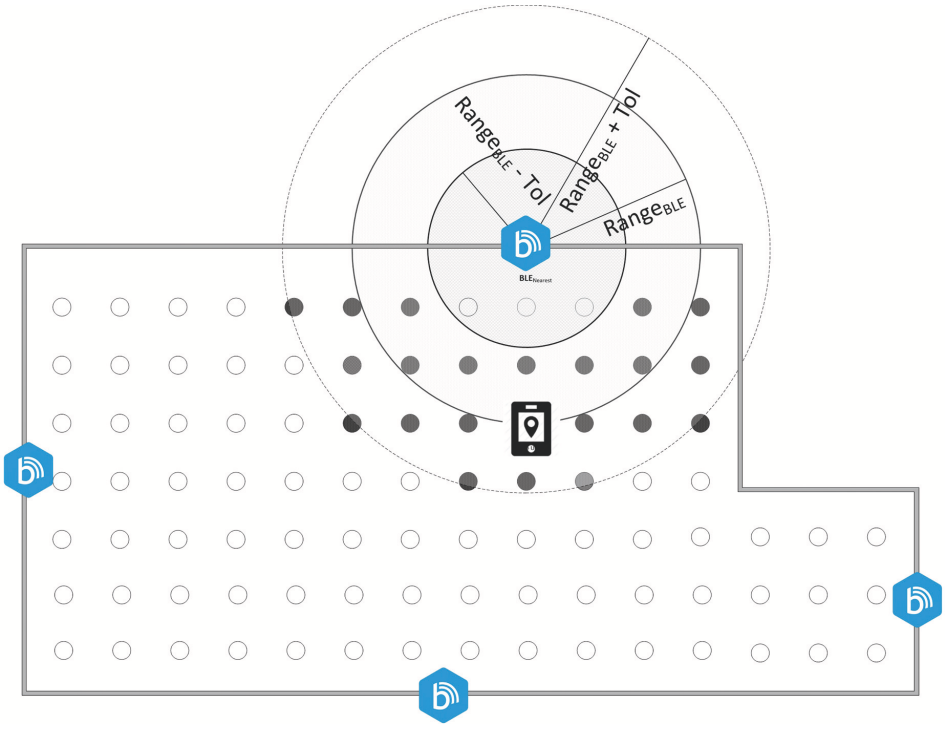

Figure 5.1 – Concept of i-KNN: BLE utilization for Radiomap Subset Generation

Tol can be either a constant number, as in this research work, or it can be dynamically calculated as a percentage $b\%$ of the distance information: $\pm Range_{BLE_i} * b\%$. In the latter case, the closer the MS user is to the BLE, the smaller the Tol will be, and hence a smaller optimized dataset will be selected. This methodology is a more optimized, since the BLE-MS user distance calculation is more reliable at smaller distances. In either case, upon calculation of area A, the optimized dataset $S : \{\ell_1, \ldots, \ell_k\}$, is extracted by utilizing the pre-calculated distances retrieved from $L : \{r_{\ell_1,BLE_1} \ldots, r_{\ell_j,BLE_i}\}$ matrix. Finally, instead of utilizing the larger initial *radiomap* D, the much smaller dataset S feeds the typical *KNN* methods in order to estimate the location of the MS user.

5.2.1.2. ***i-KNN in Pseudocode Form.*** To clarify the flow of the procedures, *i-KNN* is presented in the form of a pseudocode:

Algorithm 5.2.1: BLE FILTER(

$$D : \{\ell_1, \ldots, \ell_j\}_{WiFi}, B : \{BLE_1 \ldots, BLE_i\}$$

)

procedure FINGERPRINTS TO BLE DISTANCE(D, B)
for $i \leftarrow 1$ **to** n_B
for $j \leftarrow 1$ **to** n_D
r_{ℓ_j, BLE_i}
return $(L : \{r_{\ell_1, BLE_1} \ldots, r_{\ell_j, BLE_i}\})$

procedure BLE DISCOVERY(B)
for $i \leftarrow 1$ **to** n_{BLE}
do
if $(BLE_i \in \mathcal{B})$
then { Retrieve BLE Parameters; Sort BLEs based on Nearest
return $(BLE_{Nearest}{:}ID, RSSI, Range)$

. . . **main**
comment: Calculate BLE - Fingerprints distances
output (FINGERPRINTS TO BLE DISTANCE(D, B))
comment: Calculate filtering criteria
output (BLE DISCOVERY(B))
while $(BLE_{Nearest} != null)$
do
{ **for** $i \leftarrow 1$ **to** n_B
if $(BLE_i == BLE_{Nearest})$
then
{ **comment:** Calculate Tolerance (Tol) in [m]
$Tol \leftarrow \pm Range_{BLE_i} * b\%$
comment: Calculate Subset of Radiomap D (S)
for $j \leftarrow 1$ **to** n_L
if $((Range_{BLE_i} + Tol \leq r_{\ell_j, BLE_i})$
or $(Range_{BLE_i} - Tol \geq r_{\ell_j, BLE_i}))$
then $\ell_j \in \mathcal{S}$
return $(S : \{\ell_1, \ldots, \ell_k\})$

5.2.2. Combining IEEE 802.15.7 with 802.11

In the case of utilizing the VLC technology, as a rule of thumb it is considered that the minimal smart lighting deployment on the specific environment, is always less than 1/3 of the total number of smart lights that are required in VLP deployments. This means that depending on the space segmentation, the number of required smart lights may vary. However, in all cases, instead of deploying dense and expensive smart lighting grids that are necessary for achieving continuous overlapping of rays from several smart lights, a single light per room is required. In wide and open-plan environments, the required number of lights depends on several factors, such as the smart light transmit power (P_{Tx}), the Receiver Field of View (FOV) and sensitivity, the existence or not of concentrating/optical lens, installation height etc. Recalling Figure 2.5, typical receivers with a FOV of 160 $^{\circ}(FOV = 2 * \phi)$, when deployed at a clear ceiling-user height of $2.0m$, can cover an area of radius of approximately $11.5m$ (total coverage of 404 m^2), assuming that the illumination power is adequate.

5.2.2.1. ***vlp-KNN Algorithm Explanation***. The concept of the proposed *vlp-KNN* algorithm is analogous to the *i-KNN*: to utilize the data received from a local smart light (RSS, and/or TOF, AOA) in order to roughly estimate a probable area A enclosing the user's position. In this scenario, the aforementioned donut-shape area A, is formulated between a minimum and a maximum Radius ($R_{SL_{min}}$ and $R_{SL_{max}}$) from the the Smart Light (SL) location, taking into consideration a predefined tolerance (Tol) to accommodate any positioning error factors. As illustrated in Figure 5.12, Area A is then used to narrow down the number of candidate fingerprints to a subset ($S : \{\ell_1, \ldots, \ell_k\}$) extracted from the initial IEEE 802.11 fingerprint dataset ($D : \{\ell_1, \ldots, \ell_j\}_{WiFi}$). The filtered fingerprint data subset S is finally used as input, when implementing the typical indoor positioning algorithms (in this case the KNN).

The proposed methodology serves two purposes: Firstly, fast positioning estimation due to the utilization of a fragment of the initial fingerprint dataset and secondly improved positioning accuracy by minimizing any possible calculation errors to a very specific area A, where the user is actually located. The latter achievement is a result of the VLP property to rely only on Line of Sight rays, avoiding multipath effects. For clarity, a self explanatory pseudocode of the algorithm used to calculate the subset $S : \{\ell_1, \ldots, \ell_k\}$ is presented in algorithm 5.2.3. Finally, it is noted that all distances between SLs and all fingerprint locations are pre-calculated, for easier estimation of the subset S.

5.2.2.2. ***vlp-KNN in Pseudocode Form.*** The *vlp-KNN* filtering procedure flow is presented in the form of a self-explanatory pseudocode.

Algorithm 5.2.3: VLP-FILTER(

$$D : \{\ell_1, \ldots, \ell_j\}_{WiFi}, SL : \{SL_1 \ldots, SL_i\}$$

)

procedure FINGERPRINTS TO SL DISTANCES(D, SL)
comment: Calculate distances between all ℓ_i and SL_i
for $i \leftarrow 1$ **to** n_{SL}
for $j \leftarrow 1$ **to** n_ℓ
r_{ℓ_j, SL_i}
return $(L : \{r_{\ell_i, SL_1} \ldots, r_{\ell_j, SL_i}\})$

procedure IN RANGE SL RADIUS(SL)

for $i \leftarrow 1$ **to** n_{SL}
do
if $(SL_i \in \mathcal{SL})$
then
- Retrieve In Range SL Parameters
- $SL_{InRange}$, X_{SL}, Y_{SL}, Z_{SL}
- $AOA_{SL}, RSSI_{SL}$
- Calculate Estimated Smart Light Radius (R_{SL})
- $R_{SL} = \frac{Z_{SL} - Z_{User}}{\tan(90 - AOA_{SL})}$

return $(SL_{InRange}, R_{SL})$

. . . **main**
comment: Calculate SL - Fingerprints distances
output (FINGERPRINTS TO SL DISTANCES(D, B))
output (IN RANGE SL RADIUS(SL))
while $(SL_i! = null)$
do
- **for** $i \leftarrow 1$ **to** n_{SL}
- **if** $(SL_i == SL_{InRange})$
  - **then**
    - **comment:** Calculate Tolerance (Tol) in [m]
    - $Tol \leftarrow \pm R_{SL_i} * b\%$
    - **comment:** Calculate Subset of Radiomap D (S)
    - **for** $j \leftarrow 1$ **to** n_L
    - **if** $((R_{SL_i} + Tol \leq r_{\ell_j, SL_i})$ **or** $(R_{SL_i} - Tol \geq r_{\ell_j, SL_i}))$
      - **then** $\ell_j \in \mathcal{S}$

return $(S : \{\ell_1, \ldots, \ell_k\})$

5.3. ϕ-map Experimental Positioning Platform

Within the research work of this thesis, it was soon realized that an agile, modular fingerprint-based localization platform was needed, for testing and evaluating any newly developed algorithms or methodologies, including *i-KNN* and *vlp-KNN*. For this reason, an Android experimental platform was designed and developed, dubbed as *ϕ-map*. The platform provides access to numerous smart phone sensors and parameters related with the configuration/parameterization of both offline and online localization phases. It also provides flexibility in database management, positioning algorithm editing and User Interface (UI) setup. In the following Sections, a brief overview of ϕ-map characteristics and capabilities is presented.

5.3.1. ϕ-map Parameters

As discussed previously, *ϕ-map* provides access to a number of general parameters related with the management of the deployment environment, as well as the handling of wireless network parameters, as it is depicted in Figure 5.2.

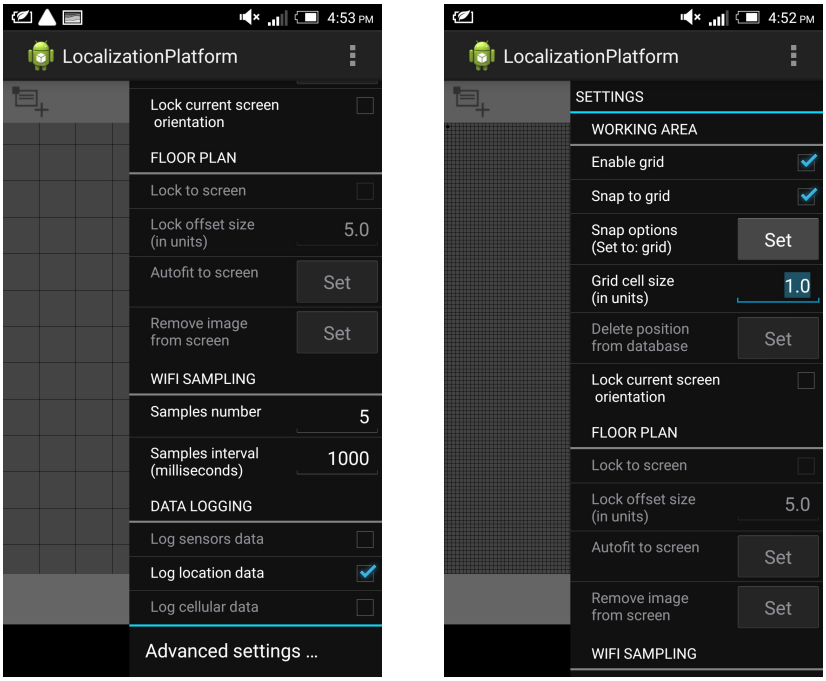

(a) *ϕ-map*: Parameters - Part 1 **(b)** *ϕ-map*: Parameters - Part 2

Figure 5.2 – *ϕ-map*: Parameters

The user is able to enable or disable an automated snap-on grid, to set the grid size and to upload a background blueprint of the study area. There is also a

provision for defining an offset to the blueprint, auto-fit to the screen, and auto-rotate. In this way the UI can be customized according to the preferences of the user. Concerning the general radio parameters, we can set the sampling interval time, the number of samples utilized for positioning purposes and the number of samples registered per position during the offline phase. Finally, a very important capability of *ϕ-map* is data logging of a wide range of parameters related to i. the localization procedure, ii. MS sensors data and iii. cellular network data. Data logs can be retrieved at any point by the researcher and analyzed in more detail in order to identify patterns, correlations and behaviours that will support performance improvement of the RTLS. Within the general parameters, an option of *Advanced Settings* was added. Through *Advanced Settings*, the user gets access to the activation and recording of a wide range of sensors, the management of multiple sites and databases, as it is depicted in figure 5.3. Through database management the user can either choose to create a new *radiomap*, restore an existing one or perform a backup for security purposes. Each newly created *radiomap* takes the name of the site - as provided by the user - along with the date and exact time stamp. Upon creation and saving of a *radiomap*, the platform can then use the information for positioning estimation.

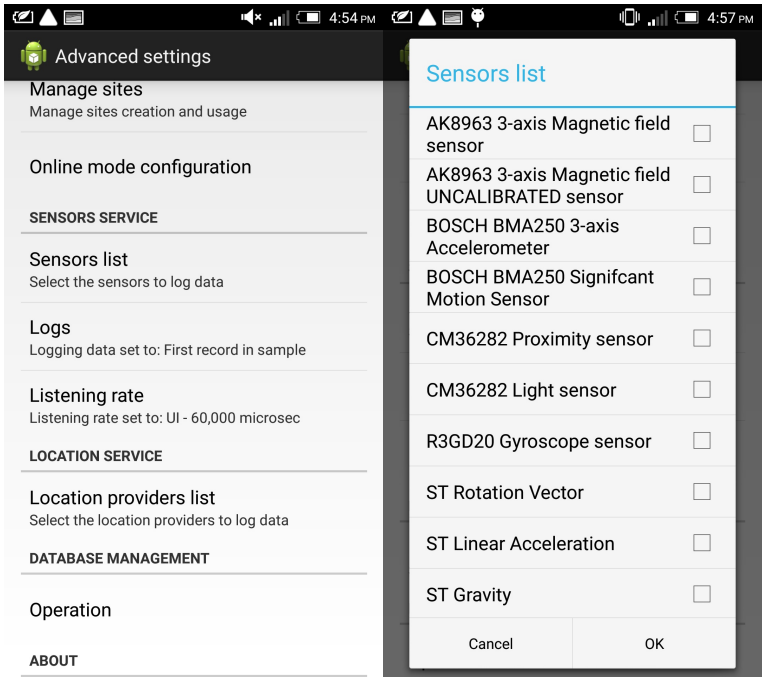

(a) *ϕ-map*: Advanced Settings - Part 1

(b) *ϕ-map*: Advanced Settings - Part 2

Figure 5.3 – *ϕ-map*: Advanced Settings

5.3.2. *ϕ-map* Operation: Offline Phase

As a fingerprint-based localization platform, *ϕ-map* provides the option to create a new *radiomap* through measurements, or to upload a *radiomap* generated through simulation. For the measurement case, the user must select the Offline Mode which can be found under *Advanced Settings*. Upon selection, the UI allows to define by "touch on screen", the measurement location point-by-point, as shown in Figure 5.4. The user moves to any desired measurement point, specifies the exact location on the blueprint and presses action button *SCAN*. The sampling procedure is initiated and the predefined number of samples are recorded into the database. The time required for sampling, is directly related to the sampling rate, which is also defined during the parameterization of the platform. It is also important to note that during the offline phase and the generation of the *radiomap*, the system also records the values retrieved by all active device sensors. The correlation between parameters can be achieved through the utilization of the time-stamp.

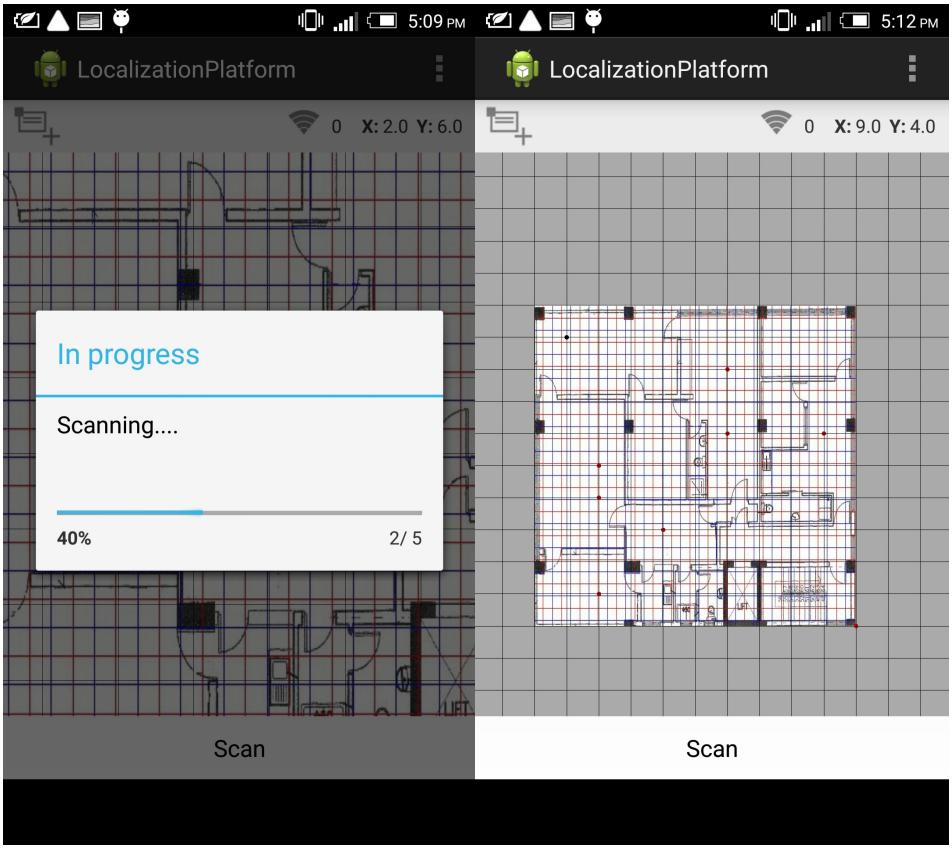

(a) *ϕ-map*: Scanning Mode UI **(b)** *ϕ-map*: Registering Fingerprints

Figure 5.4 – *ϕ-map*: Offline Phase - Scanning Mode

5.3.3. *φ-map* Operation: Online Phase

When a *radiomap* exists inside the database, generated either through measurements or simulation, the user can select the appropriate one which belongs to the area of interest. Through *Advanced Settings*, the user can now select the *Online mode* and immediately the UI switches into the *"Track me"* mode. The location estimation is performed through the selection of the desired positioning algorithm (KNN, *i-KNN*, *vlp-KNN*, WKNN, MMSE, hybrid combination with Cellular parameters etc). Some further system customization is allowed, by defining the sample size and sampling rate, during the sample collection of the online phase. As explained earlier, all data can be recorded and retrieved later for analysis. However, historical data about the user location can be visualized on the platform, as shown in Figure 5.7.

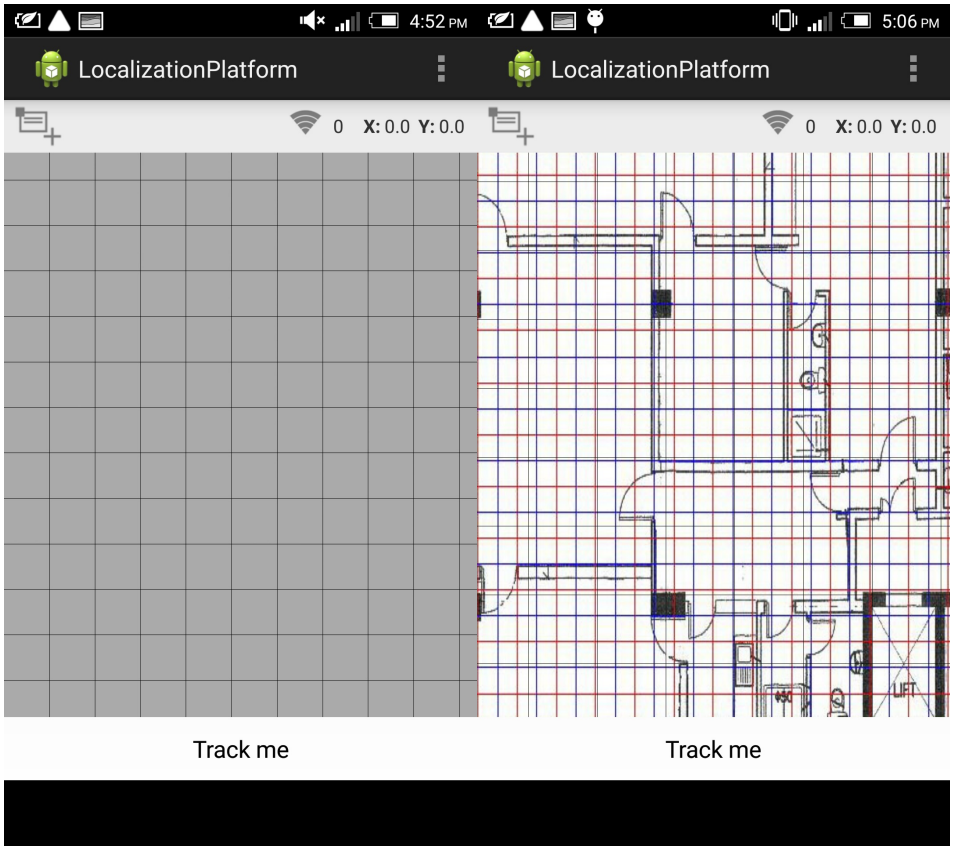

(a) *φ-map*: *"Track me"* mode UI **(b)** *φ-map*: *"Track me"* mode with blueprint

Figure 5.5 – *φ-map*: Online Phase - *"Track me"* mode

5.4. Test Environment

Both *i-KNN* and *vlp-KNN* algorithms were tested by combining actual measurements and simulations on the *ϕ-map* experimental platform. In order to accomplish this task, a *radiomap* was generated by performing a number of measurements in an indoor environment of approximately $250m^2$, while a second *radiomap* was created using *TruNET wireless* [**12**]. The wireless network utilized is composed of 6 D-Link 802.11 APs, deployed as indicated in Figure 5.6.

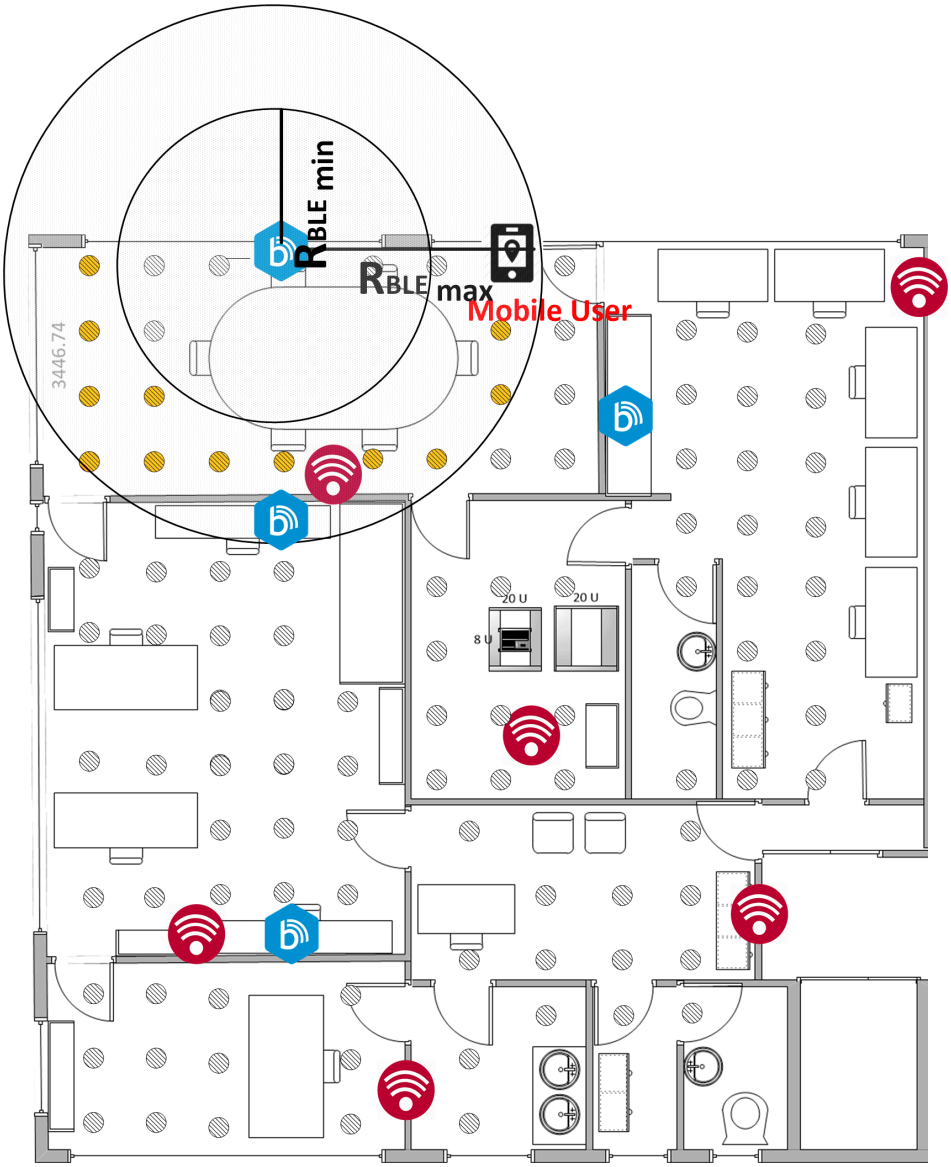

Figure 5.6 – Combined BLE and Wi-Fi Fingerprint-based Indoor Positioning

5.4.1. Radiomap from Actual Measurements

The first *radiomap* was created by measurements collected at 110 equally-spaced ($1m$ spacing) locations, at a constant height of $90cm$. At every measurement point, 30 discreet RSS samples (1 sample/sec) were recorded using an Android-based MS device. The RSS values recorded in the *radiomap* ranged from -99 dBm to -34 dBm. During the network discovering procedure, the system recorded data from 24 APs, due to the existence of other Wi-Fi networks in the proximity of the test environment. Hence a filtering procedure was implemented prior to the finalization of the dataset, leaving only the 6 APs related to the localization experiment in the final radiomap.

5.4.2. Simulated Radiomap

The second *radiomap* was generated using a 3D polarimetric Ray Tracing propagation model, implemented in *TruNET wireless* [**12**]. The building structure and the various furniture were modeled using material constitutive parameters as obtained from literature [**113**]. They were calibrated, as shown in Table 5.1, in order to better match the MS device characteristics. A detailed analysis of the Ray Tracing calibration procedure can be found in [**112**]. The same 110 measurement points, were defined as receiver cells. Finally, the 6 APs were configured as per the characteristics provided by the manufacturers.

Table 5.1 – Material Constitutive Parameters of the Test Environment

Material	**Electrical Permittivity** (F/m)	**Loss Tangent**
Concrete	3.9	0.23
Wood	2	0.025
Brick	5.5	0.03
Metal	1	1000000
Plasterboard	3	0.067
Glass	4.5	0.007

5.4.3. BLE Filtering

Initially, testing measurements were performed by implementing the simple KNN algorithm ($K = 4$) on an IEEE 802.11 typical radiomap, in order to retrieve reference benchmark values, at 12 randomly selected locations. This strategy allowed the authors to perform result analysis that could objectively depict the improvement of the localization accuracy of the positioning algorithms under study. Objective evaluation is achieved through the use of benchmark values by maintaining the external environment unmodified during the experiment execution, keeping the testing locations constant and performing the measurements under static conditions (no mobility allowed). After the retrieval of the benchmark values, the proposed *i-KNN* filtering algorithm was implemented for two different

scenarios, and test measurements were once again performed at the same 12 locations. The first scenario assumed that only one iBeacon device existed in the study area, while the second scenario took into consideration that all 4 iBeacons were deployed, as per Figure 5.6.

In all test cases an average number of 28 samples were collected, in order to ensure that the sample size was large enough for the normal distribution statistical parameters to apply. In other words, the calculated standard deviation values, and consequently any extracted confidence levels, were statistically acceptable and could provide reliable result analysis [**8**]. The user orientation was also examined for investigating the body presence effect. Finally, the influence of iBeacon number and location was also examined, by varying the number of active BLEs. The variation of the localization error in the above cases, defined the maximum tolerance Tol parameter value at $Tol = \pm 2m$. In this way, it was ensured that the user's actual location was falling within the candidate fingerprints chosen in the optimized dataset. Findings were consistent with [**91**], where BLE RSS indication fluctuated up to $10\,dB$. Error factors covered by the introduction of the Tol parameter included the actual number of active BLEs, user/device orientation, body and multipath effects.

5.4.4. VLP Filtering

The proposed *vlp-KNN* filtering algorithm was simulated for every selected test point, introducing a large tolerance $Tol = \pm 2m$, in order to accommodate large positioning errors that may occur in cases of different mobile station orientations, device diversity errors, multipath effects etc. The implementation of the *vlp-KNN* filter assumes that the mobile stations FOV has a LOS with the smart light transmitter, therefore the radius R_{SL} can be calculated either through AOA or RSS optical channel parameters. In case the connection with the VLC is lost, the *vlp-KNN* will function as a conventional KNN algorithm.

5.5. Performance Evaluation

5.5.1. *i-KNN* Algorithm

For the practical implementation and testing of the positioning algorithms *ϕ-map* was utilized extensively, providing configuration capabilities for several parameters related to KNN and *i-KNN* algorithms. The most important parameters include K value, number of samples recorded per point, time interval between each sample and Tolerance (Tol) value. As explained in Section 5.3 and illustrated in Figure 5.7, *ϕ-map* also provides the capability to select between different radiomaps (generated by both actual measurements or simulations) and to upload a 2D blueprint of the study area for user friendly visualization of the user position.

For evaluating these scenarios, the Wi-Fi Indoor Positioning system was fully deployed, and tests were performed at 12 randomly selected locations, as described previously for the benchmark (Wi-Fi only) case and the two hybrid (Wi-Fi and

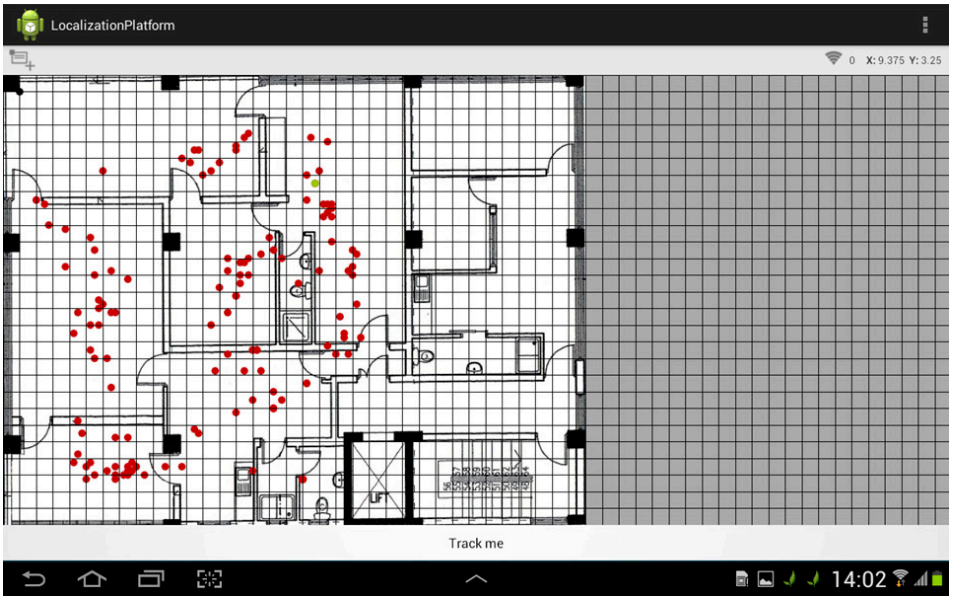

Figure 5.7 – *ϕ-map* Localization Platform

BLE) scenarios. Data retrieval was performed with the MS user stationary, in order to retrieve a statistically adequate number of samples allowing a valid statistical analysis. However, both *ϕ-map* platform and *i-KNN* algorithm can support real time moving MS users. The experimental results concerning the positioning error of the platform utilizing only the IEEE 802.11 radiomap, and implementing the typical KNN algorithm, are presented in Table 5.2. An average positioning error of $e = 4.05m$ with standard deviation $\sigma = 2.13$ is achieved for the specific environment under study. The findings of the benchmark case are aligned with the performance of other typical Wi-Fi indoor localization systems, a comparison of which is illustrated in Table 5.3. A general conclusion extracted from the aforementioned table, is that typical RSS fingerprint-based positioning systems can provide an accuracy ranging from $3m$ to $7m$, practically meaning a typical room level designation.

Test results for the first hybrid scenario (existence of a single BLE device) are shown in Table 5.4. The positioning error e is improved to $3.07m$ with a smaller standard deviation of $\sigma = 1.60$, while the utilized fingerprint dataset size is reduced to an average of 67%. At 5 out of 12 test points the *i-KNN* algorithm utilized the total number of fingerprints as included in the initial *radiomap*, since no BLE signal was identified in these specific locations, due to wall attenuation effects. Although BLE signals could penetrate single plasterboard walls and double glass windows, they were heavily weakened when transmission occurred through cement and brick walls. In those 5 test points, *i-KNN* algorithm did not have any effect and ϕ-map operated as a **Wi-Fi only** platform. During the second

Table 5.2 – Positioning Error of Wi-Fi RSS Fingerprint-based Positioning System

Test Point	$e_{average}(m)$	σ	*Radiomap size (%)*	*Samples No*
1	5.09	2.96	100	19
2	2.45	1.79	100	21
3	3.81	2.15	100	21
4	4.70	3.76	100	20
5	4.15	2.56	100	25
6	6.55	2.26	100	23
7	5.21	2.02	100	16
8	2.91	1.56	100	29
9	5.61	2.02	100	37
10	3.50	1.58	100	50
11	3.02	1.01	100	30
12	2.58	1.72	100	45

Table 5.3 – Positioning Error of Typical Indoor Wi-Fi Positioning Systems

System	*Accuracy/Error*	**Methodology**	**Complexity**
TIX[**115**]	$5.4m$	*Linear mapping of RSS*	*Light algorithm with AP modifications*
EZ [**116**]	$2.0 - 7.0m$	*Model based*	*Complex algorithm*
SDM [**117**]	$3m$	*Linear mapping of RSS*	*Light algorithm with sniffers*
Zee [**118**]	$3m$	*RSS fingerprints*	*Combined with Horus or EZ*
LiFS [**119**]	89% *room level*	*RSS fingerprints*	*Complex training phase*
WILL [**120**]	86% *room level*	*RSS fingerprints*	*Complex mapping of virtual floor*
ϕ-***map*** [**5**]	$4.05m$	*Wi-Fi RSS fingerprints*	*Light algorithm*
ϕ-***map*** [**5**]	$2.33m$	*Wi-Fi-BLE RSS fingerprints*	*Light algorithm*
AnyPlace [**121**]	$1.96m$	*Wi-Fi crowd-sourcing-based fingerprint collection*	*Light algorithm*

hybrid scenario, the full deployment of the BLE devices ensured that location information from at least one iBeacon was retrieved in all 12 test locations. Test results of this scenario are presented in Table 5.5. A radical improvement of the positioning accuracy and optimization of the utilized dataset was observed. More specifically, the error was reduced to $2.33m$ for the same study area, indicating

an improvement of 42%. Standard deviation was also significantly reduced to 1.22, depicting the much higher concentration of results around the mean values of positioning results. Additionally, the utilized dataset size was significantly reduced, ranging between 12% and 37%, depending on the test point. Taking into consideration the comparison Table 5.3, it is observed that the proposed *i-KNN* algorithm over-performs the typical Wi-Fi localization platforms. As a price for increased accuracy, the RTLS operators need to deploy a number of BLE systems to cover the maximum area of interest. Obviously, such a deployment depends on the complexity of the indoor environment; open-plan spaces require less BLE devices than wall-separated areas.

Table 5.4 – Positioning Error of Combined BLE (single BLE) and Wi-Fi RSS Fingerprint-based Positioning System

Test Point	$e_{average}(m)$	σ	*Radiomap size* (%)	*Samples No*
1	1.60	1.22	29	19
2	2.62	1.75	53	21
3	2.77	2.01	38	21
4	3.63	2.65	45	20
5	3.64	2.35	40	25
6	2.17	2.16	39	23
7	5.21	2.02	100	16
8	2.91	1.56	100	29
9	3.20	1.90	69	37
10	3.50	1.58	100	50
11	3.02	1.01	100	30
12	2.58	1.72	100	45

Figures 5.8 and 5.9 provide a visual performance comparison for the first scenario.

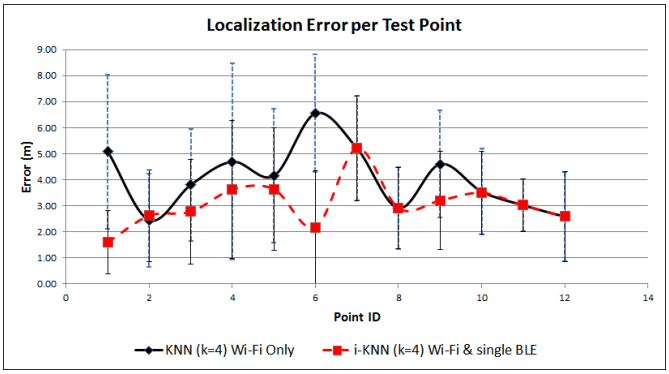

Figure 5.8 – Positioning Error Comparison: Wi-Fi only vs single BLE and Wi-Fi

Table 5.5 – Positioning Error of Combined BLE (all deployed BLEs) and Wi-Fi RSS Fingerprint-based Positioning System

Test Point	$e_{average}(m)$	σ	*Radiomap size (%)*	*Samples No*
1	1.96	1.44	22	19
2	1.70	0.93	12	21
3	1.22	0.81	12	21
4	1.52	0.62	16	20
5	2.38	1.14	12	25
6	2.12	0.63	16	23
7	2.33	0.67	16	16
8	2.91	0.65	12	29
9	3.84	1.89	37	37
10	3.17	0.79	22	50
11	2.97	1.26	28	30
12	1.87	0.55	19	45

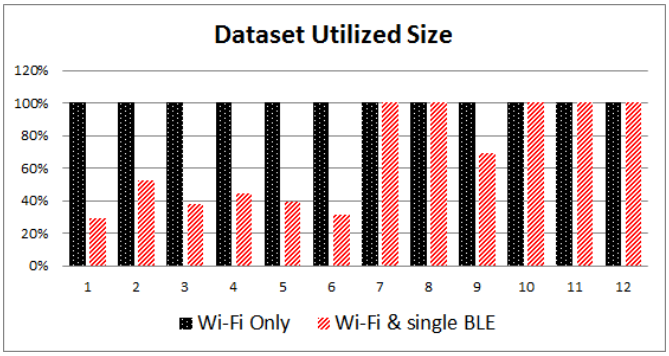

Figure 5.9 – Fingerprint Dataset Size Utilization: Wi-Fi only vs single BLE and Wi-Fi

Figures 5.10 and 5.11 refer to the outcomes of the second scenario. What is obvious from the graphs is that, the combination of Wi-Fi and BLE systems in the proposed *i-KNN* algorithm constantly outperforms the simple KNN, especially when the BLE deployment is such that it can provide adequate signal coverage in the study area. In such scenarios, accuracy is improved and positioning results fluctuate much less, as indicated by the lower standard deviation. Dataset utilization is optimized to an average of 20% for typical scenarios and can be further improved if the set Tolerance Tol factor is further optimized to a minimum value. Overall, the findings provide hard evidence that the proposed *i-KNN* algorithm improves the computational and processing requirements, provides faster and more accurate positioning and incurs lower power consumption.

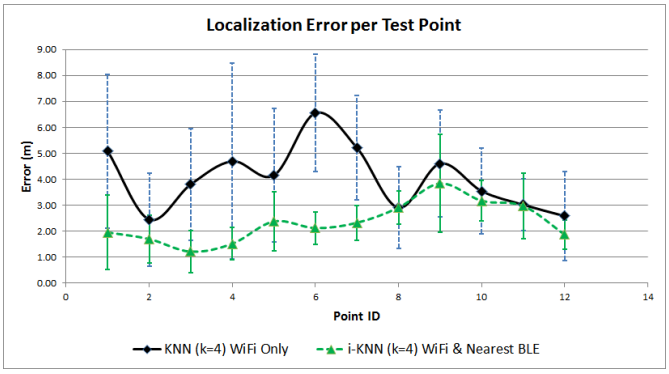

Figure 5.10 – Positioning Error Comparison: Wi-Fi only vs nearest BLE and Wi-Fi

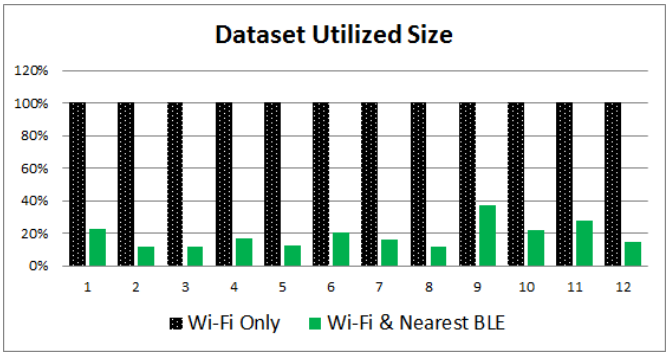

Figure 5.11 – Fingerprint Dataset Size Utilization: Wi-Fi only vs nearest BLE and Wi-Fi

5.5.2. *vlp-KNN* Algorithm

The Wi-Fi Indoor Positioning system was fully deployed, and tests were performed at 7 randomly selected locations, distributed across the whole study area, as shown with X mark in Figure 5.12.

At each test location both simple KNN and proposed *vlp-KNN* algorithms were implemented to estimate user position. The experimental results concerning the positioning error and the utilized fingerprint dataset size, are presented in Tables 5.6 and 5.7 respectively. Figures 5.13 and 5.14 provide a visual comparison between the two methods. A significant improvement on the localization accuracy is observed, from a $4.7m$ average error, the proposed algorithm recorded $1.89m$. The standard deviation σ also appears to be much smaller, pinpointing less fluctuations on the overall system performance. Finally, the utilized fingerprint dataset is reduced to approximately 20% of the initial dataset size. This finding means less computational and processing requirements, faster positioning and less power consumption.

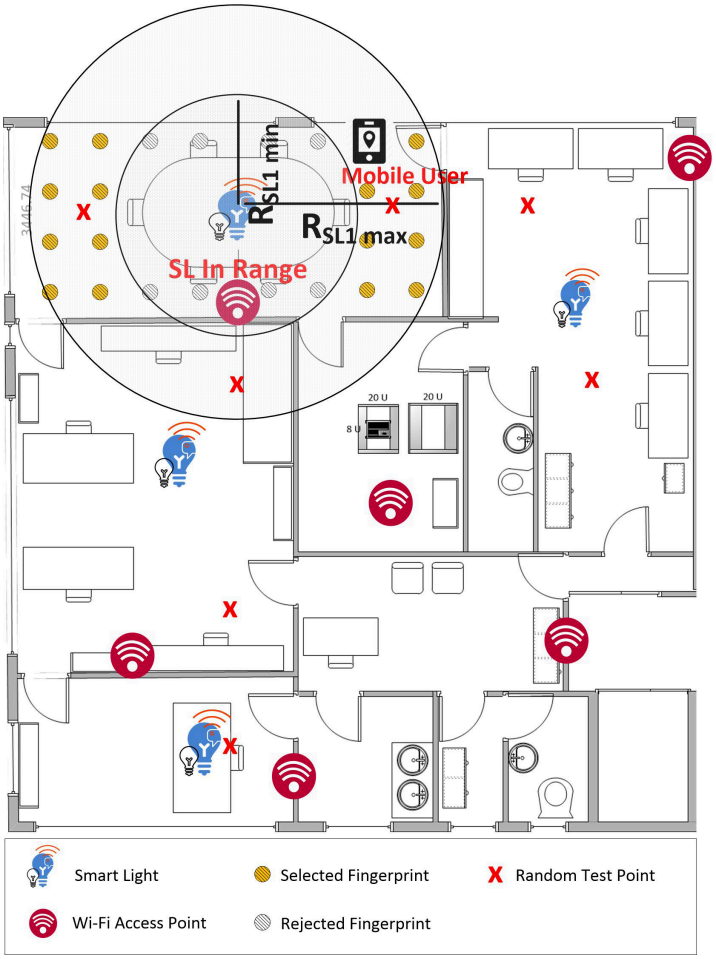

Figure 5.12 – Combined VLP and Wi-Fi Fingerprint Based Indoor Positioning

Table 5.6 – Positioning Error of Wi-Fi RSS Fingerprint-based Positioning System

Test Point	$E_{average}(m)$	σ	$RadiomapSize(\%)$
1	5.09	2.96	100
2	2.45	1.79	100
3	3.81	2.15	100
4	4.70	3.76	100
5	4.15	2.56	100
6	6.55	2.26	100
7	5.21	2.02	100

Table 5.7 – Positioning Error of Combined VLP and Wi-Fi RSS Fingerprint-based Positioning System

Test Point	$E_{average}(m)$	σ	$RadiomapSize(\%)$
1	1.96	1.44	22
2	1.70	0.93	12
3	1.22	0.81	12
4	1.52	0.62	16
5	2.38	1.14	12
6	2.12	0.63	20
7	2.33	0.67	16

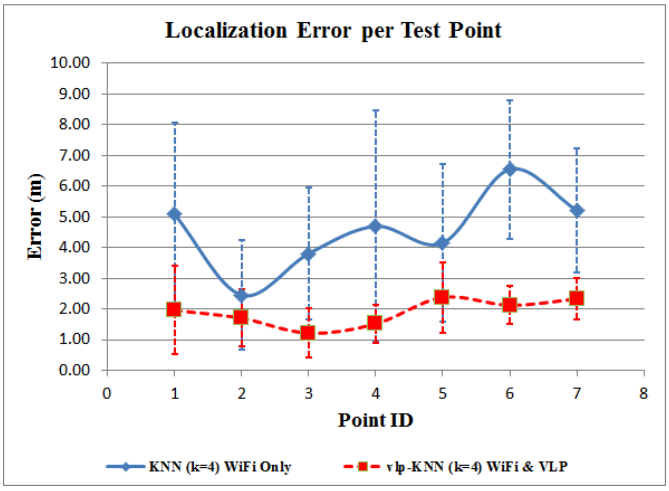

Figure 5.13 – Positioning Error Comparison: Wi-Fi only vs VLP and Wi-Fi

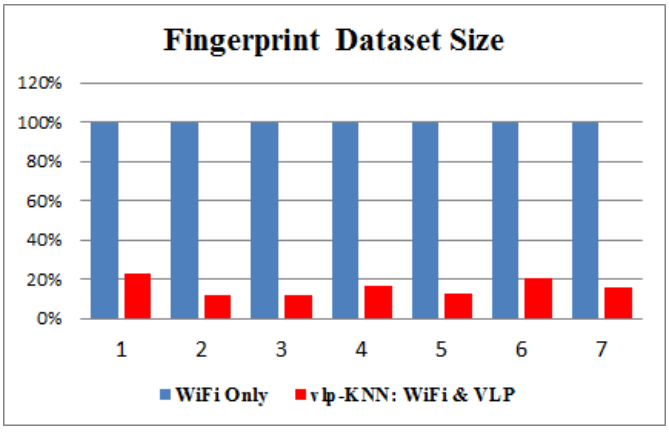

Figure 5.14 – Fingerprint Dataset Size Utilization: Wi-Fi only vs VLP and Wi-Fi

5.6. Conclusion

In this Chapter two novel algorithms were presented aiming in improving indoor localization accuracy and performance of IEEE 802.11 fingerprint-based RLTS, via the fusion of information of a second supporting wireless technology. *i-KNN* and *vlp-KNN* algorithms were the result of Wi-Fi-BLE and Wi-Fi-VLP combination respectively. The aforementioned localization algorithms are based on the same concept: to take advantage of the benefits of each technology and fuse the available information in order to enhance the performance of fingerprint–based indoor localization. Both algorithms are novel and, to the knowledge of the author, no previous research work has been proposed before. Performance evaluation indicates that both algorithms, improve localization accuracy roughly at the same level. This is an expected finding since they both filter in a similar way the same fingerprint dataset that is generated by the same IEEE 802.11 wireless network. Given the fact that a device of the supporting technology was placed in every room of the test environment, it can be safely expected that the subset extracted by the filtering algorithms concerned the fingerprints of the respective room. Consequently, the conventional KNN positioning algorithm was fed with almost the same input and for this reason the localization accuracy was similar. Computational performance increase was indicated by the reduction of the utilized dataset size, to a range between 12% and 37% of the initial radiomap size. A significant improvement in localization accuracy was also recorded and reached a 42%. The scalability of both *i-KNN* and *vlp-KNN* algorithm makes them ideal for advancing the performance of existing fingerprint based RTLS systems.

CHAPTER 6

Utilizing Polarization for Single Access Point Indoor Positioning

6.1. Introduction

A significant drawback of fingerprint-based localization systems, is that they require the deployment of several APs in order to generate a combination of unique fingerprints at each location and achieve satisfactory positioning accuracy [**9**]. Due to this characteristic, fingerprint-based localization applications and platforms cannot be easily utilized in small indoor environments (i.e., residential places or open-plan business spaces), where typically only a single AP is being deployed.

This Chapter focused on generating unique fingerprint datasets from a single Multiple Input, Multiple Output (MIMO) AP, by utilizing the antenna polarization effects arising from a single AP, and fusing the data retrieved from multiple antennas into a *multi-layered radiomap* concept. Extended analysis indicated that each antenna of the MIMO device, can be considered as an independent transmitting source. Different polarization configurations are then taken into account in order to ensure that RSS values from different antennas, at the same location, are not correlated. In this way, data retrieved from each antenna is fused to generate a single *multi-layered radiomap*, which has been found to perform satisfactory in terms of accuracy, when utilized in an RSS-based localization system.

The proposed method's performance is evaluated in a two-step procedure. Initially, by implementing deterministic and probabilistic algorithms (Weighted k-Nearest-Neighbour - WKNN, and Minimum Mean Square Error - MMSE, respectively), for a set of different antenna orientations, hence different polarization set-ups. Secondly, the uniqueness of all candidate radiomaps is examined, by calculating the correlation level of each fingerprint pair. High correlation scores indicate a high probability for localization errors and vice versa. This method requires the implementation of the "*Tolerance Based - Normal Probability Distribution* (TB-NPD)" algorithm [**9**]. The polarization mechanisms and the related research work regarding their utilization in localization are analyzed in Chapter 2, Section 2.3.

6.2. Proposed Approach

6.2.1. High Level Description of the Proposed Approach

In this Chapter, a new localization approach based on a single MIMO AP where each AP antenna acts as a separate transmitter is presented. The RSS

values consisting the fingerprint *radiomap* were purposely manipulate by carefully configuring each antenna orientation and polarization, and then fuse the retrieved information together, generating a *multi-layered radiomap*. A *Multi-layered radiomap* is defined as the unified dataset created from the fusion of RSS and antenna identification data received by each MIMO antenna. In order to achieve such a task, the MIMO AP should support and be able to be injected with a mechanism - such as *Radiotap* - which offers the capability to retrieve the additional information about frames, from the device driver into user-space applications. In this respect, *Radiotap* defines - among others - two important fields that are important for this approach: *Antenna*, a unit-less indication of the Rx/Tx physical antenna for each packet, and *Antenna Signal*, that provides the value of the RF signal power at the antenna. A typical code snippet of transmit definitions for the Atheros driver is presented below:

```
#define ATH_TX_RADIOTAP_PRESENT (                    \
    (1 << IEEE80211_RADIOTAP_TSFT)                   | \
    (1 << IEEE80211_RADIOTAP_FLAGS)                  | \
    (1 << IEEE80211_RADIOTAP_RATE)                   | \
    (1 << IEEE80211_RADIOTAP_ANTENNA)                | \
    (1 << IEEE80211_RADIOTAP_DBM_TX_POWER)           | \
    (1 << IEEE80211_RADIOTAP_XCHANNEL)               | \
    0)

struct ath_tx_radiotap_header {
    struct ieee80211_radiotap_header wt_ihdr;
    uint64_t    wt_tsf;
    uint8_t     wt_flags;
    uint8_t     wt_rate;
    uint8_t     wt_antenna;
    uint8_t     wt_txpower;
    uint32_t    wt_chan_flags;
    uint16_t    wt_chan_freq;
    uint8_t     wt_chan_ieee;
    int8_t      wt_chan_maxpow;
}
```

Having fulfilled the requirement of antenna identification and the respective RSS retrieval, the candidate radiomaps are then generated utilizing a fully deterministic simulator. *TruNET wireless* simulation tool [**12**] was utilized in the trials. On top of this simulator, a set of modules were developed to support the implementation of the following steps: i. Environment design and wireless network set-up, ii. Candidate radiomap generation, and iii. Iterative simulation and evaluation of each candidate radiomap.

Initially, the area of interest is designed in *TruNET wireless* simulator, taking into account the different building structure geometry, dimensions and material constitutive parameters. Then a list of different scenarios is created by configuring

the wireless network antennas. The wireless network, as discussed previously, is considered to be a single MIMO Access Point (AP) with a minimum of two antennas.

Afterwards, a simulation takes place for each scenario; and a candidate *multi-layered radiomap* is generated based on fused antenna information. More specifically, each AP antenna is considered as a separate transmitter and the calculated RSS values are registered in the receiver cells linked with the transmitter (antenna) ID. Depending on the scenario set-up (different antenna orientation and polarization), the RSS values vary. Finally, the candidate radiomaps are exported in a standardized template form and are passed forward for localization accuracy assessment. In order to perform the assessment, a testing dataset sample is required, which is a set of RSS fingerprints that could be retrieved either during an online phase, or can be generated through a simulator.

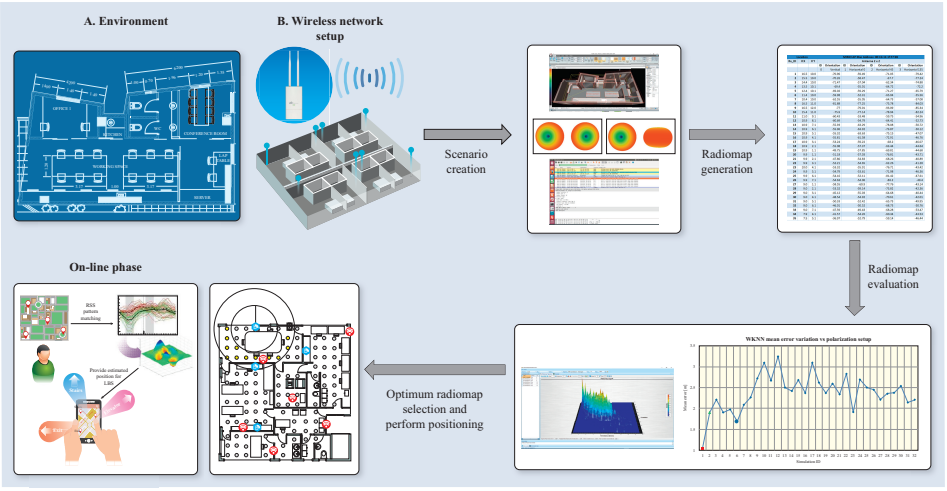

Figure 6.1 – Concept Illustration

The sample dataset size and distribution are selected in such a way so that they provide reliable and objective testing results, as per [**8**]. The localization procedure followed includes two types of localization algorithms: a deterministic (WKNN) and a probabilistic (MMSE). Each candidate radiomap is tested and its performance is evaluated with respect to the localization accuracy than it can achieve. At the last stage of the procedure, the correlation between the fingerprints in the dataset is examined and an overall correlation score for the candidate radiomaps [**9**] is provided. A high correlation score designates a higher probability for localization errors due to similarities existing between different fingerprints (locations). After the completion of the aforementioned iterative procedure, the most suitable radiomap among the candidates is selected. The selection is based on two performance metrics: minimum mean localization error and minimum correlation score. The previously described procedure is illustrated in the high level descriptive illustration of Figure 6.1.

6.2.2. Investigation of Polarization Effect in Radiomaps

Since the proposed approach relies heavily on the utilization of polarization mechanisms for optimizing the RSS datasets, its impact should be isolated and investigated in more depth. In order to eliminate any other factors that may affect the RSS indications in the receiver cells, a number of scenario set-ups is considered, simulated without any obstacles or ground effect, in pure free space loss conditions. The scenarios involve only one set of a Transmitter (Tx) and a Receiver (Rx) in the area of interest, and assume that they both have theoretical isotropic antennas. In this respect, four scenarios are created, by combining vertical and horizontal antenna polarization setups:

i. Tx: horizontal vs Rx: horizontal
ii. Tx: horizontal vs Rx: vertical
iii. Tx: vertical vs Rx: horizontal
iv. Tx: vertical vs Rx: vertical

The generated radiomaps are presented in Figures 6.2 and 6.3.

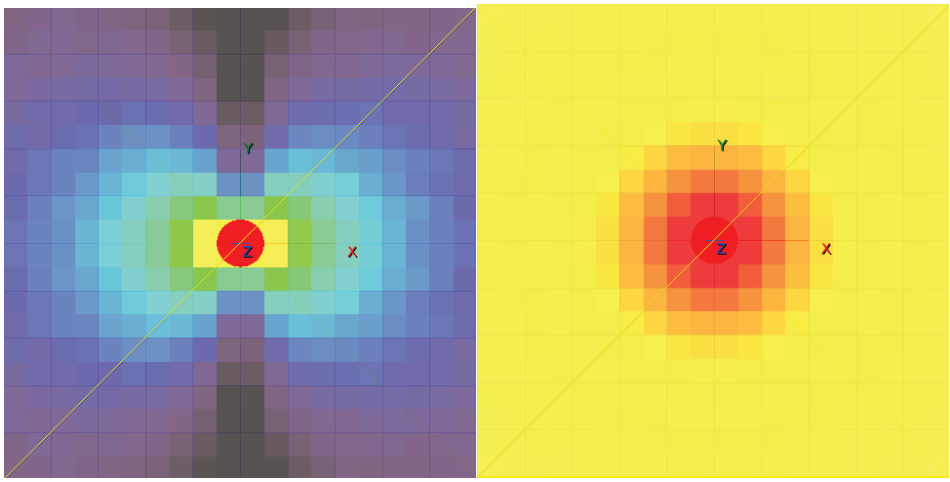

(a) Rx Horizontal **(b)** Rx Vertical

Figure 6.2 – Radiomap for Isotropic Antennas with Vertical Polarization Tx

To further investigate the variation of the RSS in each scenario, it is assumed that a mobile user is moving across the area of interest, following a diagonal path. The path is kept constant for all four radiomaps. Results shown in Figure 6.4 indicate that RSS received across Rx cells, varies significantly when the polarization of the antennas is modified.

6.3. Test Environment

The tests were performed in a laboratory area of approximately $100m^2$ which approximates a typical residential indoor floor, or a 3 bedroom flat. The 3D

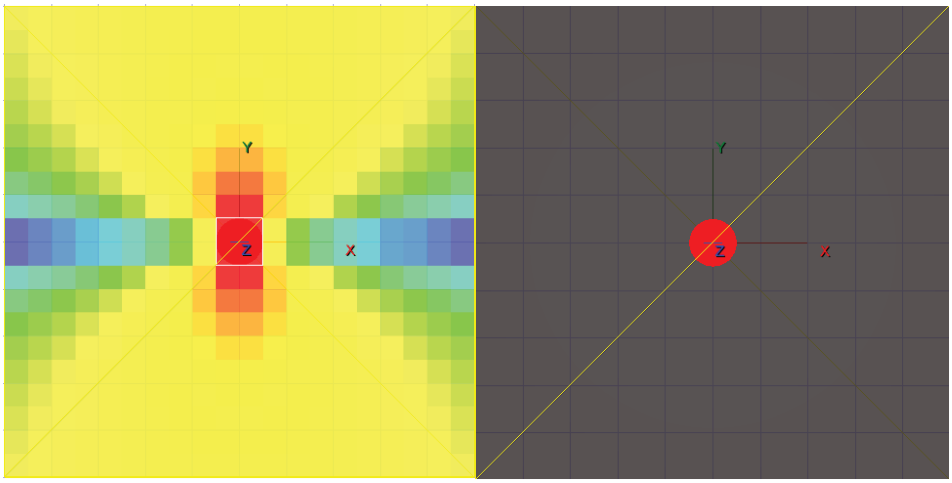

(a) Rx Horizontal **(b)** Rx Vertical

Figure 6.3 – Radiomap for Isotropic Antennas with Horizontal Polarization Tx

environment and the various different wireless network setups were simulated in *TruNET wireless*, a 3D polarimetric Ray Tracing simulator [**12**]. The building structure and large furniture were configured using material constitutive parameters obtained from literature [**113**], as per Table 6.1.

Table 6.1 – Material Constitutive Parameters of the Test Environment

Material	**El.Per.** (F/m)	**L. Tangent**
Concrete	3.9	0.23
Wood	2	0.025
Brick	5.5	0.03
Metal	1	1000000
Plasterboard	3	0.067
Glass	4.5	0.007

The generated candidate radiomaps include 406 receiver cells at a height of $1.2m$, and information retrieved by two antennas from a single 1x2 MIMO AP. The AP was intentionally positioned at the edge of the area of interest, in order to minimize the possibility of creating multiple similar fingerprints due to symmetries in the environment. A series of 12 different scenarios were created by combining different polarization setups - vertical and horizontal - as well as different antenna orientations with a changing step of 45°. The 12 scenario configuration parameters are shown in Table 6.2.

Finally, for reference purposes, a typical scenario (No 1) with five APs was created for the same environment. The radiomap generated was used for localization by implementing WKNN and MMSE algorithms, and the results were compared with the 11, single AP scenarios.

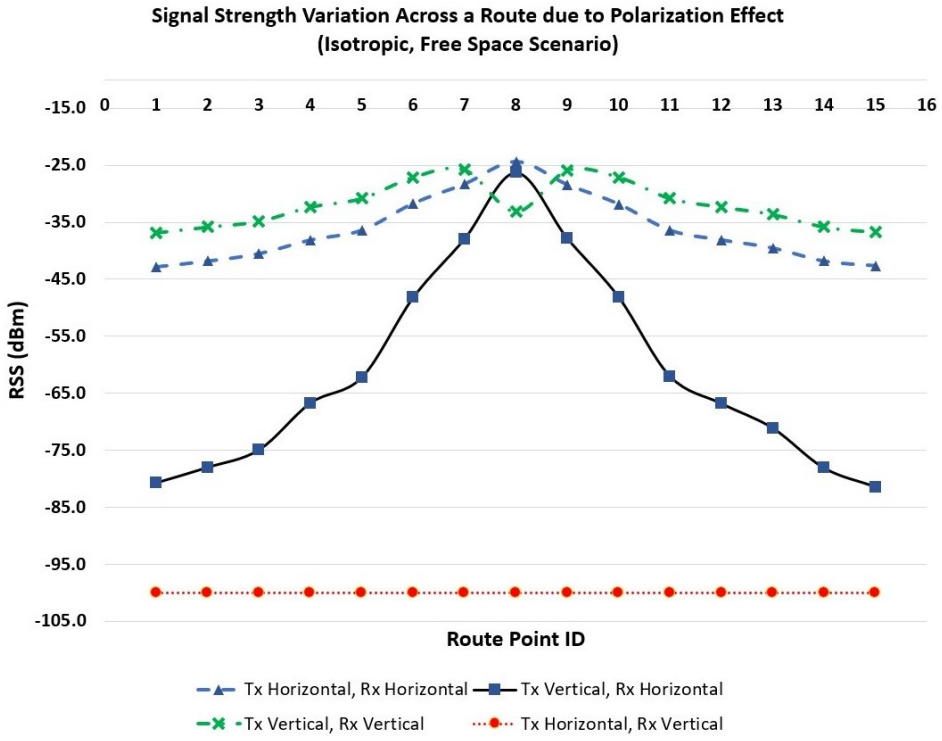

Figure 6.4 – RSS Variation Across a Route

Table 6.2 – Antenna configuration per Scenario ID

Scenario ID	Antenna 1 Polarization	Antenna 2 Polarization
2	V	V
3	H 0°	V
4	H 45°	V
5	H 90°	V
6	H 135°	V
7	H 180°	V
8	H 0°	H 0°
9	H 0°	H 45°
10	H 0°	H 90°
11	H 0°	H 135°
12	H 0°	H 180°

The effect of polarization and antenna orientation on the radiomaps is depicted in the snapshots of Figure 6.5. Figure 6.7 shows the changes in Power Delay Profile (PDP) for a randomly selected cell. It can be easily observed that the ray path's arrival time, and consequently the RSS values, may vary due to the changes in polarization and antenna orientation.

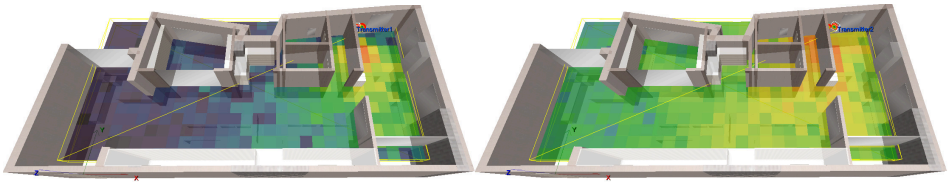

(a) H090Tx1-RSS **(b)** H045Tx2-RSS

Figure 6.5 – Radiomap vs Antenna polarization H090 and H045

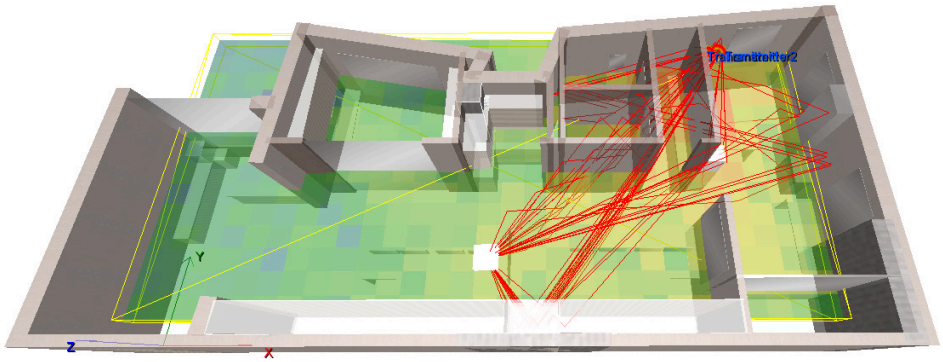

Figure 6.6 – Multipath Effect in Indoor Environment (Rx Cell 198)

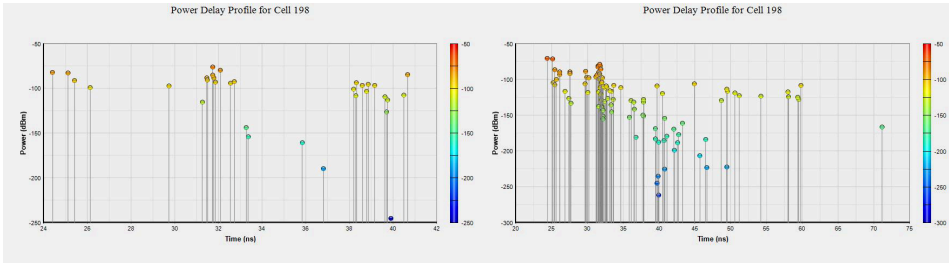

(a) H090Tx1-PDP **(b)** H045Tx1-PDP

Figure 6.7 – Power Delay Profile vs Antenna Polarization H090 and H045

6.4. Performance Evaluation

The proposed methodology was implemented for all 12 scenarios. The calculated mean error and Circular Error Probable (CEP) 95% for both WKNN and MMSE localization algorithms, are presented in Table 6.3 and Figures 6.8, 6.9, 6.10 and 6.11 respectively. The quality Correlation Score (CS) for each radiomap is illustrated in Figure 6.12.

Based on the aforementioned results, a significant variation on the localization accuracy is observed, which depends on the transmitter configuration setup. When implementing WKNN ($k = 4$), the mean error varies from $1.69m$ for scenario No.

Table 6.3 – Localization Algorithm Performance and Correlation Score per Candidate Radiomap

Scenario ID	Decision Factor				Correlation Score
	WKNN Mean Error	WKNN CEP 95%	MMSE Mean Error	MMSE CEP 95%	
2	1.91	3.41	2.17	3.78	0.371
3	2.21	4.27	2.48	4.14	0.440
4	1.91	3.69	2.11	4.19	0.355
5	1.98	3.36	2.49	5.60	0.363
6	1.69	3.45	2.29	4.27	0.314
7	2.09	3.48	2.55	4.37	0.398
8	2.27	6.22	2.82	4.97	0.442
9	2.72	4.45	2.71	4.54	0.525
10	3.01	2.99	3.08	6.07	0.591
11	2.67	9.00	3.09	5.86	0.488
12	3.25	9.85	2.52	5.01	0.657

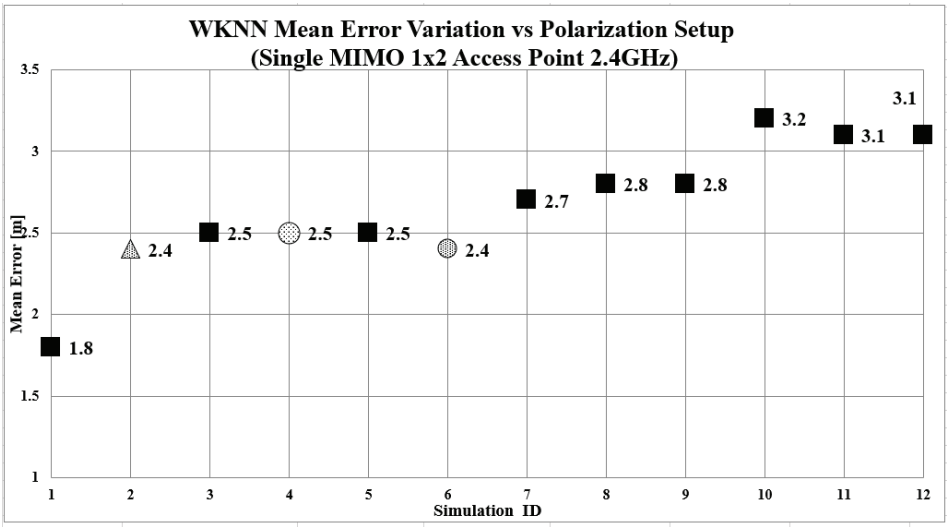

Figure 6.8 – WKNN: Mean Error per Polarization Scenario

6, and $1.91m$ for scenario No. 2 and No. 4, to $3.25m$ for scenario No. 12. A similar behaviour is noted for the mean error achieved when utilizing MMSE ($\sigma = 9$) algorithm. A minimum mean error of $2.11m$ was recorded for scenario No. 4 and $2.29m$ for scenario No. 6, to a maximum of $3.09m$ for scenario No. 11. The quality evaluation of the candidate radiomaps supports the above findings, indicating that the most appropriate radiomaps for indoor positioning utilization are No. 6 ($CS = 0.314$) and No. 4 ($CS = 0.355$). The localization accuracy that can be achieved with the proposed methodology, is comparable to the benchmark scenario No. 1, where 5 APs were used. More specifically, although utilizing the

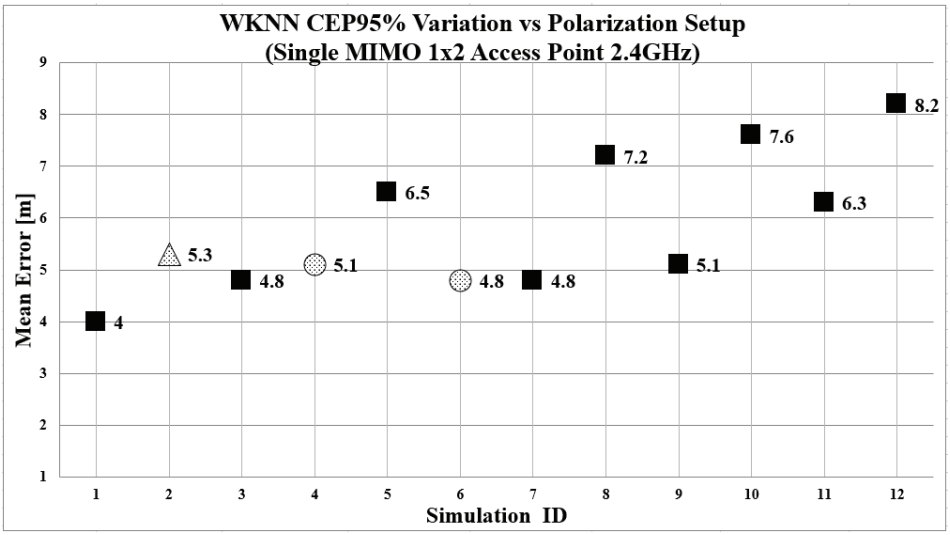

Figure 6.9 – WKNN: CEP95 per Polarization Scenario

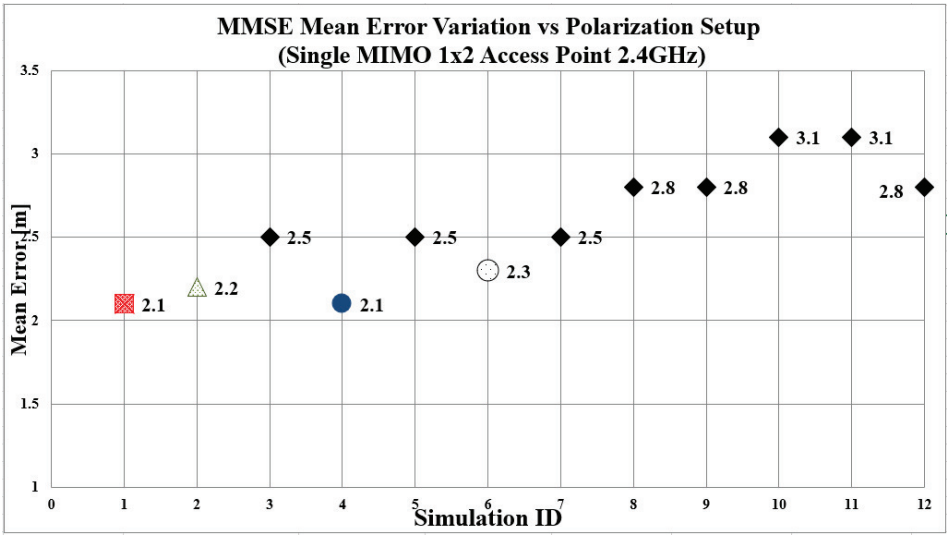

Figure 6.10 – MMSE: Mean Error per Polarization Scenario

information from 5 different APs leads to a minimum of $1.04m$ mean error, still the $1.69m$ error accomplished by a single AP is satisfactory and provides a much more tangible solution for individual residences. Another observation that is worth mentioning, is related to scenario 2, which scored the second best performance. In this scenario, the configuration of both antennas was set to Vertical Polarization. The RSS differences occur only due to the spatial separation of the antennas. On the other hand, it is noted that both scenario No. 4 and scenario No. 6, which performed best, were configured with their antennas having a 45° angle

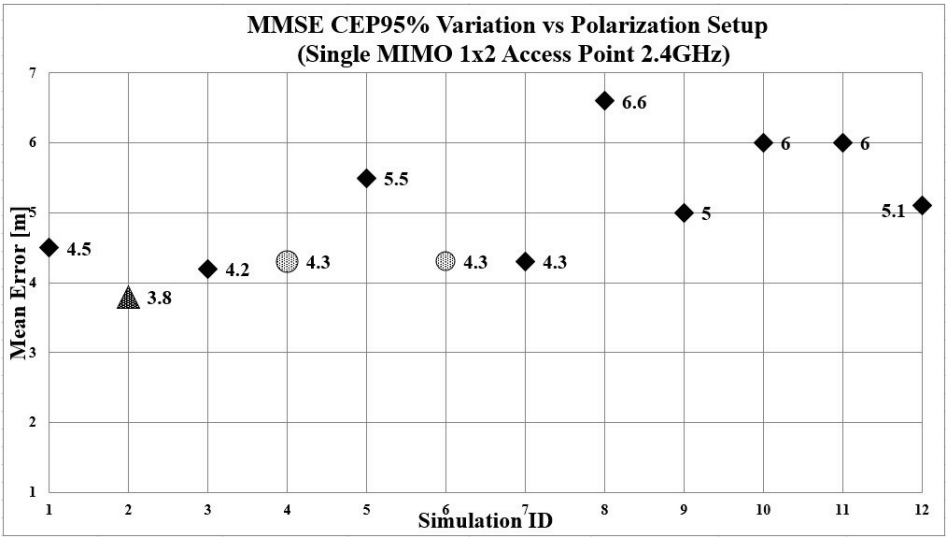

Figure 6.11 – MMSE: CEP95 per Polarization Scenario

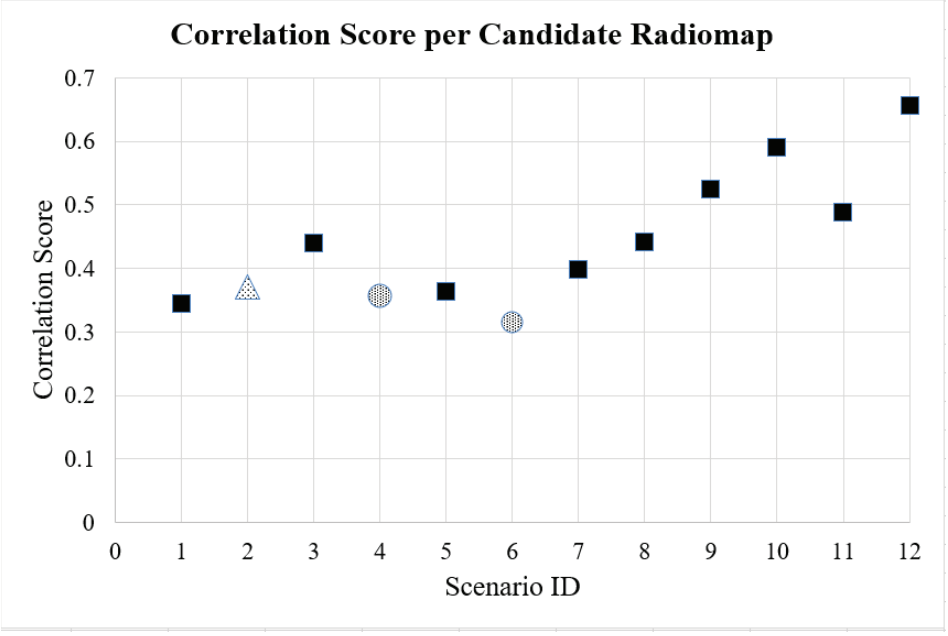

Figure 6.12 – Correlation Score per Polarization Scenario

between them. Finally, it can be safely assumed that by utilizing more complex MIMO devices (i.e., 4x4), and a proper antenna polarization configuration, the localization accuracy achieved can be further improved.

6.5. Conclusion

In this Chapter, a novel approach is presented in performing indoor localization by utilizing a single MIMO AP. The novelty of the approach lies on multiple antenna information fusion, for the purposes of generating a high quality radiomap and utilizing it in an RSS fingerprint-based indoor localization system. Antenna information retrieved is optimized by taking into consideration antenna polarization effects. Testing and evaluation of the proposed methodology indicates that satisfactory localization accuracy can be achieved, providing in this way a more tangible and affordable solution for single AP owners. The research may be further expanded by investigating more complex MIMO device antenna configurations.

CHAPTER 7

Conclusion and Future Work

7.1. Conclusion

Nowadays, outdoor and indoor localization of people, vehicles, equipment and assets is an essential service required by a vast number of applications. In outdoor environments, GNSS is the dominant type of positioning service, but alternative solutions are still vital due to the vulnerability of GNSS to attacks and spoofing of satellite signals. In indoor environments, the research challenges are still very active and ongoing, despite the fact that the research community has been investigating the topic for decades. The rapid technological and computational advances have opened the road for new categories of services and have increased the demand by the users in turns of quality of service and quality of experience. Mobility, accessibility, as well as fast and effective accomplishment of tasks have been the main driving factors in our era. The booming in the IoT and Wireless Sensor Networks (WSN), including Body Sensor Networks (BSN), has also generated new opportunities and demands related to localization as a service.

Numerous positioning techniques and methodologies have been proposed, as described in Section 2. Focusing in the indoor requirements, it was noted that the most popular technique is currently fingerprinting, due to the simplicity of the related positioning algorithms, their satisfactory accuracy, as well as the ability to utilize widely used, off-the-shelf wireless networks, such as Wi-Fi and Bluetooth. The most important disadvantages of fingerprint-based platforms are related to the following:

(1) **Calibration requirements** in order to enable the underlying radiomaps, which are used during the location estimation, to be device-independent.
(2) **Sensitivity to dynamic changes in the environment and interference**, that result in increased mean and maximum positioning errors. Such errors are inflated by the inherent characteristics of fingerprint "best match" methodology.
(3) **Labour intensive and time consuming radiomap generation during the offline phase**. Especially focusing in measurement campaigns, these are becoming less attractive due to their static and inflexible nature.
(4) **Requirement for the deployment of several access points** to serve as transmitting nodes and provide satisfactory distinction between each pair of fingerprints and hence, less positioning errors.

The research work of this thesis was concentrated exactly on providing novel approaches and practical solutions to face all the aforementioned challenges. The

device diversity concept was investigated in [**1**] and [**2**] and analyzed in Chapter 3. Novel solutions and algorithms on information fusion and combination of heterogeneous technologies are presented in Chapters 4 and 5 respectively. Related scientific work [**3**], [**4**], [**5**] and [**6**] has also been published. The last drawback of fingerprint-based platforms, which is related to the requirement of multiple access point deployment, is investigated in Chapter 6. In this Chapter a methodology for single access point localization, by utilizing the polarization effects that occur in indoor environments is proposed. Such a solution is actually and practically implementable in residential and small office areas where usually only one single access point is being deployed.

Finally, in the area of RTLS performance evaluation, contribution have been made towards the development of *TBNPD* algorithm, as per [**9**], which is extensively utilized in Chapter 6.

Last but not least, for the actual implementation of the initial novel concepts, the test and evaluation of new positioning algorithms, an experimental versatile localization platform called *ϕ-map* was created. This platform was developed in Android and supports a wide range of functions and capabilities.

7.2. Future Work

It is the author's personal belief that the research work presented in this thesis, and especially the algorithms presented in relation to information fusion, can be further expanded and find practical implementation by the industry. Special notice should be given to the proposed novel methodology for single MIMO AP positioning that takes advantage of the polarization effects. The concept of accessing all MIMO device antennas separately, and considering them as independent emitters, can provide new positioning capabilities, when the information retrieved is utilized effectively.

Additionally, the developed *ϕ-map* localization platform is modular and expandable and can further accommodate different types of positioning algorithms and evaluation techniques, in order to be utilized for the evaluation of new concepts. Typical examples for future investigation are the following:

(1) Fusion of information from an actually deployed Visible Light Positioning System with Wi-Fi and BLE information, in order to produce a triple heterogeneous technology localization platform.
(2) Dynamic radiomap update by utilizing crowd sourcing data collection and automatic filtering.
(3) 3D indoor positioning by combining fingerprinting with inertial sensors.
(4) Enhanced positioning algorithm for minimizing the antenna orientation effects.

In a more general approach of future work, several topics can be identified that are foreseen to be especially active for the research community in the coming years. **Information fusion** and combination of heterogeneous wireless technologies for

improving RTLS performance is considered to be an ongoing and open-ended challenge. Radio and non-radio parameters availability and diversity is vast and increasing rapidly. Issues on selecting and filtering such information or mitigating the effects of interference are challenges to be faced. Future work, will unavoidably involve the introduction of **artificial intelligence** in positioning algorithms, as well as in the high level management and optimization of localization platforms.

As discussed in this thesis, location information is becoming more and more critical in the provision of a vast number of services. It is currently being investigated on how to better support self-organizing networks in 5G era. However, the nature of such information - monitoring and tracking of everybody and everything - invades deeply in privacy and sensitive security aspects. Such an issue puts a burden on the shoulders of the research community: the responsibility to provide adequate security mechanisms to protect the confidentiality aspects from any type of attack. Hence, it is also expected that localization topics will be even more related and associated with **security** topics, ethical and non-ethical hacking, satellite spoofing cyber-attacks etc.

It is envisioned that future work of this thesis will focus in the following areas:

(1) Firstly, the fusion of information from heterogeneous wireless technologies, as well as data from other sensors (i.e, microphone, temperature, pressure) that can be found in a modern smart phone.
(2) Following that, the combination of positioning with machine learning, in order to study potential performance improvements of the positioning methods in large fingerprint databases. The resiliency of the positioning algorithms in fast changing environments and dynamic interference can be investigated.
(3) Finally, one can investigate how to take advantage of the computational power of new Graphics Processing Units (GPUs) in two directions: i. leveraging real-time Ray Tracing to detect significant changes in an environment, during the online phase of positioning, and ii. use the efficiency of parallel programming of GPUs to increase the performance of positioning algorithms when they have to deal with very large fingerprinting databases.

In the scope of these studies, the ϕ-map platform, as well as the *TruNET wireless* simulator, which will provide the testing platforms for newly created algorithms and methodologies, will be further extended and developed.

Bibliography

[1] M. Raspopoulos, C. Laoudias, L. Kanaris, A. Kokkinis, C.G. Panayiotou, and S. Stavrou. 3d ray tracing for device-independent fingerprint-based positioning in wlans. In *Positioning Navigation and Communication (WPNC), 2012 9th Workshop on*, pages 109–113, March.

[2] Marios Raspopoulos, Christos Laoudias, Loizos Kanaris, Akis Kokkinis, Christos Panayiotou, and Stavros Stavrou. Cross device fingerprint-based positioning using 3D ray tracing. In *Mobile Computing Symposium (IWCMC2012-Mobile Computing)*, Limassol, Cyprus, August 2012.

[3] Akis Kokkinis, Marios Raspopoulos, Loizos Kanaris, Antonio Liotta, and Stavros Stavrou. Map-Aided fingerprint-based indoor positioning. In *2013 IEEE 24th International Symposium on Personal, Indoor and Mobile Radio Communications: Fundamentals and PHY Track (PIMRC'13 - Fundamentals and PHY Track)*, pages 265–269, London, United Kingdom, September 2013.

[4] A. Kokkinis, L. Kanaris, M. Raspopoulos, A. Liotta, and S. Stavrou. Optimizing route prior knowledge for map-aided fingerprint-based positioning systems. In *The 8th European Conference on Antennas and Propagation (EuCAP 2014)*, pages 2141–2144, April 2014.

[5] Loizos Kanaris, Akis Kokkinis, Antonio Liotta, and Stavros Stavrou. Fusing bluetooth beacon data with wi-fi radiomaps for improved indoor localization. *Sensors*, 17(4), 2017.

[6] Loizos Kanaris, Akis Kokkinis, Antonio Liotta, and Stavros Stavrou. Combining smart lighting and radio fingerprinting for improved indoor localization. In *Networking, Sensing and Control (ICNSC), 2017 IEEE 14th International Conference on*, pages 447–452. IEEE, 2017.

[7] Loizos Kanaris, Akis Kokkinis, Antonio Liotta, Marios Raspopoulos, and Stavros Stavrou. A binomial distribution approach for the evaluation of indoor positioning systems. In *20th International Conference on Telecommunications (ICT 2013)*, Casablanca, Morocco, 2013.

[8] Loizos Kanaris, Akis Kokkinis, Giancarlo Fortino, Antonio Liotta, and Stavros Stavrou. Sample size determination algorithm for fingerprint-based indoor localization systems. *Computer Networks*, 101:169–177, 2016.

[9] Loizos Kanaris, Akis Kokkinis, Antonio Liotta, and Stavros Stavrou. Quality of fingerprint radiomaps for positioning systems. In *2017 24th International Conference on Telecommunications (ICT) (ICT 2017)*, Limassol, Cyprus, May 2017.

[10] L. Kanaris, A. Kokkinis, M. Raspopoulos, A. Liotta, and S. Stavrou. Improving rss fingerprint-based localization using directional antennas. In *The 8th European Conference on Antennas and Propagation (EuCAP 2014)*, pages 1593–1597, April 2014.

[11] Akis Kokkinis, Aristodemos Paphitis, Loizos Kanaris, Charalampos Sergiou, and Stavros Stavrou. Demo: Physical and network layer interconnection module for realistic planning of iot sensor networks. In *Proceedings of the 2018 International Conference on Embedded Wireless Systems and Networks*, EWSN ’18, pages 201–202, USA, 2018. Junction Publishing.

[12] Fractal Networx Limited. TruNET wireless, www.fractalnetworx.com, 2017.

[13] Alan Bensky. *Wireless Positioning Technologies and Applications*. Artech House, Inc., Norwood, MA, USA, 2007.

[14] Min Chen. Towards smart city: M2m communications with software agent intelligence. *Multimedia Tools and Applications*, 67(1):167–178, 2013.

[15] D. Zhang, L.T. Yang, M. Chen, S. Zhao, M. Guo, and Y. Zhang. Real-time locating systems using active rfid for internet of things. *Systems Journal, IEEE*, PP(99):1–10, 2014.

[16] Hao Ji, Lei Xie, Chuyu Wang, Yafeng Yin, and Sanglu Lu. Crowdsensing: A crowd-sourcing based indoor navigation using rfid-based delay tolerant network. *Journal of Network and Computer Applications*, 52(0):79 – 89, 2015.

[17] D. Macagnano, G. Destino, and G. Abreu. Indoor positioning: A key enabling technology for iot applications. In *Internet of Things (WF-IoT), 2014 IEEE World Forum on*, pages 117–118, March 2014.

[18] H. Liu, H. Darabi, P. Banerjee, and J. Liu. Survey of wireless indoor positioning techniques and systems. *IEEE Transactions on Systems, Man, and Cybernetics, Part C (Applications and Reviews)*, 37(6):1067–1080, Nov 2007.

[19] K. Al Nuaimi and H. Kamel. A survey of indoor positioning systems and algorithms. In *Proc. Int Innovations in Information Technology (IIT) Conf*, pages 185–190, 2011.

[20] Reza Zekavat and R. Michael Buehrer. *IEEE Press Series on Digital and Mobile Communication*. IEEE, 2012.

[21] J. A. del Peral-Rosado, R. Raulefs, J. A. Lopez-Salcedo, and G. Seco-Granados. Survey of cellular mobile radio localization methods: From 1g to 5g. *IEEE Communications Surveys Tutorials*, 20(2):1124–1148, Secondquarter 2018.

[22] S. S. Cherian and A. N. Rudrapatna. Lte location technologies and delivery solutions. *Bell Labs Technical Journal*, 18(2):175–194, Sept 2013.

[23] Q. D. Vo and P. De. A survey of fingerprint-based outdoor localization. *IEEE Communications Surveys Tutorials*, 18(1):491–506, Firstquarter 2016.

[24] A. Tahat, G. Kaddoum, S. Yousefi, S. Valaee, and F. Gagnon. A look at the recent wireless positioning techniques with a focus on algorithms for moving receivers. *IEEE Access*, 4:6652–6680, 2016.

[25] R. M. Alkan, H. Karaman, and M. Sahin. Gps, galileo and glonass satellite navigation systems: Gps modernization. In *Proceedings of 2nd International Conference on Recent Advances in Space Technologies, 2005. RAST 2005.*, pages 390–394, June 2005.

[26] M. Richharia and L.D. Westbrook. *Satellite Systems for Personal Applications: Concepts and Technology*. Wireless Communications and Mobile Computing. Wiley, 2011.

[27] Jacek Januszewski. Visibility and geometry of global satellite navigation systems constellations. *Artificial Satellites*, 50:169–180, 12 2015.

[28] S. Mumtaz, K. M. S. Huq, J. Rodriguez, S. Ghosh, E. E. Ugwuanyi, M. Iqbal, T. Dagiuklas, S. Stavrou, L. Kanaris, I. D. Politis, A. Lykourgiotis, T. Chrysikos, P. Nakou, and P. Georgakopoulos. Self-organization towards reduced cost and energy per bit for future emerging radio technologies - sonnet. In *2017 IEEE Globecom Workshops (GC Wkshps)*, pages 1–6, Dec 2017.

[29] A.K.M. Mahtab Hossain and Wee-Seng Soh. A survey of calibration-free indoor positioning systems. *Computer Communications*, 66(0):1 – 13, 2015.

[30] S. He and S.G. Chan. Wi-fi fingerprint-based indoor positioning: Recent advances and comparisons. *Communications Surveys Tutorials, IEEE*, 18(1):466–490, Firstquarter 2016.

[31] S. De Lausnay, L. De Strycker, J. P. Goemaere, B. Nauwelaers, and N. Stevens. A survey on multiple access visible light positioning. In *2016 IEEE International Conference on Emerging Technologies and Innovative Business Practices for the Transformation of Societies (EmergiTech)*, pages 38–42, Aug 2016.

[32] F. Wen and C. Liang. Fine-grained indoor localization using single access point with multiple antennas. *IEEE Sensors Journal*, 15(3):1538–1544, March 2015.

[33] Jose Rabadan, Victor Guerra, Rafael Rodrguez, Julio Rufo, Martin Luna-Rivera, and Rafael Perez-Jimenez. Hybrid visible light and ultrasound-based sensor for distance estimation. *Sensors*, 17(2), 2017.

[34] P. Mirowski, Tin Kam Ho, Saehoon Yi, and M. Macdonald. Signalslam: Simultaneous localization and mapping with mixed wifi, bluetooth, lte and magnetic signals. In *Indoor Positioning and Indoor Navigation (IPIN), 2013 International Conference on*, pages 1–10, Oct 2013.

[35] Li Li, Wang Yang, and Guojun Wang. Intelligent fusion of information derived from received signal strength and inertial measurements for indoor wireless localization. *AEU - International Journal of Electronics and Communications*, 70(9):1105 – 1113, 2016.

[36] You Li, Yuan Zhuang, Peng Zhang, Haiyu Lan, Xiaoji Niu, and Naser El-Sheimy. An improved inertial/wifi/magnetic fusion structure for indoor navigation. *Information Fusion*, 34:101 – 119, 2017.

[37] A. Kokkinis, M. Raspopoulos, L. Kanaris, A. Liotta, and S. Stavrou. Map-aided fingerprint-based indoor positioning. In *Personal Indoor and Mobile Radio Communications (PIMRC), 2013 IEEE 24th International Symposium on*, pages 270–274, Sept 2013.

[38] Zhenlong Song, Gangyi Jiang, and Chao Huang. A survey on indoor positioning technologies. In Qihai Zhou, editor, *Theoretical and Mathematical Foundations of Computer Science*, pages 198–206, Berlin, Heidelberg, 2011. Springer Berlin Heidelberg.

[39] Abdulrahman Alarifi, AbdulMalik Al-Salman, Mansour Alsaleh, Ahmad Alnafessah, Suheer Al-Hadhrami, Mai A. Al-Ammar, and Hend S. Al-Khalifa. Ultra wideband indoor positioning technologies: Analysis and recent advances. *Sensors*, 16(5), 2016.

[40] B. Amer and A. Noureldin. Rss-based indoor positioning utilizing firefly algorithm in wireless sensor networks. In *2016 11th International Conference on Computer Engineering Systems (ICCES)*, pages 329–333, Dec 2016.

[41] Nasrullah Pirzada, M Yunus Nayan, Fazli Subhanc M Fadzil Hassan, and Muhammad Amir Khan. Device-free localization technique for indoor detection and tracking of human body: A survey. *Procedia - Social and Behavioral Sciences*, 129(0):422 – 429, 2014. 2nd International Conference on Innovation, Management and Technology Research.

[42] A.K.M.M. Hossain and Wee-Seng Soh. A comprehensive study of bluetooth signal parameters for localization. In *Personal, Indoor and Mobile Radio Communications, 2007. PIMRC 2007. IEEE 18th International Symposium on*, pages 1–5, Sept 2007.

[43] Mikkel Kjærgaard. A taxonomy for radio location fingerprinting. In *3rd international conference on Location-and context-awareness*, pages 139–156. Springer-Verlag, 2007.

[44] A. Ishimaru. *Electromagnetic Wave Propagation, Radiation, and Scattering*. Prentice Hall, 1991.

[45] M.F. Cátedra and J. Perez. *Cell Planning for Wireless Communications*. Artech House mobile communications library. Artech House, 1999.

[46] Y. Okumura, E. Ohmori, T. Kawano, and K. Fukuda. Field strength and its variability in VHF and UHF land-mobile radio service. *Review of the Electrical Communication Laboratory*, 16(9-10):825–873, 1968.

[47] M. Hata. Empirical formula for propagation loss in land mobile radio services. *IEEE Transactions on Vehicular Technology*, 29(3):317–325, Aug 1980.

[48] European Cooperation in the Field of Scientific and Technical Research. *Digital mobile radio: COST 231 view on the evolution towards 3rd generation systems*. 1996.

[49] J. D. Parsons and M. F. Ibrahim. Signal strength prediction in built-up areas. part 2: Signal variability. *IEE Proceedings F - Communications, Radar and Signal Processing*, 130(5):385–391, August 1983.

[50] K. Allsebrook and J. D. Parsons. Mobile radio propagation in british cities at frequencies in the vhf and uhf bands. *IEEE Transactions on Vehicular Technology*, 26(4):313–323, Nov 1977.

[51] J. Walfisch and H. L. Bertoni. A theoretical model of uhf propagation in urban environments. *IEEE Transactions on Antennas and Propagation*, 36(12):1788–1796, Dec 1988.

[52] S. Phaiboon. An empirically based path loss model for indoor wireless channels in laboratory building. In *TENCON '02. Proceedings. 2002 IEEE Region 10 Conference on Computers, Communications, Control and Power Engineering*, volume 2, pages 1020 – 1023 vol.2, oct. 2002.

[53] H. Hashemi. The indoor radio propagation channel. *Proceedings of the IEEE*, 81(7):943–968, July 1993.

[54] D. Molkdar. Review on radio propagation into and within buildings. *IEE Proceedings H - Microwaves, Antennas and Propagation*, 138(1):61–73, Feb 1991.

[55] A. Hills, J. Schlegel, and B. Jenkins. Estimating signal strengths in the design of an indoor wireless network. *Wireless Communications, IEEE Transactions on*, 3(1):17 – 19, jan. 2004.

[56] Manuel F. Catedra and Jesus Perez. *Cell Planning for Wireless Communications*. Artech House, Inc., Norwood, MA, USA, 1st edition, 1999.

[57] G.E. Athanasiadou and A.R. Nix. A novel 3-D indoor ray-tracing propagation model: The path generator and evaluation of narrow-band and wide-band predictions. *IEEE Transactions on Vehicular Technology*, 49(4):1152–1168, 2000.

[58] S.R. Saunders. *Antennas and propagation for wireless communication systems*. Wiley, 2007.

[59] I. Guvenc and C. Chong. A survey on toa based wireless localization and nlos mitigation techniques. *IEEE Communications Surveys Tutorials*, 11(3):107–124, rd 2009.

[60] S. A. Zekavat, A. Kolbus, X. Yang, Z. Wang, J. Pourrostam, and M. Pourkhaatoun. A novel implementation of doa estimation for node localization on software defined radios: Achieving high performance with low complexity. In *2007 IEEE International Conference on Signal Processing and Communications*, pages 983–986, Nov 2007.

[61] R. Schmidt. Multiple emitter location and signal parameter estimation. *IEEE Transactions on Antennas and Propagation*, 34(3):276–280, March 1986.

[62] Janis Werner, Jun Wang, Aki Hakkarainen, Nikhil Gulati, Damiano Patron, Doug Pfeil, Kapil Dandekar, Danijela Cabric, and Mikko Valkama. Sectorized antenna-based doa estimation and localization: Advanced algorithms and measurements. *IEEE Journal on Selected Areas in Communications*, pages 1–1, 11 2015.

[63] R. Harle. A survey of indoor inertial positioning systems for pedestrians. *IEEE Communications Surveys Tutorials*, 15(3):1281–1293, Third 2013.

[64] Y. Cheng, Q. Meng, Y. Liu, M. Zeng, L. Xue, and S. Ma. Fusing sound and dead reckoning for multi-robot cooperative localization. In *2016 12th World Congress on Intelligent Control and Automation (WCICA)*, pages 1474–1478, June 2016.

[65] Seongwoo Jang, Kyungjae Ahn, Jongseong Lee, and Yeonsik Kang. A study on integration of particle filter and dead reckoning for efficient localization of automated guided vehicles. In *2015 IEEE International Symposium on Robotics and Intelligent Sensors (IRIS)*, pages 81–86, Oct 2015.

[66] W. Kang and Y. Han. Smartpdr: Smartphone-based pedestrian dead reckoning for indoor localization. *IEEE Sensors Journal*, 15(5):2906–2916, May 2015.

[67] P. Bahl and V.N. Padmanabhan. RADAR: an in-building RF-based user location and tracking system. In *IEEE International Conference on Computer Communications INFOCOM*, volume 2, pages 775–784, 2000.

[68] Teemu Roos, Petri Myllymaki, Henry Tirri, Pauli Misikangas, and Juha Sievanen. A probabilistic approach to wlan user location estimation. *International Journal of Wireless Information Networks*, 9:155–164, 2002. 10.1023/A:1016003126882.

[69] Yiming Ji, Saad Biaz, Santosh Pandey, and Prathima Agrawal. ARIADNE: a dynamic indoor signal map construction and localization system. In *4th ACM international conference on Mobile systems, applications and services*, pages 151–164, 2006.

[70] A. Hatami and K. Pahlavan. Comparative statistical analysis of indoor positioning using empirical data and indoor radio channel models. In *3rd IEEE Consumer Communications and Networking Conference (CCNC)*, volume 2, pages 1018–1022. IEEE, 2006.

[71] K. El-Kafrawy, M. Youssef, A. El-Keyi, and A. Naguib. Propagation modeling for accurate indoor wlan rss-based localization. In *Proc. IEEE 72nd Vehicular Technology Conf. Fall (VTC 2010-Fall)*, pages 1–5, 2010.

[72] V. Honkavirta, T. Perala, S. Ali-Loytty, and R. Piche. A comparative survey of WLAN location fingerprinting methods. In *6th Workshop on Positioning, Navigation and Communication (WPNC)*, pages 243–251, 2009.

[73] Binghao Li, James Salter, Andrew G Dempster, Chris Rizos, et al. Indoor positioning techniques based on wireless lan. In *LAN, First IEEE International Conference on Wireless Broadband and Ultra Wideband Communications*, pages 13–16, 2006.

[74] P. Prasithsangaree, P. Krishnamurthy, and P.K. Chrysanthis. On indoor position location with wireless lans. In *Personal, Indoor and Mobile Radio Communications, 2002. The 13th IEEE International Symposium on*, volume 2, pages 720–724 vol.2, Sept.

[75] Wilson Yeung, JunYang Zhou, and Joseph Ng. Enhanced fingerprint-based location estimation system in wireless LAN environment. *Emerging Directions in Embedded and Ubiquitous Computing*, pages 273–284, 2007.

[76] P Bahl, VN Padmanabhan, and A Balachandran. Enhancements to the RADAR user location and tracking system. *Microsoft Research, Tech. Rep. MSR-TR-00-12*, February 2000.

[77] S. Saha, K. Chaudhuri, D. Sanghi, and P. Bhagwat. Location determination of a mobile device using ieee 802.11b access point signals. In *2003 IEEE Wireless Communications and Networking, 2003. WCNC 2003.*, volume 3, pages 1987–1992 vol.3, March 2003.

[78] H. Laitinen, J. Lahteenmaki, and T. Nordstrom. Database correlation method for GSM location. In *53rd IEEE Vehicular Technology Conference (VTC2001-Spring)*, volume 4, pages 2504–2508, 2001.

[79] P. Kemppi and S. Nousiainen. Database correlation method for multi-system positioning. In *63rd IEEE Vehicular Technology Conference (VTC2006-Spring)*, volume 2, pages 866–870, 2006.

[80] M.A. Youssef, A. Agrawala, and A. Udaya Shankar. WLAN location determination via clustering and probability distributions. In *IEEE International Conference on Pervasive Computing and Communications (PerCom)*, pages 143–150, 2003.

[81] M. Youssef and A. Agrawala. Handling samples correlation in the horus system. In *INFOCOM 2004. Twenty-third AnnualJoint Conference of the IEEE Computer and Communications Societies*, volume 2, pages 1023 – 1031 vol.2, march 2004.

[82] Moustafa Youssef and Ashok Agrawala. The Horus WLAN location determination system. In *3rd ACM International Conference on Mobile systems, applications, and services*, pages 205–218, 2005.

[83] Lin Liao, D. Fox, Jeffrey Hightower, H. Kautz, and D. Schulz. Voronoi tracking: location estimation using sparse and noisy sensor data. In *Intelligent Robots and Systems, 2003. (IROS 2003). Proceedings. 2003 IEEE/RSJ International Conference on*, volume 1, pages 723–728 vol.1, 2003.

[84] F. Evennou, F. Marx, and E. Novakov. Map-aided indoor mobile positioning system using particle filter. In *Proc. IEEE Wireless Communications and Networking Conf*, volume 4, pages 2490–2494, 2005.

[85] Bluetooth SIG. Bluetooth technology website, 2017.

[86] Apple Inc. ibeacon for developers, 2017.

[87] H. K. Fard, Y. Chen, and K. K. Son. Indoor positioning of mobile devices with agile ibeacon deployment. In *2015 IEEE 28th Canadian Conference on Electrical and Computer Engineering (CCECE)*, pages 275–279, May 2015.

[88] S. Gowrishankar, N. Madhu, and T. G. Basavaraju. Role of ble in proximity based automation of iot: A practical approach. In *2015 IEEE Recent Advances in Intelligent Computational Systems (RAICS)*, pages 400–405, Dec 2015.

[89] V. Chandel, N. Ahmed, S. Arora, and A. Ghose. Inloc: An end-to-end robust indoor localization and routing solution using mobile phones and ble beacons. In *2016 International Conference on Indoor Positioning and Indoor Navigation (IPIN)*, pages 1–8, Oct 2016.

[90] K. Antevski, A. E. C. Redondi, and R. Pitic. A hybrid ble and wi-fi localization system for the creation of study groups in smart libraries. In *2016 9th IFIP Wireless and Mobile Networking Conference (WMNC)*, pages 41–48, July 2016.

[91] Y. Peng, W. Fan, X. Dong, and X. Zhang. An iterative weighted knn (iw-knn) based indoor localization method in bluetooth low energy (ble) environment. In *2016 Intl IEEE Conferences on Ubiquitous Intelligence Computing, Advanced and Trusted Computing, Scalable Computing and Communications, Cloud and Big Data Computing, Internet of People, and Smart World Congress (UIC/ATC/ScalCom/CBDCom/IoP/SmartWorld)*, pages 794–800, July 2016.

[92] Pavel Kriz, Filip Maly, and Tomas Kozel. Improving indoor localization using bluetooth low energy beacons. *Mobile Information Systems*, 2016:11, 2016.

[93] H. S. Kim, D. R. Kim, S. H. Yang, Y. H. Son, and S. K. Han. An indoor visible light communication positioning system using a rf carrier allocation technique. *Journal of Lightwave Technology*, 31(1):134–144, Jan 2013.

[94] M. S. Rahman, M. M. Haque, and Ki-Doo Kim. High precision indoor positioning using lighting led and image sensor. In *14th International Conference on Computer and Information Technology (ICCIT 2011)*, pages 309–314, Dec 2011.

[95] Ye-Sheng Kuo, Pat Pannuto, Ko-Jen Hsiao, and Prabal Dutta. Luxapose: Indoor positioning with mobile phones and visible light. In *Proceedings of the 20th Annual International Conference on Mobile Computing and Networking*, MobiCom '14, pages 447–458, New York, NY, USA, 2014. ACM.

[96] Y. Nakazawa, H. Makino, K. Nishimori, D. Wakatsuki, and H. Komagata. Indoor positioning using a high-speed, fish-eye lens-equipped camera in visible light communication. In *International Conference on Indoor Positioning and Indoor Navigation*, pages 1–8, Oct 2013.

[97] M. Yasir, S. W. Ho, and B. N. Vellambi. Indoor positioning system using visible light and accelerometer. *Journal of Lightwave Technology*, 32(19):3306–3316, Oct 2014.

[98] S. De Lausnay, L. De Strycker, J. P. Goemaere, N. Stevens, and B. Nauwelaers. Optical cdma codes for an indoor localization system using vlc. In *2014 3rd International Workshop in Optical Wireless Communications (IWOW)*, pages 50–54, Sept 2014.

[99] W. Burnside and K. Burgener. High frequency scattering by a thin lossless dielectric slab. *IEEE Transactions on Antennas and Propagation*, 31(1):104–110, Jan 1983.

[100] K. Sato, H. Kozima, H. Masuzawa, T. Manabe, T. Ihara, Y. Kasashima, and K. Yamaki. Measurements of reflection characteristics and refractive indices of interior construction materials in millimeter-wave bands. In *1995 IEEE 45th Vehicular Technology Conference. Countdown to the Wireless Twenty-First Century*, volume 1, pages 449–453 vol.1, Jul 1995.

[101] R. Szumny, K. Kurek, and J. Modelski. Attenuation of multipath components using directional antennas and circular polarization for indoor wireless positioning systems. In *Microwave Conference, 2007. European*, pages 1680–1683, 2007.

[102] M. Barralet, Xu Huang, and D. Sharma. Effects of antenna polarization on rssi based location identification. In *2009 11th International Conference on Advanced Communication Technology*, volume 01, pages 260–265, Feb 2009.

[103] A. Cidronali, S. Maddio, G. Giorgetti, I. Magrini, S. K. S. Gupta, and G. Manes. A 2.45 ghz smart antenna for location-aware single-anchor indoor applications. In *2009 IEEE MTT-S International Microwave Symposium Digest*, pages 1553–1556, June 2009.

[104] A. Cidronali, S. Maddio, G. Giorgetti, and G. Manes. Analysis and performance of a smart antenna for 2.45-ghz single-anchor indoor positioning. *Microwave Theory and Techniques, IEEE Transactions on*, 58(1):21–31, 2010.

[105] Jirapat Sangthong, Sathaporn Promwong, and Pichaya Supanakoon. Comparison of uwb fingerprinting with vertical and horizontal polarizations for indoor localization. In *ECTI-CON2010: The 2010 ECTI International Confernce on Electrical Engineering/Electronics, Computer, Telecommunications and Information Technology*, pages 588–592, 2010.

[106] Z. Szalay and L. Nagy. Utilization of linearly and circularly polarized antennas for indoor positioning. In *2015 17th International Conference on Transparent Optical Networks (ICTON)*, pages 1–4, July 2015.

[107] M. Wallbaum and S. Diepolder. Benchmarking wireless lan location systems wireless lan location systems. In *Mobile Commerce and Services, 2005. WMCS '05. The Second IEEE International Workshop on*, pages 42 –51, july 2005.

[108] Yiming Ji, S. Biaz, Shaoen Wu, and Bing Qi. Optimal sniffers deployment on wireless indoor localization. In *Computer Communications and Networks, 2007. ICCCN 2007. Proceedings of 16th International Conference on*, pages 251 –256, aug. 2007.

[109] Yiming Ji. *Location Determination Within Wireless Networks*. VDM Publishing House Ltd, March 2009.

[110] Yiming Ji and Lei Chen. Dynamic indoor location determination: Mechanisms and robustness evaluation. In *Proc. Sixth Int Autonomic and Autonomous Systems (ICAS) Conf*, pages 70–77, 2010.

[111] J. Kim, M. Ji, Y. Cho, Y. Lee, and S. Park. Performance evaluation of fingerprint based location system using dynamic collection. In *2013 International Conference on ICT Convergence (ICTC)*, pages 950–954, Oct 2013.

[112] J. Jemai, R. Piesiewicz, and T. Kurner. Calibration of an indoor radio propagation prediction model at 2.4 GHz by measurements of the IEEE 802.11b preamble. In *IEEE 61st Vehicular Technology Conference (VTC 2005-Spring)*, volume 1, pages 111–115, 2005.

[113] S. Stavrou and SR Saunders. Review of constitutive parameters of building materials. In *Antennas and Propagation, 2003.(ICAP 2003). Twelfth International Conference on (Conf. Publ. No. 491)*, volume 1, pages 211–215. IET, 2003.

[114] Jun geun Park, D. Curtis, S. Teller, and J. Ledlie. Implications of device diversity for organic localization. In *Proc. IEEE INFOCOM*, pages 3182–3190, 2011.

[115] Youngjune Gwon and Ravi Jain. Error characteristics and calibration-free techniques for wireless lan-based location estimation. In *Proceedings of the Second International Workshop on Mobility Management &Amp; Wireless Access Protocols*, MobiWac '04, pages 2–9, New York, NY, USA, 2004. ACM.

[116] Krishna Chintalapudi, Anand Padmanabha Iyer, and Venkata N. Padmanabhan. Indoor localization without the pain. In *Proceedings of the Sixteenth Annual International Conference on Mobile Computing and Networking*, MobiCom '10, pages 173–184, New York, NY, USA, 2010. ACM.

[117] Hyuk Lim, Lu-Chuan Kung, Jennifer C. Hou, and Haiyun Luo. Zero-configuration indoor localization over ieee 802.11 wireless infrastructure. *Wirel. Netw.*, 16(2):405–420, February 2010.

[118] Anshul Rai, Krishna Kant Chintalapudi, Venkata N. Padmanabhan, and Rijurekha Sen. Zee: Zero-effort crowdsourcing for indoor localization. In *Proceedings of the 18th Annual International Conference on Mobile Computing and Networking*, Mobicom '12, pages 293–304, New York, NY, USA, 2012. ACM.

[119] Zheng Yang, Chenshu Wu, and Yunhao Liu. Locating in fingerprint space: Wireless indoor localization with little human intervention. In *Proceedings of the 18th Annual International Conference on Mobile Computing and Networking*, Mobicom '12, pages 269–280, New York, NY, USA, 2012. ACM.

[120] Zheng Yang, Chenshu Wu, Yunhao Liu, and Wei Xi. Will: Wireless indoor localization without site survey. *IEEE Transactions on Parallel & Distributed Systems*, 24:839–848, 2013.

[121] A. Nikitin, C. Laoudias, G. Chatzimilioudis, P. Karras, and D. Zeinalipour-Yazti. Indoor localization accuracy estimation from fingerprint data. In *2017 18th IEEE International Conference on Mobile Data Management (MDM)*, pages 196–205, May 2017.

List of Publications

The research work published in scientific papers or presented in conferences is the following:

[1] Akis Kokkinis, Loizos Kanaris, Marios Raspopoulos, Antonio Liotta, and Stavros Stavrou. Optimizing route prior knowledge for map-aided fingerprint-based positioning systems. In Antennas and Propagation (EuCAP), 2014 8th European Conference on, pages 21412144. IEEE, 2014.

[2] Akis Kokkinis, Aristodemos Paphitis, Loizos Kanaris, Charalampos Sergiou, and Stavros Stavrou. Physical and network layer interconnection module for realistic planning of IoT sensor networks. In Proceedings of the 2018 International Conference on Embedded Wireless Systems and Networks, pages 201202. Junction Publishing, 2018.

[3] Akis Kokkinis, Marios Raspopoulos, Loizos Kanaris, Antonio Liotta, and Stavros Stavrou. Map-aided fingerprint-based indoor positioning. In Personal Indoor and Mobile Radio Communications (PIMRC), 2013 IEEE 24th International Symposium on, pages 270274. IEEE, 2013.

[4] Marios Raspopoulos, Christos Laoudias, Loizos Kanaris, Akis Kokkinis, Christos G Panayiotou, and Stavros Stavrou. 3D ray tracing for device-independent fingerprint-based positioning in WLANs. 2012.

[5] Marios Raspopoulos, Christos Laoudias, Loizos Kanaris, Akis Kokkinis, Christos G Panayiotou, and Stavros Stavrou. Cross device fingerprint-based positioning using 3D ray tracing. In Wireless Communications and Mobile Computing Conference (IWCMC), 2012 8th International, pages 147152. IEEE, 2012

[6] Loizos Kanaris, Akis Kokkinis, Giancarlo Fortino, Antonio Liotta, and Stavros Stavrou. Sample size determination algorithm for fingerprint-based indoor localization systems. Computer Networks, 101:169177, 2016.

[7] Loizos Kanaris, Akis Kokkinis, Antonio Liotta, Marios Raspopoulos, and Stavros Stavrou. A binomial distribution approach for the evaluation of indoor positioning systems. In Telecommunications (ICT), 2013 20th International Conference on, pages 14. IEEE, 2013.

[8] Loizos Kanaris, Akis Kokkinis, Antonio Liotta, and Stavros Stavrou. Combining smart lighting and radio fingerprinting for improved indoor localization. In Networking, Sensing and Control (ICNSC), 2017 IEEE 14th International Conference on, pages 447452. IEEE, 2017.

[9] Loizos Kanaris, Akis Kokkinis, Antonio Liotta, and Stavros Stavrou. Fusing bluetooth beacon data with Wi-Fi radiomaps for improved indoor localization. Sensors, 17(4):812, 2017.

[10] Loizos Kanaris, Akis Kokkinis, Antonio Liotta, and Stavros Stavrou. Quality of fingerprint radiomaps for positioning systems. In Telecommunications (ICT), 2017 24th International Conference on, pages 15. IEEE, 2017.

[11] Loizos Kanaris, Akis Kokkinis, Marios Raspopoulos, Antonio Liotta, and Stavros Stavrou. Improving RSS fingerprint-based localization using directional antennas. In Antennas and Propagation (EuCAP), 2014 8th European Conference on, pages 15931597. IEEE, 2014.

[12] Akis Kokkinis, Loizos Kanaris, Antonio Liotta, and Stavros Stavrou. Fusing antenna information for improved single access point indoor localization. Sensors, MDPI, 2019, Submitted

Curriculum Vitae

Akis Kokkinis received a BSc in Aviation Science from the Hellenic Airforce Academy in Athens, with a diploma thesis in computer aided flight planning (Operational Navigation Flight Planning, including 3D RADAR coverage, RADAR Prediction and Visualization Features) in 1998. Since 2010, he is a member of the R&D department of Sigint Solutions Ltd, as a Software Architect and lead developer for several telecommunication platforms, such as TruNET, a 3D Ray Tracing Simulator. Additionally, he is heavily involved in FP6, FP7 and national ICT funded projects where Sigint Solutions Ltd carries out research work on multiple layers of the OSI protocol stack. Examples of these projects include UNITE (FP6), FUTON (FP7), WHERE (FP7) and COGEU (FP7). During his PhD (TU/e) he has been concentrating on the investigation of enhanced hybrid indoor positioning algorithms. He has published several peer-reviewed papers and presented his work at international conferences. He has developed an experimental, fingerprint-based indoor positioning platform (*ϕ-map*) and interconnected a Physical Layer simulator (*TruNET wireless*) with a Network Layer simulator (*Cooja*) in order to investigate Wireless Sensor Networks (WSN) in the aspects of indoor localization.